

DEPARTMENT OF CHEMISTRY, UNIVERSITY OF JYVÄSKYLÄ
RESEARCH REPORT No. 178

**METHOD DEVELOPMENT FOR DETERMINATION AND
RECOVERY OF RARE EARTH ELEMENTS FROM
INDUSTRIAL FLY ASH**

BY

SIIRI PERÄMÄKI

Academic Dissertation for the Degree of
Doctor of Philosophy

*To be presented, by permission of the Faculty of Mathematics and Science of the
University of Jyväskylä, for public examination in Auditorium YlistöKem4,
on December 12th, 2014 at 12 noon.*



UNIVERSITY OF JYVÄSKYLÄ

Copyright ©, 2014
University of Jyväskylä
Jyväskylä, Finland
ISBN 978-951-39-6001-8
ISSN 0357-346X

ABSTRACT

Perämäki, Siiri

Method development for determination and recovery of rare earth elements from industrial fly ash

Jyväskylä: University of Jyväskylä, 2014, p. 88

(Department of Chemistry, University of Jyväskylä Research Report Series ISSN 0357-346X)

ISBN 978-951-39-6001-8

Rare earth elements (REE) are important in numerous high technology applications and in addition their supply risk is high, which gives rise to studying new sources for rare earth elements. Rare earth element concentrations in industrial fly ash samples collected from Finnish power plants, using a mixture of peat and biomass as a fuel, have been determined. Two sample pre-treatment methods, ultrasound- and microwave-assisted acid digestions, have been applied to fly ash samples. Measurement conditions for inductively coupled plasma-optical emission spectrometry (ICP-OES) have been optimized to reach robust plasma conditions and the reliability of the analysis has been investigated by using a standard reference material, synthetic samples, a method of standard addition, and a comparison analysis with inductively coupled plasma-mass spectrometry (ICP-MS). Most rare earth elements in fly ash samples are enriched compared to concentrations in earth's crust, and some ashes have total rare earth element concentrations as high as 560 mg kg⁻¹.

A leaching procedure using dilute sulfuric acid as a leaching reagent has been developed for the dissolution of rare earth elements from fly ash. Optimization of the sulfuric acid leaching resulted in approximately 70 % of the rare earth elements being dissolved from the fly ash samples. Recovery of rare earth elements from the sulfuric acid leachate has been investigated using oxalate precipitation and liquid-liquid extraction. Conditions for oxalate precipitation were optimized, and it was found to be quantitative but non-selective towards rare earth elements. Liquid-liquid extraction with bis(2-ethylhexyl)phosphoric acid (D2EHPA) was found most suitable to concentrate rare earth elements before precipitation as oxalates. After optimization of process parameters, recovery of light and heavy rare earth elements was achieved. A specific liquid-liquid extraction procedure for scandium recovery was also developed.

Keywords: rare earth element, fly ash, ICP-OES, optimization, robust plasma, leaching, precipitation, liquid-liquid extraction.

Author's address Siiri Perämäki
Department of Chemistry
P.O. Box 35
FI-40014 University of Jyväskylä
siiri.e.peramaki@jyu.fi

Supervisor Docent Ari Väisänen
Department of Chemistry
University of Jyväskylä
Jyväskylä, Finland

Reviewers Professor Antonio Canals
Department of Analytical Chemistry
University of Alicante
Alicante, Spain

Senior Researcher Sirpa Peräniemi
University of Eastern Finland
School of Pharmacy
Kuopio, Finland

Opponent Professor Paavo Perämäki
Department of Chemistry
University of Oulu
Oulu, Finland

PREFACE

This doctoral thesis was conducted at Jyväskylä University's Chemistry Department during the years 2011–2014. Docent Ari Väisänen has supervised my work, to whom I express my deepest gratitude. Thank you for your skillful guidance and never-ending enthusiasm during these years, and for creating an inspiring and supporting atmosphere in our group. I also express my thanks to Prof. Jussi Valkonen for guidance at the beginning of this project and for encouraging me to start my Ph.D. studies. The referees, Prof. Antonio Canals and Senior Researcher Sirpa Peräniemi, are gratefully acknowledged for their valuable comments and suggestions regarding this dissertation.

Jyväskylän Energia Oy is gratefully obliged for the financial support during this work, and particularly the Development Manager Risto Ryymin for guiding this project forward and for providing a fresh outlook on several aspects. My sincere thanks go to all the team members at the university and other collaborating companies, who have been a vital part of this project. Ville Soikkeli, M.Sc., is especially recognized for collaboration at the beginning of this work. A special thank you goes to Antti Tiihonen, M.Sc., for helpful collaboration regarding this project and for the numerous inspiring conversations.

I am grateful to all the wonderful people in the Chemistry Department for making these years very special for me. I particularly want to thank all my roommates at work, current and previous; it has been a pleasure sharing a workspace with you and getting to know you. I also want to thank all the people I have had the pleasure of teaching and working beside in the laboratory and with ICP; I have learned much from the experience. Esa Lehtimäki, M.Sc., is acknowledged for his ability to make even the most routine lab work fun: the lab would have been a lot quieter without you. Thank you also for the people in the coffee room for enjoyable conversations during lunches and coffee breaks. Hannu Salo and Hannu Lamberg are acknowledged for their helpful expertise with scanning electron microscopy and particle size analysis, respectively.

Lastly, I want to thank my friends and family for their support during this time. My greatest gratitude I owe to my husband and best friend, Henri, who has always been there for me through all the ups and downs. Thank you for your endless love and support, and for making everything worthwhile.

Jyväskylä 28.11.2014

Siiri Perämäki

CONTENTS

ABSTRACT
PREFACE
CONTENTS
ABBREVIATIONS

1	AIMS OF THE STUDY	9
2	REVIEW OF THE LITERATURE	10
2.1	Introduction.....	10
2.2	Rare earth elements	11
2.2.1	Properties	11
2.2.2	Compounds.....	13
2.2.3	Applications	15
2.2.4	Abundance	16
2.2.5	Resources.....	17
2.2.6	Production.....	19
2.2.7	Prices	19
2.3	REE separation processes	20
2.3.1	Fractional crystallization and precipitation	21
2.3.2	Ion exchange	22
2.3.3	Liquid-liquid extraction	23
2.4	Industrial fly ash.....	26
2.4.1	Production and composition	26
2.4.2	Utilization.....	27
2.4.3	REE in fly ash.....	28
2.5	ICP-OES.....	30
2.5.1	Introduction	30
2.5.2	Optimization of measurement conditions.....	31
2.5.3	Interferences.....	33
2.6	Reliability of analytical results.....	35
3	EXPERIMENTAL	37
3.1	Samples	37
3.2	Reagents	37
3.3	Instrumentation.....	39
3.4	Optimization of ICP-OES measurement	40
3.5	Experimental procedures.....	42
3.5.1	Digestion.....	43
3.5.2	Leaching	44
3.5.3	Precipitation.....	45

3.5.4	Liquid-liquid extraction	46
4	RESULTS AND DISCUSSION	47
4.1	Development of REE analysis	47
4.2	Optimization of measurement conditions	51
4.2.1	Robustness of plasma with <i>aqua regia</i> samples	51
4.2.2	Robustness of plasma with sulfuric acid samples	53
4.2.3	Acid effect in sulfuric acid samples	54
4.2.4	REE recovery in robust and non-robust plasma conditions ...	55
4.3	Properties of fly ash	57
4.4	Leaching of REEs from fly ash	59
4.4.1	Initial leaching experiments	59
4.4.2	Concentration of sulfuric and nitric acid	60
4.4.3	Leaching time and temperature	61
4.4.4	Leachate re-circulation	62
4.4.5	Optimized leaching procedure	64
4.5	REE precipitation as oxalates	65
4.5.1	Initial precipitation experiments	65
4.5.2	Effects of pH	65
4.5.3	Molar amount of oxalic acid	66
4.5.4	Mixing time and temperature	67
4.5.5	Optimized precipitation procedure	68
4.6	REE concentration using liquid-liquid extraction	68
4.6.1	Initial liquid-liquid extraction experiments	68
4.6.2	Optimization of liquid-liquid extraction	69
4.6.3	Optimization of stripping	72
4.6.4	Scandium stripping	75
4.6.5	Scrubbing of organic phase	75
4.6.6	Optimized liquid-liquid extraction procedure	75
5	CONCLUSIONS	77
	REFERENCES	79

ABBREVIATIONS

α	Separation factor
A:O-ratio	Aqueous to organic ratio
BEC	Background equivalent concentration
c	concentration
CCD	Charged-coupled device
D	Distribution coefficient
D2EHPA	Bis(2-ethylhexyl) hydrogen phosphate (IUPAC) Di(2-ethylhexyl)phosphoric acid
EDTA	Ethylenediaminetetraacetic acid
EHEHPA	2-ethylhexyl (2-ethylhexyl) phosphonate
EIE	Easily ionized elements
HREE	Heavy rare earth elements
ICP-MS	Inductively coupled plasma mass spectrometry
ICP-AES	Inductively coupled plasma atomic emission spectrometry
ICP-OES	Inductively coupled plasma optical emission spectrometry
istd	internal standard
IUPAC	International Union of Pure and Applied Chemistry
Ln	Rare earth element
LnM	Rare earth element compound with non-rare earth element
LOD	Limit of detection
LOQ	Limit of quantification
LREE	Light rare earth elements
MSF	Multicomponent spectral fitting
m/z	mass-to-charge ratio

n	number of replicates
NA	not available
NiMH	Nickel-metal hydride
NIST	National Institute of Standards and Technology
p.a.	pro analysis
RE	Rare earth
REE	Rare earth element
REM	Rare earth metal or mineral
REO	Rare earth oxide
RSD	Relative standard deviation
SEM	Scanning electron microscope
SRM	Standard reference material
TBP	Tributyl phosphate
v/v	Volume to volume ratio
w/w, %	weight percentage
XRF	X-ray fluorescence

1 AIMS OF THE STUDY

Industrial fly ash contains considerable concentrations of rare earth elements, and due to large production volumes, coal fly ash has been studied widely for rare earth element recovery. Although several methods have been developed, rare earth element recovery from coal fly ash is not in commercial use. Fly ashes from combustion power plants using different types of fuels have not been studied as closely. The focus of this study was to develop methods for the determination and recovery of rare earth elements in fly ash from power plants using biomass as a partial fuel.

The first step was to investigate the properties of fly ash and to develop an accurate and reliable analysis method for the determination of rare earth element concentrations. ICP-OES was used in the analysis of rare earth elements, and the measurement conditions were optimized. Standard reference material, synthetic samples and ICP-MS analysis were used in confirming accurate results. Several dissolution methods were employed to examine the total concentrations of rare earth elements in fly ash samples.

The second step of this study was to leach rare earth elements from fly ash with good recovery and as high concentrations in leachate as possible. The leaching of the matrix elements should be minimized; hence, the use of dilute acid is preferred over concentrated solutions. Leaching reagent should be selective for rare earth elements over matrix elements, and ideally it would be widely available and affordable. Leaching conditions were optimized to achieve maximum dissolution.

In the final phase of this research, a rare earth element concentrate was produced from the fly ash leachate. Requirements from the concentrate were good yield of REEs and sufficient purity. Precipitation and liquid-liquid extraction were possible routes to achieving a concentrate. Availability and cost of extraction reagents were important aspects in liquid-liquid extraction.

2 REVIEW OF THE LITERATURE

2.1 Introduction

Rare earth elements' market availability has become an increasingly important aspect for the modern society due to supply risks and increasing demand in various areas of production. China is the main producer of REEs with more than 90 % of the market in 2013, and it is also estimated to have the largest known REE reserves of any single country.¹ The high economic importance and supply risk concerning REEs has evoked the European Union to classify rare earth elements among the 20 critical materials in their report in 2014.² Rare earth elements have been among the critical materials since the 2010 listing.³ Export restrictions and rare earth quotas implemented by China have made rare earths' supply risk the highest of the critical materials, with China producing 99 % of heavy rare earth elements (HREE) and 87 % of light rare earth elements (LREE). The U.S. Department of Energy has also classified neodymium, europium, terbium, dysprosium, and yttrium as being critical in their 2011 Critical Materials Strategy.⁴ Recycling rare earth elements has been well-researched especially on a small scale; but has not been widely utilized: less than 1 % of REEs were recycled in 2011.⁵

Meanwhile, industrial fly ashes from combustion power plants are produced in large volumes, and their usage is only at 25 % on a global scale.⁶ The world's power demands will increase in the future with population growth and industrialization of developing countries, and while renewable energy sources are a partial solution, demand, especially in China and India, is most likely going to be met with coal or mixed fuel power plants producing various ashes. This gives rise to studies with the purpose of generating valuable fractions from fly ash. Coal fly ash utilization is a widespread research area, and especially at times of material crises, coal fly ash has been utilized in several ways.⁷ In the former Soviet Union and the United States uranium was collected from coal for nuclear industries during the post-World War II period, and during the germa-

mium crisis in the early 1960s, methods for germanium recovery from coal fly ash were developed.⁷

When more attention is being paid on the uncertain availability and unevenly distributed resources of rare earth elements, fly ash has been suggested as a new source for REEs. This idea was introduced more than 20 years ago, when coal beds with high rare earth element content were discovered in the Russian Far East.⁷ Since then, the concentrations of rare earth elements in coal fly ashes have been studied extensively; moreover, REE concentrations in fly ash from biomass, medical waste, animal waste, sewage sludge, and municipal solid waste incinerators have been determined.⁸⁻¹¹ In several publications, however, only the possible toxicity of rare earth elements in fly ash has been evaluated rather than recovery possibilities.¹²

Compared to the conventional recovery of rare earth elements from ores, the recovery process from ashes can be more efficient because crushing and grinding are not necessary. Some methods for rare earth element recovery from coal fly ash have been suggested, for example, in the patent by Joshi *et al.*¹³ published in 2013, it is proposed that rare earth elements are leached from fly ash using nitric acid, followed by liquid-liquid extraction with tributyl phosphate (TBP) in kerosene and finally ion exchange. A considerable portion of the literature concerning rare earth element recovery is published in Chinese, and only the abstracts are available in English. According to the data from Chemical Abstracts of the American Chemical Society, the number of REE related publications from China has increased at a rapid pace during the last decade and has overtaken other countries in publication numbers.¹⁴ Translation of some Chinese articles has revealed that many articles lack proper background information, for example, on the reagents used, and offer no useful information on the REE recovery processes.¹⁵

2.2 Rare earth elements

2.2.1 Properties

Rare earth elements are a group of 17 chemically similar metallic elements (table 1) corresponding to scandium (atomic number 21), yttrium (39), and elements from lanthanum to lutetium (57-71). The latter subgroup (La-Lu) is called “lanthanoids” according to IUPAC nomenclature, but the term “lanthanides” is still used frequently. The abbreviation Ln is commonly used, and it refers to either lanthanoids or all rare earth elements; in this thesis, it is used to denote all rare earth elements. The terms rare earth (RE) and rare earth metal, or mineral (REM) are also used often in the place of rare earth element. Rare earth elements are sometimes divided into subgroups, and these divisions have a multitude of definitions and can cause confusion. Subgroups used in this thesis are as follows: light rare earth elements (LREEs), also known as the cerium group, which contains elements from lanthanum to gadolinium, and heavy rare earth

elements (HREEs), also known as the yttrium group, which contains elements from terbium to lutetium and yttrium. Scandium is not included in group classifications due to its deviating properties.¹⁶

The similarity of chemical properties between rare earth elements and their compounds is due to their electronic configuration (table 1). Scandium, yttrium, and lanthanum are the first elements in the series of transition elements (*d*-elements) with the ground state electronic configuration of $ns^2(n-1)d^1$ ($n=4, 5$ or 6). The 14 elements from cerium to lutetium are called the inner transition elements (*f*-elements) with the electron configuration of $6s^25d^14f^{n-1}$ or $6s^24f^n$. $5d$ and $4f$ orbitals are energetically very close to each other, which explains the filling order observed for Ce, Gd, and Lu.¹⁷

TABLE 1 Rare earth elements, their chemical symbols, atomic numbers, electronic ground state configurations, and usual oxidation states.¹⁷

Element	Symbol	Atomic number	Configuration	Oxidation states
Scandium	Sc	21	[Ar]4s ² 3d ¹	3
Yttrium	Y	39	[Kr]5s ² 4d ¹	3
Lanthanum	La	57	[Xe]6s ² 5d ¹	3
Cerium	Ce	58	[Xe]4f ¹ 6s ² 5d ¹	3, 4
Praseodymium	Pr	59	[Xe]4f ³ 6s ²	3, 4
Neodymium	Nd	60	[Xe]4f ⁴ 6s ²	3
Promethium*	Pm	61	[Xe]4f ⁵ 6s ²	3
Samarium	Sm	62	[Xe]4f ⁶ 6s ²	3, 2
Europium	Eu	63	[Xe]4f ⁷ 6s ²	3, 2
Gadolinium	Gd	64	[Xe]4f ⁷ 6s ² 5d ¹	3
Terbium	Tb	65	[Xe]4f ⁹ 6s ²	3, 4
Dysprosium	Dy	66	[Xe]4f ¹⁰ 6s ²	3
Holmium	Ho	67	[Xe]4f ¹¹ 6s ²	3
Erbium	Er	68	[Xe]4f ¹² 6s ²	3
Thulium	Tm	69	[Xe]4f ¹³ 6s ²	3, 2
Ytterbium	Yb	70	[Xe]4f ¹⁴ 6s ²	3, 2
Lutetium	Lu	71	[Xe]4f ¹⁴ 6s ² 5d ¹	3

*Radioactive

Many of the rare earth elements' chemical properties are a result of the lanthanoid contraction: the overall decrease in atomic and ionic radii as the atomic number increases from lanthanum to lutetium. There is a general consensus that the reason for this contraction is the incomplete mutual shielding of $4f$ -electrons. As a consequence of the shape of the orbitals, the electrons shield one another quite poorly, and when the atomic number increases, the effective nuclear charge felt by the electrons increases. This results in a steady decrease in size across the lanthanoid series. The similarity of yttrium to heavy rare earth elements is explained by similarities in outer electronic configuration and the lanthanoid contraction: atomic and ionic radii of lanthanides decrease close to yttrium's in the holmium to erbium range. Figure 1 illustrates the lanthanoid

contraction, but it should be noted that values for ionic radii increase with increasing coordination number and that there are no absolute values for ionic radii. Europium and ytterbium have much larger metallic radii than the other lanthanoids, which implies that they contribute fewer electrons to metal-metal bonding.¹⁷

Rare earth elements have low ionization potentials and are therefore highly electropositive and occur primarily as ionic compounds. This is the consequence of their valence shells consisting of deeply buried 4f orbitals, where the 4f electrons are not available for covalent bonding. All rare earth elements occur at oxidation state +3 in solutions and solid compounds, and some REEs also occur at +2 and +4 states. This is due to the special stability of empty, half-filled, and full *f*-shell; hence, Ce⁴⁺ and Tb⁴⁺ (*f*⁰ and *f*⁷) and Eu²⁺ and Yb²⁺ (*f*⁷ and *f*¹⁴) can occur. The properties of di- and tetravalent cations are clearly different compared to the trivalent cations, which allows them to be easily separated from other REEs using selective oxidation or reduction.¹⁶

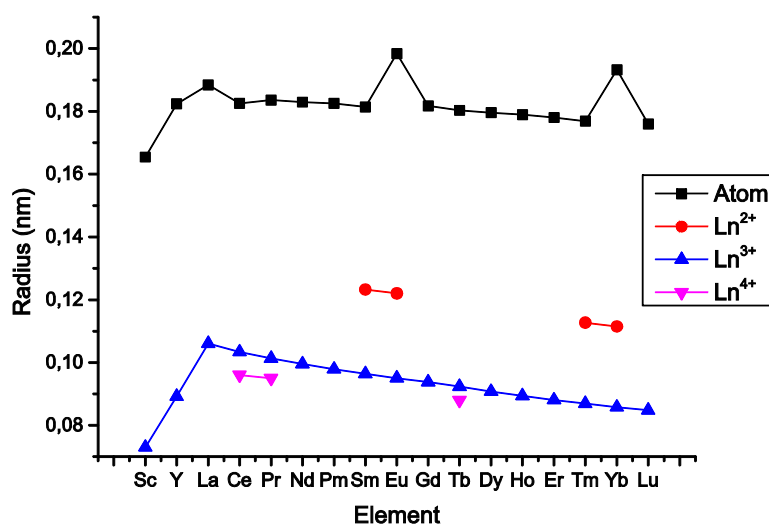


FIGURE 1 Radius of rare earth element atoms and ions displaying the lanthanoid contraction. Data for atoms: half the interatomic distance in room temperature, Ln²⁺; at coordination number 8 in difluorides, Ln³⁺; at coordination number 6, Ln⁴⁺; at coordination number 8 in dioxides.¹⁷

2.2.2 Compounds

In solutions and crystalline compounds, coordination numbers above 6 are typical for rare earth cations, except for scandium. Larger trivalent LREE cations occur usually at coordination numbers 8–10 and smaller HREE cations at coordination numbers 6–8.¹⁵ Aqua complexes are usually 9 coordinated.¹⁷

All rare earth elements form dihydrides in a reaction with molecular hydrogen, and most REEs also form trihydrides. These hydrides are typically non-stoichiometric. Dihydrides form mostly cubic structures; and trihydrides hex-

agonal. Dihydrides are metal conductors, except for YH_2 and EuH_2 , and as trihydride composition is approached, the materials begin to exhibit semiconducting properties. Hydrides formed by hydrogenation of binary LnM alloys (where M is a non-REE metal) can absorb and desorb significant amounts of hydrogen efficiently and reversibly, which gives rise to possible commercial applications as hydrogen storages.^{17, 18 p. 23}

Sesquioxides (Ln_2O_3) except for Ce, Pr, and Tb, are formed by oxidation of rare earth metals with oxygen at elevated temperatures, or by thermal or pyrohydrolytic decomposition of hydroxides, halides, and certain oxoacids. REE sesquioxides have high melting points (in the range of 2,200-2,400 °C) and high enthalpies of formation (-1,907.9 kJ mol⁻¹ for Sc_2O_3 , -1,661 kJ mol⁻¹ for Eu_2O_3). REE dioxides can only be prepared under strongly oxidizing conditions, except for CeO_2 , which is produced by air oxidation. EuO is the only easily obtained monoxide of the REEs, produced by reducing Eu_2O_3 . Other monoxides have been observed as metastable compounds or stable compounds under extreme conditions, such as high pressure.¹⁷

Hydroxides $\text{Ln}(\text{OH})_3$ are obtained as hydrates when ammonia or other bases are used to precipitate Ln^{3+} . $\text{La}(\text{OH})_3$ is a sparingly soluble strong base, and the base strength and solubility decrease in the series towards $\text{Lu}(\text{OH})_3$. These properties are utilized in several rare earth element separation processes. Hydroxides react with carbon dioxide to form basic carbonates. Furthermore, the precipitation of Ln^{3+} ions by solutions of alkali metal carbonates yields the sparingly soluble hydrated or basic carbonates. There is little knowledge on rare earth element peroxides, only Ce peroxide is known.¹⁷

REE sulfates crystallize from solution as octahydrates, except for La which forms nonahydrate. Hydrated sulfates can be thermally decomposed to anhydrous form, which is fairly soluble. REE sulfates are of industrial importance due to sulfuric acid's use in digestion of REE ores. Double sulfates $\text{Ln}_2(\text{SO}_4)_3 \cdot \text{Na}_2\text{SO}_4 \cdot n\text{H}_2\text{O}$ are important in separating LREEs from HREEs.¹⁷

Rare earth elements react with nitrogen to give nitrides. A slow reaction occurs between rare earth elements and nitrogen at 1000 °C, and when ammonia is used at 700 °C, the reaction occurs more quickly. REE nitrides form cubic structures, and they have very high melting points and decomposition temperatures.^{18 p. 23} They are ionic compounds with metallic conductivity or semiconductors. Nitrides are sensitive to hydrolysis, except for ScN , and have to be handled in a moisture-free environment. Rare earth element nitrates crystallize as hydrates $\text{Ln}(\text{NO}_3)_3 \cdot n\text{H}_2\text{O}$ from dilute nitric acid solution.¹⁷ Nitrates are very soluble in water, are moderately soluble in certain organic solvents, and have important applications in rare earth element separation using liquid-liquid extraction. Certain double nitrates have been used in rare earth element fractional crystallization.¹⁷

All rare earth elements except for europium form trihalides (LnX_3), where X is F, Cl, Br, or I. Sparingly soluble trifluorides are obtained from aqueous solutions by precipitation with hydrogen fluoride. Trichlorides crystallize as hexa- or heptahydrates by carefully evaporating rare earth element's hydrochloric

acid solutions. Anhydrous trichlorides are very soluble in water and certain organic solvents. Tribromides and triiodides are formed in the same way as chlorides. Tetrafluorides of Ce and Pr are the only tetrahalides that occur. Many dihalides have been prepared, and they are either salt-like compounds or compounds with a metallic character. Thermodynamically stable difluorides are known only for Eu, Sm, and Yb.¹⁷

Rare earth elements form a variety of chalcogenides, and they have a wide range of structural, electrical, and magnetic properties. Most REE chalcogenides are very sensitive to hydrolysis; and can only be handled and prepared in moisture-free conditions. Several carbides are known for the rare earth elements (LnC_2 , Ln_2C_3 , Ln_2C , Ln_3C_4)^{18 p. 24}, and they can be synthesized directly from the elements.¹⁷ The largest carbide group is dicarbides, which are high-melting, highly involatile metallic conductors. They typically crystallize in a tetragonal structure.¹⁷

Rare earth elements resemble the elements of group 2 more than 3d transition elements when REE complex forming properties are considered. The reason for this behavior is the deeply buried 4f orbitals that are not available for forming hybrid orbitals, which could form covalent bonds. In addition, the large size of Ln^{3+} ion compared to other trivalent cations leads to smaller electrostatic forces of attraction. Hence, only very strong ligands are able to form thermodynamically stable REE complexes that are isolable. Technically important chelating agents in rare earth element separation include certain ketones and especially tributyl phosphate and 2,4-pentanedione (acetylacetonone).¹⁷

2.2.3 Applications

Rare earth elements and their compounds have a wide variety of applications in various fields of industry.¹⁶ Their demand has increased due to use in several high-technology applications, for example, phosphors for electronic displays, high strength permanent magnets, alloying agents in metallurgy, and applications in a number of renewable energy technologies.¹⁵ The most important applications of rare earths are in catalysts, metallurgy, magnets, electronics and in optical, medical, and nuclear technologies. Rare earth elements are not interchangeable in many of the applications, as a specific rare earth element is essential. The requirements of selected REEs in common applications are presented in table 2. For example, magnet and phosphor manufacturers require Eu and Tb, two of the least abundant REEs, for their applications, while petroleum catalysts manufacturers require La and Ce that are among the most abundant REEs.¹⁵

Rare earth elements are used in a variety of catalytic reactions. The oldest application is in oil cracking, where rare earth nitrates or chlorides are added into zeolite for improved gasoline yields and reduction in the formation of coke and light hydrocarbons. REEs are also used as catalysts in a number of other reactions. REEs' high affinity to oxygen and sulfur is utilized in metallurgy, where mischmetal (mixture of mainly Ce, La, and Nd) is employed to trap O and S since they deteriorate the properties of steel or cast iron. REEs are widely used in alloys to improve properties, and while mischmetal is commonly used

due to its affordable pricing; the use of pure rare earth metals results in better properties in the alloy. The first application of REEs in magnets was samarium in SmCo₅-magnets, but samarium's scarcity and high price limited its applications. The neodymium-iron-boron magnet (Nd₂Fe₁₄B) was developed in 1984 and has numerous applications, the most important being electric engines in hybrid and electric vehicles, wind turbines, and hard disk computer drives.¹⁷

The distribution of rare earth element end use in the United States in 2013 had catalysts as the most common (65 %) end use of rare earth elements. Metallurgy and alloys are also an important application of REEs with 19 % of the end use. REEs are also used in permanent magnets (9 %) and glass polishing (6 %) and various other areas of industry. Catalysts have gained more end use in the U.S. in recent years; in 2008, the most common use was metallurgy and alloys at 29 percent, while catalysts were only at 27 %.¹⁹ It should be noted that the data can be rather different in other countries.

TABLE 2 Rare earth element requirement percentages for different applications (modified from Long *et al.*²⁰, data originally from Lynas Corporation 2010).

Application	La	Ce	Pr	Nd	Sm	Eu	Gd	Tb	Dy	Y	Other
Magnets			23.4	69.4			2.0	0.2	5.0		
Battery alloys	50.0	33.4	3.3	10.0	3.3						
Metal alloys	26.0	52.0	5.5	16.5							
Auto catalyst	5.0	90.0	2.0	3.0							
Petroleum refining	90.0	10.0									
Polishing compounds	31.5	65.0	3.5								
Glass additives	24.0	66.0	1.0	3.0						2.0	4.0
Phosphors	8.5	11.0				4.9	1.8	4.6		69.2	
Ceramics	17.0	12.0	6.0	12.0						53.0	
Other	19.0	39.0	4.0	15.0	2.0		1.0			19.0	

2.2.4 Abundance

Although their name suggests that they are rare, REEs are moderately abundant elements in the earth's crust (table 3), for example, more abundant than common copper and zinc.¹⁸ pp. 58-59 They are, however, widely distributed in low concentrations, which in addition to difficult isolation processes during the time of their discovery is the reason for the term "rare". The first rare earth element was discovered in 1794 when a "new earth" was detected, now known as yttrium. By the turn of the 19th century, all naturally occurring rare earth elements had been found, and in 1947, the REE group was complete with the discovery of radioactive promethium using nuclear reactions. Rare earth elements occur in nature in association with each other, except for radioactive promethium, which occurs as a fission product of uranium or as a result of actions of cosmic rays. REE abundance follows the Oddo-Harkins rule: elements with even-atomic numbers are more stable and hence more abundant than the adjacent odd-

atomic number elements.¹⁶ The most abundant REE in the earth's crust is cerium (20–70 mg kg⁻¹), followed by neodymium and lanthanum, with heavier REEs being less abundant, and tulium being the least abundant rare earth element (0.2–1 mg kg⁻¹).^{18 p. 58}

Rare earth elements occur in nature in their oxidized form in salts and minerals due to their electropositive nature and high affinity for oxygen. Most rare earth element statistics are hence expressed as rare earth oxides (REO). Rare earth elements occur in a large number of minerals in oxidic compounds, such as oxides, carbonates, phosphates, and silicates. REEs are present as mixtures with 10–300 mg kg⁻¹ levels in many rock formations: basalts, granites, gneisses, shales, and silicate rocks.^{18 p. 59}

TABLE 3 Rare earth element's abundance (mg kg⁻¹) in the earth's crust (modified from Extractive Metallurgy of Rare Earths^{18 p. 58}).

Element	Abundance (mg kg ⁻¹)
La	5–39
Ce	20–70
Pr	3.5–9.2
Nd	12–41.5
Sm	4.5–8
Eu	0.14–2.0
Gd	4.5–8.0
Tb	0.7–2.5
Dy	4.5–7.5
Ho	0.7–1.7
Er	2.5–6.5
Tm	0.2–1
Yb	0.33–8
Lu	0.8–1.7
Y	28–70
Sc	5–22

2.2.5 Resources

The most important mineral resources for REEs are bastnäsite, monazite, and xenotime. Bastnäsite is a fluorocarbonate mineral (figure 2) containing approximately 70 % REO, of which the majority are lighter elements. Bastnäsite resources include a large deposit in Bayan Obo in China, and at Mountain Pass, California in the U.S. Bastnäsite has replaced monazite as the main mineral in REE recovery during the last 50 years due to production of the mines mentioned above. Monazite is a phosphate mineral containing mainly light rare earth elements and, unlike bastnäsite, 4–12 % of thorium and a variable amount of uranium.¹⁵ Monazite has been recovered from Van Rhynsdorp and Na-boomspruit in South Africa, from Colorado in the U.S., and from Bayan Obo in

China. Xenotime is an yttrium phosphate containing approximately 67 % REO, of which most are heavier elements. It is usually found with monazite as a minor component, but the concentration of HREEs makes it an important resource. Other important heavy rare earth element sources are ion-adsorption clays, where REEs are present as ions. Several other rare earth minerals have also been used or are in use for rare earth element recovery: apatite, brannerite, euxenite, gadolinite, loparite and uraninite.^{18 pp. 61-63}



FIGURE 2 REE minerals from left: bastnasite, monazite and xenotime with rutile.²¹⁻²³

While the world's REE resources are large (table 4), the availability of individual rare earth elements is highly polarized. The most important REE minerals are enriched with rare earths of low atomic number and depleted with rare earths of higher atomic number, hence making low atomic number REEs more available. In the U.S. Geological Survey Mineral Commodity Summaries¹, China is estimated to have the largest REO reserves of any single country, with 40 % of the world's REO reserves. The second largest reserves are in Brazil with 16 % of the estimated total, and the third largest are in United States with 10 %. There are, however, differences in resource estimates, and according to other data, China's REE reserves are 25 % of the world's total, while Brazil has the largest reserves with 37 %.²⁴

TABLE 4 Estimated rare earth mine production and reserves in tons and percentages in 2013.¹

Country	Reserves		Production	
	REO (t)	REO (%)	REO (t)	REO (%)
United States	13,000,000	9.5	4,000	3.6
Australia	2,100,000	1.5	2,000	1.8
Brazil	22,000,000	16.1	140	0.1
China	55,000,000	40.4	100,000	89.5
India	3,100,000	2.3	2,900	2.6
Malaysia	30,000	0.0	100	0.1
Russia	*		2,400	2.1
Vietnam	*		220	0.2
Other	41,000,000	30.1	NA	
Total	140,000,000		110,000	

* Included in other

NA Not available

2.2.6 Production

In the 1950s, rare earth elements were mined in South Africa, India, and Brazil. From the 1960s to 1980s, Mountain Pass mine in California was the largest global source of REEs. China began its large scale REE production in 1990s with cheaper prices, which led to the shutdown of several mines that were not able to compete with lower prices. Mountain Pass mine was also closed in 2002, leaving China as the major producer of REEs.²⁵ In 2013, China controlled the market with 90 % of the world's mine production (table 4).¹ Most of China's production comes from REE recovery as a by-product of iron ore mining in Bayan Obo.^{18 pp. 83-85} United States is the second largest producer with 4 % of the mine production, followed by India, Russia, and Australia. Other countries produce minor amounts of rare earth elements. In most deposits, REEs are recovered as co- or by-products of other minerals.¹⁶ This is due to the low concentrations in the reserves: in most cases, the mining and production costs cannot be compensated by the market value of rare earth elements. Only in Mountain Pass California were rare earth elements mined as primary products of a bastnäsite deposit. Large amounts of ore have to be processed to achieve small amounts of pure rare earth elements; for example, at Mountain Pass, one metric ton of ore produced 100 g of Eu_2O_3 , and as a by-product 200 g of radioactive thorium.¹⁶

The Chinese government has steadily limited its yearly export of REO in recent years due to resource depletion and environmental regulations.¹⁵ From 2009 to 2010, China's export quota decreased by 40 % from 50,150 to 30,250 tons.²⁶ China's export quota is estimated to be 32,000–35,000 t for 2011–2015.²⁴ The new quota system has evoked new producers to enter the REE market, although they face a lot of challenges: limited technical knowledge outside China, production of radioactive waste, high capital cost of a new processing plant, uncertainty of market price, and uneven demand for individual REEs.¹⁵

Rare earth elements were produced in Finland in the 1960s and 1970s at Typpi Oy's fertilizer factory in Oulu. The raw material was at first apatite from the Kola Peninsula, and later on a rare earth element concentrate recovered as a by-product from the Korsnäs lead mine, which is currently in the possession of Tasman Metals, Ltd. Other rare earth element deposits in Finland include Katajakangas and Kontioaho (Tasman Metals Ltd. has the prospecting rights) and Kuusamo's gold, copper, and cobalt deposit, where Dragon Mining company is investigating the possibility of recovering REEs as a by-product of gold ore. Several investigations are under way to open rare earth element mines in Finland, but currently, there is no REE production in Finland. By far the largest deposits in Fennoscandia are in Kola Peninsula, where REEs are being produced in the Karnasurt deposit.²⁷

2.2.7 Prices

Prices of REEs are not widely available but are found from selected producers. Prices are prone to fluctuations due to a few large producers and are not set like,

for example, with platinum group metals. There are two distinct phases in rare earth element price development: rare earth element production quantities increased up to 2007, lowering the average prices, and since 2007 the annual production has remained fairly the same at 134,000 tons, forcing the prices up.²⁶ REE metal and oxide prices in December 2013 and May 2014 from HEFA Rare Earth Canada Co. Ltd. are presented in table 5.²⁸ Prices for holmium, thulium, ytterbium, and lutetium were not available. Light REEs have the lowest prices, while the heavier are more expensive. Scandium has currently the highest price of the presented REEs.

TABLE 5 Rare earth metal and oxide prices (USD kg⁻¹) from HEFA Rare Earth Canada Co. Ltd. in December 2013 and May 2014.²⁸

Element and purity	Price USD kg ⁻¹	
	Dec. 2013	May 2014
La metal ≥ 99%	13	12.5
La oxide ≥ 99.5%	6.05	5.8
Ce metal ≥ 99%	12	12
Ce oxide ≥ 99.5%	5.5	5.5
Pr metal ≥ 99%	175	175
Pr oxide ≥ 99.5%	134	125
Nd metal ≥ 99.5%	94	95
Nd oxide ≥ 99.5%	69	68
Sm metal ≥ 99.9%	30	30
Eu oxide ≥ 99.99%	1,100	980
Gd metal 99.9%	95	95
Gd oxide ≥ 99.5%	44	41
Tb metal ≥ 99.9%	1,900	1,200
Tb oxide ≥ 99.5%	950	800
Dy metal ≥ 99%	750	600
Dy oxide ≥ 99.5%	525	500
Er metal ≥ 99.9%	225	215
Er oxide ≥ 99.5%	69	72
Y metal ≥ 99.9%	75	74
Y oxide ≥ 99.99%	20	19
Sc metal 99.9%	15,500	17,500
Sc oxide ≥ 99.95%	7,000	7,200
Mischmetal ≥ 99%	10	10

2.3 REE separation processes

Separation of rare earth elements from each other is based on the differences in acidities resulting from the lanthanide contraction. This gives rise to differences in the solubility of salts, hydrolysis of cations, and the formation of complex

species, which are the foundation of rare earth element separation processes. The occurrence of tetravalent (Ce, Pr, and Tb) and divalent (Sm, Eu, and Yb) cations allows them to be separated after selective oxidation or reduction. This is due to the distinctly different chemical behavior of tetra- and divalent cations compared to the trivalent species.^{16-18 pp. 17-18}

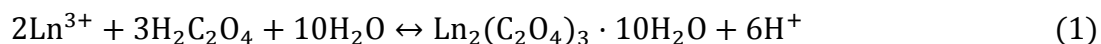
2.3.1 Fractional crystallization and precipitation

Fractional crystallization and fractional precipitation are the basic methods in REE separations, and were widely used in the twentieth century, but have now been replaced by ion exchange and liquid-liquid extraction.¹⁶

In fractional crystallization, a part of a salt in a solution is precipitated either by a temperature change or by evaporation of a saturated solution. The composition of the formed crystals is different compared to the original solution due to different solubilities of the components. The result is a crystal crop with fewer soluble components and a solution enriched with more soluble components. A number of REE salts and double salts have been used in separation with fractional crystallization. For example double ammonium nitrates have been used in lanthanum removal and to separate praseodymium and neodymium.^{18 pp. 161-162}

In fractional precipitation, a part of the rare earth elements are removed from the solution by the addition of a chemical reagent, which forms a less soluble compound. The rest of the REEs in solution are recovered by further precipitation as the same or different compound. Several compounds have been used in REE fractional precipitation, with hydroxides and double sulfates being the most widely used. For example, double chromate precipitation has been used to separate other rare earth elements from yttrium.^{18 pp. 162-163}

From concentrated rare earth element solutions with few impurities, rare earth elements can be precipitated as a group. This is usually preceded by some other concentration techniques, such as liquid-liquid extraction or ion exchange. The most common technique is to precipitate REEs as oxalates using oxalic acid. The reaction involved is the following:



After precipitation as oxalates, REEs can be thermally treated into oxides. Oxalate precipitation has been studied, for example, in rare earth element recovery from weathered clays.²⁹ Another widely used technique in REE group separation is precipitation as double-sulphates:



REE sulphates can further be converted to hydroxides. Double-sulphate precipitation has been investigated, for example, in rare earth element recovery from spent NiMH batteries^{30, 31} and monazite leach liquor³².

2.3.2 Ion exchange

Ion exchange is used to treat solutions with low concentrations of REEs and is used in applications where very high purity REEs are needed. Ion exchange was the most common separating technology in the 1950s, and the main commercial process used ammonium ethylene diamine tetraacetate as the complexing agent. Ion exchange was largely replaced by liquid-liquid extraction during the next decade, but it is still used in high purity applications.^{18 pp. 163-168}

In an ion exchange resin or an ion exchanger, there are negative or positive ions attached to an insoluble organic matrix. In a cation exchange resin, the ions are positive and in an anion exchange resin, they are negative. When the resin is brought into contact with a salt solution, the ions in the organic resin can be replaced by the ions in the solution. Typically, the ion with a higher charge displaces the one with a lower charge, and if the ions have the same charge, the ion with the larger radius displaces the ion with a smaller radius. Displacement also occurs according to the law of mass action.^{18 pp. 163-168}

After the adsorption stage, where the ions in the solution are loaded into the resin, the ions are desorbed from the resin into a solution in an elution stage. If a solution contains several ions that exhibit selectivity in the exchange, ion exchange can be called ion exchange separation. The distribution of a component between two phases has a constant value in equilibrium conditions. The distribution ratio D_A of component A in phases 1 and 2 is given in the equation:

$$D_A = \frac{c_{A1}}{c_{A2}} \quad (3)$$

where c_{A1} is the concentration of A in phase 1 and c_{A2} the concentration of A in phase 2. Similarly, for component B,

$$D_B = \frac{c_{B1}}{c_{B2}} \quad (4)$$

A comparison of D_A and D_B tells how the two components are distributed in the different phases. The relation of the distribution ratios is called the separation factor α :

$$\alpha_B^A = \frac{D_A}{D_B} \quad (5)$$

When the separation factor is close to 1, no separation can be achieved between components A and B, and when α clearly differs from 1, separation between components is possible.^{18 pp. 163-168}

In modern applications, typically sulfonated polystyrene or its Na^+ salt is used as a resin. The cations exchange with H^+ or Na^+ and are then removed from the resin utilizing a complexing agent, such as EDTA^{4-} . The formation constants of EDTA complexes increase from La to Lu, which allows for the separation to 99.9 % pure components.^{16, 17}

2.3.3 Liquid-liquid extraction

Liquid-liquid extraction, also called solvent extraction, is the most common technique used in rare earth element separation. Acidic, basic, and neutral extractants are the most common industrial extractants and include bis(2-ethylhexyl) phosphoric acid (D2EHPA), 2-ethylhexyl (2-ethylhexyl) phosphonate (EHEHPA), tributyl phosphate (TBP), versatic 911, versatic 10, and Aliquat 336 (figure 3). The behavior of these extractants is well-known and a widely published research area and some industrial extraction processes are also known such as the Molycorp process used in Mountain Pass California.¹⁸ pp.177-180

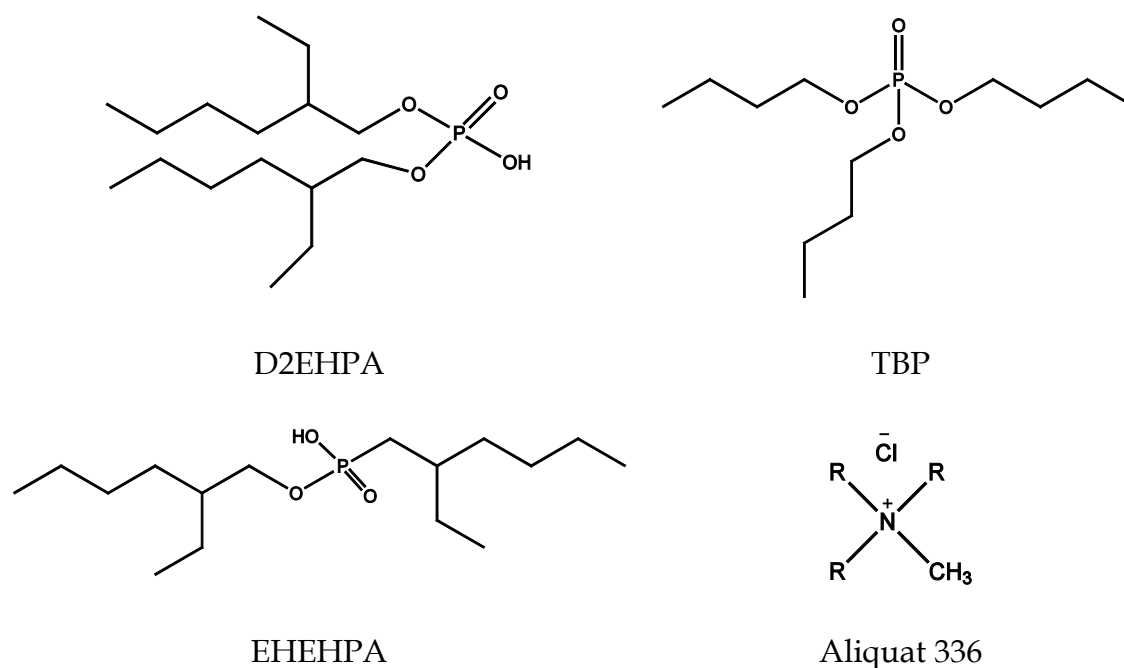


FIGURE 3 Structures of bis(2-ethylhexyl) phosphoric acid (D2EHPA), tributyl phosphate (TBP), 2-ethylhexyl (2-ethylhexyl) phosphonate (EHEHPA), and Aliquat 336 (R = C₈ or C₁₀ linear alkane chain).

In liquid-liquid extraction, two immiscible liquids are mixed, and the solutes are separated between the two liquid phases. One of the liquid phases is aqueous and the other organic. In the loading stage of liquid-liquid extraction, the solutes are transferred from the aqueous phase to the organic phase, which is scrubbed with a suitable aqueous phase to remove impurities transferred into the organic phase. In the following stripping stage, the solutes are removed from the organic phase back into an aqueous phase (figure 4). Distribution factor D and separation coefficient α presented earlier regarding ion exchange also apply to liquid-liquid extraction. Modern separation processes use liquid-liquid extraction due to its several advantages over other techniques. Some of the advantages are high loading of rare earths in the organic phase, which allows for

solutions with concentrations as high as 100-140 g REO l⁻¹ to be treated, and the use of continuous countercurrent processes. ^{18 pp. 168-177}

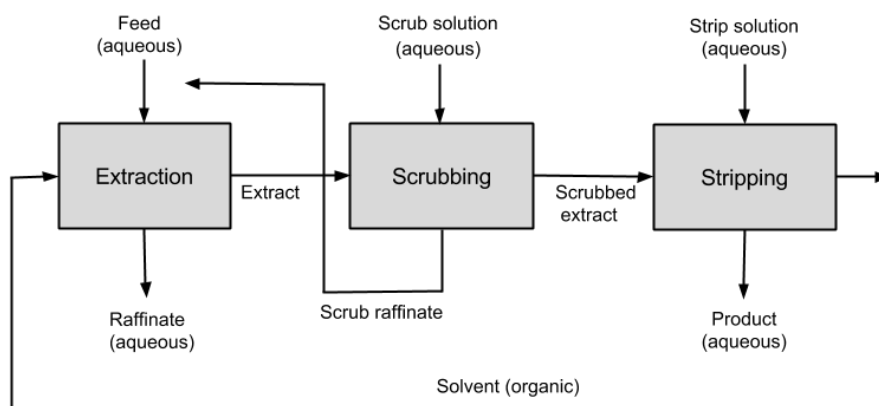


FIGURE 4 Flowsheet for typical liquid-liquid extraction process, modified from *Extractive Metallurgy of Rare Earths*.^{18 p. 168}

The organic phase used in liquid-liquid extraction usually consists of two or more chemicals. The extractant collects the rare earth elements in the organic phase, and a suitable solvent is used to dissolve the extractant, which is usually too viscous to be used on its own in practical applications. Kerosene and certain aromatics are commonly used as solvents. A modifier can also be added into the organic phase to improve the hydrodynamics of the system. The use of extractant mixtures can have synergistic effects on the distribution coefficient. This is the case when the distribution coefficient of a mixture is greater than the sum of the distribution coefficients of the extractants used.^{18 pp. 168-177}

Acidic extractants

Acidic extractants include organophosphorus acids, carboxylic acids, and naphthenic acids. They react according to the following cation exchange reaction:



The hydrogen in the extractant is usually displaced by the extracted metal, and a neutral organic soluble complex is formed. Extraction and stripping stages are, therefore, governed by the pH of the aqueous solution.^{18 pp. 168-177}

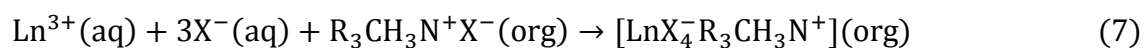
For organophosphorus acids, the extraction efficiency increases with increasing atomic number. A possible explanation for this trend could be the increase in electrostatic attraction between the extractant anion and the rare earth element cation, as the size of the cation decreases. The increase in solution acidity via liberation of hydrogen ions during metal loading has an adverse effect on metal extraction. This can be avoided by saponification of the extractant with sodium hydroxide. D2EHPA is the most widely available and studied extract-

ant of the organophosphorus acids.³³⁻⁴¹ It can be used in several aqueous media, and it gives suitable separation factors for all REEs, the average between two adjacent rare earth elements being 2.5. Distribution coefficients in D2EHPA increase with an increasing atomic number and decrease with increasing temperature. The distribution coefficient is also influenced by the diluent used with the organophosphorus acid and decreases in the following order: kerosene>cyclohexane>tetrachloromethane>xylene>benzene. Kerosene is the most common solvent used with organophosphorus acids.^{18 pp. 168-177} EHEHPA has replaced D2EHPA in many applications due to high separation factors between adjacent rare earths.^{33, 41-45} The extraction efficiency of rare earths in EHEHPA also increases with increasing atomic number as with D2EHPA, but not to the same extent.^{18 pp. 168-177} Other phosphoric acids have also been studied for rare earth element recovery.⁴⁶⁻⁴⁹

Carboxylic acids (C₇-C₁₅) are widely available extractants and also relatively inexpensive. The most common carboxylic acids used in REE liquid-liquid extraction are versatic acids R₁R₂(CH₃)CCOOH, where R₁ and R₂ are branched alkyl groups. Versatic 911 has 9 to 11 carbon atoms and versatic 10 has 10 carbon atoms.^{18 p. 174}

Basic extractants

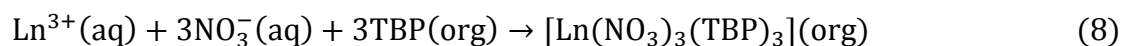
Basic extractants include long-chain quaternary ammonium salts R₃CH₃N⁺X⁻, where R₃ is a C₈-C₁₂ group and X is nitrate or thiocyanate. Basic extractants react with REE according to an anion exchange reaction:



The extent of extraction and stripping is dependent on the concentration of X⁻ in the aqueous phase. Extraction in thiocyanate and nitrate systems display interestingly different behaviors. In the thiocyanate system, the extraction efficiency increases with increasing atomic number, but in the nitrate system, the effect is the opposite. It is possible that steric and electrostatic effects influence the stability of several complexes and hence their extractability. The most common basic reactant is Aliquat 336. High purity yttrium is produced using a combination of ammonium salts and carboxylic acids in liquid-liquid extraction.^{18 p. 176}

Neutral extractants

Neutral extractants include phosphate esters, phosphonate esters, phosphinate esters, and phosphine oxides. The most used neutral extractant is tributyl phosphate (TBP),^{35, 50} which reacts according to the solvation reaction:



TBP works well in a nitrate medium, where 170-190 g REO L⁻¹ can be loaded into the organic phase. Separation factors for adjacent rare earth elements are in

the range of 1.2–2.2, making TBP and other neutral extractants less useful in separations than, for example, phosphoric acids.^{18 pp.168-177}

2.4 Industrial fly ash

2.4.1 Production and composition

Fly ash is one of the residues formed in combustion processes. Fly ash particles solidify while suspended in exhaust gases and are captured by electrostatic precipitators or bag filters. Coal fly ash is the most widely produced fly ash in the world with 750 million tons produced annually.⁶ Currently, biomass is emerging as a fuel resource since it is a source for carbon neutral energy, and it does not contribute to the greenhouse effect.⁵¹ At the present biomass contributes to 8–15 % of the world's energy supplies. Since the annual global growth of biomass is estimated at 112–220 billion tonnes, the potential for utilization is vast. There are no statistics on how much ash is generated in biomass combustion worldwide, but it was estimated that 480 million tons of biomass ash could be generated annually.⁵¹

Composition of fly ash varies considerably depending on the fuel used in the combustion process, but it mainly consists of metal oxides in different proportions. In table 6, the main components in coal fly ash, wood ash, and peat ash are presented. The main components in coal fly ash are in decreasing order: SiO_2 , Al_2O_3 , Fe_2O_3 , CaO , MgO , K_2O , Na_2O , and TiO_2 .⁶ The variation range in main components of wood ash is larger than that of coal fly ash, but it seems that biomass ash has a higher CaO content than coal fly ash. The water soluble fraction of biomass ash is high (up to 61.0 %) compared to 0.2–7.2 % for coal ash.⁵¹

TABLE 6 Weight percentage ranges of main components in coal fly ash from Europe⁶, wood ash and peat ash.⁵¹

Component	Weight %		
	Coal fly ash	Wood ash	Peat ash
SiO_2	28.5–59.7	1.86–68.18	37.53
Al_2O_3	12.5–35.6	0.12–15.12	20.14
Fe_2O_3	2.6–21.2	0.37–9.54	13.83
CaO	0.5–28.9	5.79–83.46	9.97
MgO	0.6–3.8	1.10–14.57	2.14
Na_2O	0.1–1.9	0.22–29.82	0.10
K_2O	0.4–4	2.19–31.99	1.12
P_2O_5	0.1–1.7	0.66–13.01	2.75
TiO_2	0.5–2.6	0.06–1.20	0.31
SO_3	0.1–12.7	0.36–11.66	12.11

In addition to the main components, fly ashes contain an extensive part of the periodic table in lower concentrations, usually including noteworthy concentrations of toxic elements. Fly ash morphology has been studied using scanning electron microscopy (SEM), which has revealed that fly ash consists of solid spheres, hollow spheres (or cenospheres), and irregularly shaped unburned carbon.⁶

2.4.2 Utilization

The coal fly ash utilization rate is at 47 % in Europe, while the remaining ash is used in mining restoration (45 %), disposed of (6 %) and stockpiled (2 %). In United States, 39 % of coal fly ash is utilized, while the global estimate is only 25 %. The complexity of fly ash is the foremost obstacle between large scale utilization. Coal fly ash use in Europe in 2008 is presented in figure 5.⁶

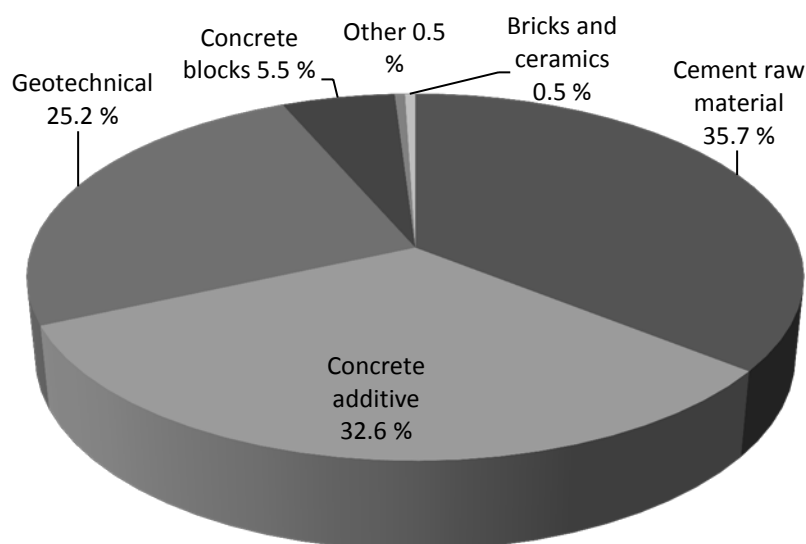


FIGURE 5 Coal fly ash use as percentages in Europe in 2008.⁶

Coal fly ash is mainly used as a substitute material in the construction industry. The use of coal fly ash in construction materials is prevalent, but the application of biomass ash is not yet as common and is prohibited by several standards. Coal fly ash also has geotechnical applications, for example, as an asphalt filler, pavement base course, soil amendment agent, and engineering or structural fill. Biomass ash has its largest application possibilities in soil amendment and fertilization. Biomass ash can provide nutrients and alkaline character to the soil, but at the same time, several problems can arise from its use: unavailability of nutrients, hazardous trace elements, ground water contamination, dust emissions, and so on. Use of semi-biomass ash, such as municipal solid waste ash and sewage sludge ash, is not recommended in soil amendment since the concentrations of hazardous components is usually high.⁵²

Future utilization possibilities for coal fly ash include use as an absorbent in removal of, for example, heavy metals and phenols from waste waters, use as a soil amelioration agent in agriculture, Al, Ti, Ge, and Ga recovery, use in catalysts, glass, etc. Fly ash has considerable adsorption capacity for several heavy metals and compounds, such as NH_3 , NO_x , PO_4 , SO_x , phenols, and pesticides.⁶ The major potential implementations of biomass ash are soil amendment and fertilization, in the construction industry and sorbents, and to a lesser extent the synthesis and production of minerals, ceramics, and other materials.⁵²

2.4.3 REE in fly ash

Rare earth element concentrations in coal fly ash have been investigated in detail, and there is comprehensive knowledge of their occurrence.⁵³⁻⁶⁷ Accumulation of REEs in coal fly ash in fairly high concentrations (table 7) has initiated a lot of research aiming at their recovery.^{7, 13, 68, 69} Some studies are available where rare earth element content has been determined in fly ash, where different fuels have been used: wood, wheat, and rice straw⁹, food scrap, animal waste, horticulture waste, sewage sludge⁸, medical waste,¹⁰ and municipal solid waste¹¹. Several studies focus on determining whether there could be harmful environmental effects due to rare earths by studying their leachability.¹² Utilization of these kinds of fly ashes as rare earth element resources has gained little attention due to low concentrations of REEs. The most common analysis technique in the determination of REE concentrations in different ashes has been ICP-MS^{8-11, 53, 56, 58, 60, 66, 67, 70}, while ICP-OES has been used occasionally⁶⁹ and instrumental neutron activation analysis (INAA), especially in publications dating a few decades ago^{9, 55, 59, 61-65}.

Zhang *et al.*⁸ determined rare earth element concentrations in several ashes by digesting the samples in a Teflon beaker using nitric acid, perchloric acid, and hydrofluoric acid. Rare earth element concentrations were determined using ICP-MS, resulting in 53.7 mg kg⁻¹ of REEs in food scrap ash, 80.9 mg kg⁻¹ in animal waste ash, 101 mg kg⁻¹ in horticulture waste ash, 130 mg kg⁻¹ in sewage sludge ash, and 83.1 mg kg⁻¹ in incinerator bottom ash. Compared to concentrations in the crust, food scrap ash was enriched with Sm, Eu, Tb, Sc, and Gd, and incinerator bottom ash was enriched with Eu and Tb. Other REEs were fairly normally distributed.

Zhao *et al.*¹⁰ studied medical waste ashes using the same digestion method as Zhang *et al.*⁸ and determined rare earth element concentrations in the samples using ICP-MS. Analysis of the ash samples resulted in total rare earth element concentrations of 42.0–78.9 mg kg⁻¹ in bottom ash samples and 10.2 mg kg⁻¹ in a fly ash sample. Concentrations of Gd and La were enriched compared to concentrations in the crust, the most likely reasons being the use of gadolinium as a chelating agent in the medical field and lanthanum as a glass additive in medical instruments and in some drugs. According to the sequential extraction performed on the ashes, REEs were mostly present in the residual fraction (47.0–87.7 %), and to a lesser extent in the organic fraction (1.8–31.9 %).

TABLE 7 REE concentration range in coal fly ashes from United Kingdom, Poland, and China.^{53, 67}

Element	Concentration range (mg kg ⁻¹)
La	41.9-110
Ce	86.6-225
Pr	9.4-27
Nd	37.2-106
Sm	7.1-20
Eu	2.0-4.1
Gd	7.4-20.1
Tb	1.2-2.8
Dy	6.9-15.8
Ho	1.4-3.1
Er	3.7-9
Tm	0.5-1.3
Yb	3.4-8.4
Lu	0.5-1.2
Y	37.3-86

In a report for the California Energy Commission, Thy *et al.*⁹ examined several ashes and determined rare earth element concentrations using INAA for Sc and ICP-MS for the other REEs. Samples were dissolved using microwave-assisted digestion with nitric acid, hydrochloric acid, and hydrofluoric acid. Total REE concentrations of 0.6–33.2 mg kg⁻¹ were determined in wheat and rice straw ashes, 87.9–90.0 mg kg⁻¹ in straw blend ashes, 17.3 mg kg⁻¹ in cattle manure ash, 9.5–91.2 mg kg⁻¹ in wood ashes, and 81.8 mg kg⁻¹ in a biomass ash from a commercial plant in California. Concentrations in ashes show considerable variations between different biomass types and also among similar samples.

The average content of rare earth elements in coal fly ash is 400 mg kg⁻¹, but coal ashes with REE concentrations higher than 1,000 mg kg⁻¹ are common; even concentrations as high as 17,000 mg kg⁻¹ of REEs have been reported in coal ash.⁷ Rare earth elements appear to be concentrated on the smaller size classes in coal fly ash^{53, 56}, which may offer routes for concentrating REEs. Rare earth oxide content of 1,000 mg kg⁻¹ has been suggested to be the cut-off grade for profitable utilization.⁷ Another criterion for utilization-suitable fly ash is that it should be abundant in critical REEs and have few excessive elements, such as cerium. Rare earth elements are classified according to Seredin⁷¹ as critical: Nd, Eu, Tb, Dy, Y, and Er; uncritical: La, Pr, Sm, and Gd; and excessive: Ce, Ho, Tm, Yb, and Lu.

There are two possible deposition routes for rare earths into fly ash: surface deposition, where rare earth elements are vaporized during combustion and are then deposited on the fly ash particles, or accompaniment, where rare earth elements melt with the ash components and are distributed into the fly ash. A study by Kashiwakura *et al.*,⁷⁰ where europium has been used to model rare earth elements suggests both types of occurrences. Wavelength-dispersive

spectrometry electron microprobe analysis on cerium occurrence in coal fly ash by Hower *et al.*⁵⁴ also supports this assumption. It has an important effect on dissolution of rare earth elements from fly ash: rare earth elements deposited on the surface of the fly ash are easily dissolved, but rare earth elements inside the fly ash particles are dissolved more gradually.

2.5 ICP-OES

2.5.1 Introduction

ICP-OES, also called inductively coupled plasma-atomic emission spectrometry (ICP-AES), is one of the most popular techniques in elemental analysis due to its simultaneous multi-element detection, wide dynamic range, and ability to measure most elements in the periodic table (elements from Li to U except for C, N, O, and the noble gases). High throughput of up to 60 elements in one minute is one of the key factors in making ICP-OES so common in modern laboratories.^{72 pp. 2-3} Compared to its main competitor ICP-MS, an emission based technique is more affordable, can withstand higher dissolved solid content, and is easier to use, but on the other hand, ICP-MS has lower detection limits in most cases and is able to measure isotopes.

Inductively coupled plasma is used to excite the atoms in the sample to emit light. The plasma is generated in a quartz torch using most commonly argon gas to form the plasma. Radio frequency of 27 or 40 MHz is applied around the quartz torch traditionally with an induction coil, or newly developed Flat Plates™⁷³, and a high voltage spark is given to produce “seed” electrons and ions. In the high temperature of the plasma, which can reach 10,000 K in the hottest zone, most elements are ionized. The plasma can be viewed two ways: radially from the side of the plasma or axially from the end of the plasma along the analyte channel.^{72 pp. 32-34} Radial viewing was used in ICP instruments before axial measurement, which was developed to improve sensitivity by following the analyte signal for a longer distance. Axial viewing of the plasma improves detection limits but increases the amount and severity of spectral interferences.^{72 pp. 11-17}

Sample is commonly introduced into the plasma as a fine aerosol, i.e. a mixture of liquid droplets and argon gas, called nebulizer gas or carrier gas. The sample aerosol is produced in the nebulizer as the nebulized gas passes through the nebulizer and spray chamber. Larger droplets and droplets with high velocity are removed into the drain in the spray chamber, to allow only the right size aerosol to reach the plasma. Auxiliary gas is used to push the plasma away from the injector tip if necessary and prevent deposition of solid particles on the tip. The cool tail of the plasma is removed using a shear gas in order to reduce interferences in axial viewing.^{72 pp. 39-55}

When the sample aerosol is introduced into the plasma through the injector, the solvent is evaporated, solid particles are vaporized, chemical bonds are

broken, and atoms are formed. Most elements are also ionized and further excited to emit light. The ionization energy of argon is 15.68 eV, and while most metals have ionization energies of approximately 7–8 eV, excess energy is used to further excite the ions. The excitation is very short-lived lasting only 10^{-8} s, and when the system returns to a lower energy state, the energy difference between the two states is released as a photon. The wavelength of the photon is specific for each element, and this is how different elements can be differentiated. Most wavelengths are in the ultra violet and visual range, and some instruments have different detectors for the specific ranges. Atomic and ionic transitions are separated by the use of Roman numeral I for atomic transition and II for ionic transition. The possible transitions occurring in the plasma for one single element are numerous, and this allows one to measure the element at several different wavelengths but also makes the spectra more complex.^{72 pp. 18-24, 74 pp. 2-11}

The wavelengths are separated from each other using a diffraction grating after which they are directed into the detector(s). Modern instruments use charged-coupled device (CCD) detectors, where pixels convert incoming photons into electrical charges, the same principle as in digital cameras. The computer then compares the emission intensity of the sample to the calibration standards and calculates the concentration in the sample.^{72 p. 65}

2.5.2 Optimization of measurement conditions

Method development for ICP-OES includes selection of sample introduction system, plasma conditions, appropriate wavelengths, background correction points, and correction of possible interferences.^{72 pp. 99-101}

Sample introduction

Selection of appropriate nebulizer and spray chamber for a given application is crucial in achieving accurate results. The nebulizer is used to produce an aerosol from the liquid sample and argon gas. Most common nebulizer types are pneumatic concentric nebulizer and cross-flow nebulizer, which are in use in most ICP-laboratories. Other nebulizer types are also available, such as micro-nebulizers designed to operate at low liquid flow rates^{75, 76}, and nebulizers for the analysis of samples with high dissolved solids content.^{77 pp. 1-76}

Spray chamber is used adapt aerosol properties to requirements of the plasma. The main goal is to separate coarse droplets from the primary aerosol, which results in a maximum analyte transport efficiency of about 2–4 %. Most widely used spray chambers are the double-pass spray chamber and the cyclonic spray chamber. Double-pass spray chamber is efficient in removal of coarse droplets but has high loss of aerosol, more memory effects and long rinsing times. Cyclonic spray chamber has less aerosol loss leading to higher signals and better limits of detection, has low memory effects, and short rinsing times, but the signal can be noisier and the position of nebulizer tip is critical. The

conventional cyclonic spray chamber is made out of glass, but for hydrofluoric acid applications, PTFE has also been used as a material for cyclonic spray chambers⁷⁸. Other available spray chamber options are single-pass spray chamber, and low inner volume spray chamber.^{77 pp. 77-118}

Robustness of plasma

Argon ICP has a high kinetic temperature, yet energy transfer in the plasma can still be inefficient, affecting the results when difficult sample matrices are analyzed.^{72 pp. 27-32} In robust conditions, energy transfer from the plasma to the sample is efficient, which ensures good excitation of analytes even in very complex sample matrices. Plasma conditions should, therefore, be optimized to achieve robust plasma, ergo conditions where the analyte signal is not significantly affected by the changes in the matrix composition (major elements, reagents, such as acids and solvents). In robust conditions, plasma temperature, electron number density, and species spatial distribution are not modified when different samples are introduced into the plasma. The attributes mentioned above are difficult to measure; hence, the intensity ratio of an elements ionic and atomic line can be used to estimate robustness.⁷⁹

The most common practice is to use the intensity ratio of Mg II (280.270 nm) and Mg I (285.213 nm) introduced by Mermet⁸⁰, while other intensity ratios have also been used successfully in the estimation of robustness. When Mg II/I ratio is 8 or higher, the plasma is considered to be robust. This applies to radial viewing of the plasma; when axial viewing is used, robust conditions can be achieved with a lower Mg II/I ratio. There is usually no need to compensate for different wavelength responses, except for when echelle grating is utilized. The two Mg lines can be in different diffraction orders or in different locations in the same order, which influences the diffraction efficiency. This can be compensated for by multiplying the ratio with a correction factor ϵ , which is the ratio of background emission measured at Mg I 285.213 nm and at Mg II 280.270 nm.⁸¹

Several instrument parameters have an effect on the robustness: plasma power, carrier gas flow rate, inner diameter of the injector, use of sheathing gas, presence of molecular gases, and viewing height when radial viewing is used. Optimization of these parameters using the Mg II/I ratio leads to robust plasma. Usually robust plasma conditions are achieved using a nebulizer gas flow rate below 0.6 l min⁻¹, plasma power above 1,400 W and an injector inner diameter of at least 2 mm.⁸⁰

Velitchkova *et al.*⁸² optimized ICP-OES operating conditions for REE determination in 10 g l⁻¹ Eu₂O₃ and Lu₂O₃ matrices. The Mg II (280.270 nm)/Mg I (285.213 nm) intensity ratio was used to evaluate the robustness of the plasma. The highest plasma power of 1,300 W and lower sheathing gas flow rate of 0–0.2 l min⁻¹ with a 0.4 l min⁻¹ carrier gas flow rate resulted in the highest Mg II/I ratio. In pure solvent, a line intensity ratio of 14 was achieved in robust plasma conditions, and in europium and lutetium matrices, the ratio was 11.5–12.5.

Wavelength selection

When selecting the analytical wavelength, the approximate concentration of the analyte in samples should be known. If the analyte is present in trace concentrations, the most sensitive line should be used. In wavelength tables, attributes, such as background equivalent concentration (BEC), signal to background ratio, and intensity, describe the sensitivity of the line. If high concentrations are expected, a less sensitive line can be used. It is also important to select a wavelength free of spectral interference caused by the sample matrix; consequently sufficient knowledge on the sample components is needed to identify interferences in the spectra. Resolution of the spectrometer determines whether there is spectral overlap in a specific line or not. In practice, it is preferred to select several wavelengths for one element and check if they are suitable. In simultaneous spectrometers, the available wavelengths are set, and the analyst can choose from these lines. When using a sequential or an array spectrometer, there is more flexibility in line selection but also more work in method development.⁷² pp. 101-118

Background correction

Background correction is used in ICP-OES to correct for the background emission present in all measurements. Background emission originates from argon emission lines and a continuum, which covers the whole wavelength range used. Matrix elements in the sample can increase the emission of the background or decrease it. An increase in background is observed when a matrix element has an intense emission line near an analytical line. The intensity of the background decreases when the sample being aspirated cools the plasma down. This is the case when the sample has high dissolved solids content, for example, a 10 % sodium chloride solution.⁷² pp. 125-134

Background correction is performed by setting background correction points on each side of the analyte peak. These points are measured with every sample run, and the area below the background correction points is subtracted from the net signal of the analyte. The use of only one background correction point can be justified when, on the other side of the analyte peak, the spectra is very complex with interference peaks. Great care should be practiced when choosing the positions of background correction points, as incorrectly setting the points could cause significantly erroneous results.⁷² pp.125-134 In some instruments, background correction can be done automatically via software.⁸³

2.5.3 Interferences

Interferences observed in ICP-OES technique are categorized as spectral and non-spectral, also called matrix effects. Spectral interferences can stem from matrix elements, argon emission lines (mostly in the range of 300–600 nm), carbon and silicon lines, and rotation oscillations of molecules, which produces a dis-

tinctive molecular band spectrum; for example, oscillations of OH radicals cause band spectra in the range of 280–330 nm. ^{72 pp.104-118, pp. 146-147}

Non-spectral interferences occur due to changes in sample transport, nebulization, and excitation conditions in the plasma. This can be caused by variations in physical properties of the sample, especially viscosity, density, surface tension and volatility. Acids present in most samples as a result of solid digestion, sample preparation, or analyte stabilization are a common cause of non-spectral interferences.^{84, 85} At acid concentrations below 1 % (v/v), an increase in the net intensity is observed, and with higher concentrations, a signal suppression is detected. The combination of two or more acids results in an effect more complex than the addition of single effects, depending on the nature of the interference.⁸⁵ Use of robust plasma conditions and cyclonic spray chamber can reduce the severity of acid effects.^{84, 86, 87} The presence of easily ionized elements (EIE) can also enhance or depress the analyte signal intensity. The effect of EIEs on ICP-OES is complex, and its origin is not yet clear.^{88, 89}

Acid effects on rare earth element line intensities were studied by Brenner *et al.*^{90, 91} It was found that all REE line intensities decreased similarly as the hydrochloric acid concentration in the sample increased. However with increasing nitric acid concentration, REE line intensities did not respond as a group, but instead, each line was suppressed to a different extent.⁹⁰ Differences in rare earth element ionization energies and oxide dissociation energies have been suggested as reasons for REE line intensities' different responses in the nitric acid matrix.⁹¹

Correction of spectral interferences

Spectral interferences can be corrected using inter-element correction or multivariate regression. Inter-element correction is used when there is direct overlap, and it applies only to a limited extent to partial overlap. An undisturbed wavelength of the interfering element is measured, and its contribution is subtracted from the analyte line with the interference. Use of this technique also increases the collective error of the analysis and hence leads to poorer reproducibility and limits of detection. Usually, in the case of direct overlap, it is better to use another more suitable wavelength if possible.^{72 pp. 135-136}

Multivariate regression is used to correct for partial overlap, and some ICP-OES manufacturers have their own techniques integrated in spectrometer software.^{92, 93} PerkinElmer was the first manufacturer to introduce a multivariate regression technique called "Multi-component Spectral Fitting" (MSF) in their software. This process includes analyzing a blank solution, single element solutions of all interfering elements, and a single element solution of the analyte. Scaling factors are used to calculate the concentration of the analyte rather than the intensity as is usually done. Because this correction method uses more spectral information than a normal measurement, the total error of the analysis decreases; thus, reproducibility and limits of detection are improved.^{72 pp. 136-146}

Correction of non-spectral interferences

Non-spectral interference can be corrected using several methods: matrix matching, use of an internal standard, calibration by analyte addition, addition of surfactants, or an ionization buffer. In the matrix matching technique, standard solutions are matched to the sample solutions or vice versa. If the samples are matched to the calibration standards, usually this is conducted by diluting the samples, which eliminates most of the non-spectral interferences. This is not always possible due to low concentrations of analytes in the samples. When calibration standards are matched to the samples, the acid matrix, digestion reagents and the main components in the matrix are added to the standards. This introduces a contamination risk to the standard solutions, and the components added in higher concentrations should be of highest purity.^{72 pp. 147-153}

An internal standard can be used to overcome non-spectral interferences when samples have lots of variation and dilution is not possible. Internal standardization can also be used to improve precision and long term stability. An element, or two or more elements, selected as an internal standard is added in the same concentration to all samples and standards. The changes in the intensity of the internal standard are used to correct intensities of the analyte.⁷² To achieve the best results with internal standardization, the analyte line and internal standard line should behave in the same way as changes in the measurement conditions occur. Utilization of robust plasma conditions improves the efficiency of internal standardization, which can be difficult in non-robust conditions, as interferences can arise from changes in sample transport as well as changes in the plasma.^{94, 95} Plasma viewing mode has also been found to factor in the effectiveness of internal standardization: radial viewing mode gives better results than axial viewing due to incorporation of atomization zone in axial viewing.⁹⁶

Calibration with analyte addition (also known as standard addition) allows optimum correction of non-spectral interferences but is very time consuming if there are lots of samples and analytes. In analyte addition, a known quantity or quantities of analyte is added into the sample, and the calibration is executed individually for all samples.^{72, 97}

2.6 Reliability of analytical results

All analyses contain errors to some extent. These errors can be divided into three categories: gross, random, and systematic errors. Gross errors are defined as serious deviations from the true value, and are very easily noticed. Gross errors can occur, for example, when an instrument is not working correctly. Random errors are present in all analyses and can be identified by carrying out several replicate analyses, where the results are spread evenly around the mean. There is a multitude of reasons for random errors from small changes in analytical conditions to human factors. Systematic errors change the analysis result

continuously in the same direction; consequently, the average result differs from the true value. The total systematic error of the analysis is called the bias.⁹⁸ pp. 3-4

In an ideal situation, the analytical results are accurate, i.e. true and precise. Trueness can be described as “closeness of agreement between the average of an infinite number of replicate measured quantity values and a reference quantity value”⁹⁹. Measurement precision is defined as “closeness of agreement between indications or measured quantity values obtained by replicate measurements on the same or similar objects under specified conditions”⁹⁹. Precision of a given result can be quantified using the standard deviation (s) of replicate analyses:

$$s = \sqrt{\frac{\sum_i (x_i - \bar{x})^2}{n-1}} \quad (9)$$

where \bar{x} is the average result of the replicate analyses, x_i is the numerical value for a single replicate analysis, and n is the number of replicates.⁹⁸ pp. 20-21 Variance or coefficient of variation also describe analytical precision,⁹⁹ and relative standard deviation (RSD) is commonly used to express variance as percentages.

Reference materials, or certified reference materials, can be used to evaluate the precision of analytical results. Designated properties of the reference material are accurately determined by a number of selected laboratories, and the uncertainties of the results are given at a certain level of confidence. There are reference materials available in numerous sample matrices, but the availability of especially certified reference materials is sometimes poor. It is useful to use several reference materials of different compositions in the development of an analytical method. The yield of obtained results compared to the reference material is usually given when the results are presented.¹⁰⁰

Recovery tests, also known as spiking, can also be used to ensure reliable analytical results. A known concentration of an analyte is added into the sample, and the concentrations in the spiked and original sample are determined. The recovery of the analyte addition can reveal bias in the analysis. The concentration of the addition is usually selected at the midway of the working range.¹⁰⁰

The sensitivity of an instrument is crucial when trace concentrations are analyzed. Sensitivity can be quantified by using the limit of detection (LOD): the lowest concentration of an analyte that gives a significantly different signal from the blank signal. There are several ways of calculating the limit of detection, and it is important to report how the value for limit of detection has been computed. One way of calculating the limit of detection is:

$$LOD = y_B + 3s_B \quad (10)$$

where y_B is the blank signal and s_B the standard deviation of the blank.⁹⁸ pp. 120-121 This technique has been used to calculate the limits of detection in this thesis.

3 EXPERIMENTAL

3.1 Samples

Several fly ash samples collected from energy wood incineration plants in Finland were analyzed during this work. Results are presented for A, B, C and D fly ash samples. All the incineration plants use mixed fuels containing energy wood and peat as a major fuel. Fly ash samples were collected with an electrostatic precipitator. Real fly ash samples were used throughout the process development presented in this thesis.

Coal fly ash standard reference material, SRM 1633b, certified by the National Institute of Standards and Technology (NIST) was used to confirm the accuracy of rare earth element concentration analysis. The concentrations of rare earth elements in SRM 1633b are informed as noncertified values only (table 8) and concentrations of Er, Pr, and Y are not informed.

3.2 Reagents

Ultrapure water of 18.2 M Ω cm resistivity was produced using Elga PURELAB Ultra Analytic, and was used throughout the work. Chemicals used in this study are collected in table 9.

Multi-element standard solutions of 10 mg l⁻¹ were supplied by PerkinElmer, and their composition is presented in table 10. Single element standard solutions for beryllium, magnesium, manganese and silicon (1,000 mg l⁻¹) were supplied by PerkinElmer. For iron, aluminum, potassium and sodium 10,000 mg l⁻¹ solutions were prepared from their inorganic salts and were used for adjusting the matrix of synthetic samples.

TABLE 8 Certified values for matrix elements in SRM 1633b and noncertified values for rare earth elements.

Certified values		Noncertified values	
Element	w-%	Element	mg kg ⁻¹
Al	15.05 ± 0.27	La	94
Ca	1.51 ± 0.06	Ce	190
Fe	7.78 ± 0.23	Nd	85
Mg	0.482 ± 0.008	Sm	20
K	1.95 ± 0.03	Eu	4.1
Si	23.02 ± 0.08	Gd	13
Na	0.201 ± 0.003	Tb	2.6
S	0.2075 ± 0.0011	Dy	17
Ti	0.791 ± 0.014	Ho	3.5
		Tm	2.1
		Yb	7.6
		Lu	1.2
		Sc	41

TABLE 9 Chemicals, their suppliers, and purities.

Chemical	Supplier	Purity/concentration
Ammonium hydroxide solution	Sigma-Aldrich	puriss p.a., approx. 25 % NH ₃
Bis(2-ethylhexyl)phosphate	Aldrich	97 %
Hydrochloric acid	Sigma-Aldrich	puriss p.a., ≥37 %
Hydrofluoric acid	AnalaR NORMAPUR	40 %
Kerosene	Sigma-Aldrich	reagent grade, low odor
Nitric acid	Sigma-Aldrich	puriss p.a., ≥65 %
Oxalic acid-2-hydrate	Riedel-de-Häen	≥99.5 %
Sulfuric acid	Sigma-Aldrich	puriss p.a., 95-97 %

TABLE 10 Multi-element standards supplied by PerkinElmer.

Multi-element standard, c(mg l ⁻¹)	Elements
Multi-element standard 1, 10 mg l ⁻¹	Ce, Dy, Er, Gd, Ho, La, Lu, Nd, Pr, Sm, Sc, Tb, Th, Tm, Y, and Yb
Multi-element standard 2, 10 mg l ⁻¹	Al, Ag, As, Ba, Be, Bi, Ca, Cd, Co, Cr, Cs, Cu, Fe, Ga, In, K, Li, Mg, Mn, Na, Ni, Pb, Rb, Se, Sr, Tl, U, V, and Zn
Multi-element standard 3, 10 mg l ⁻¹	B, Ge, Mo, Nb, P, Re, S, Si, Ta, Tl, W, and Zr

3.3 Instrumentation

Two PerkinElmer ICP-OES instruments were used in analyses conducted during this work. Majority of the analyses presented in this thesis, including the optimization of ICP-OES measurement conditions, were performed with the PerkinElmer Optima 8300 with a PerkinElmer S10 Autosampler. Instrument operating conditions are presented in table 11. The PerkinElmer Optima 4300DV with a PerkinElmer AS-90Plus Autosampler was used in the beginning of the study, mainly in the analysis of samples from early leaching studies and rare earth element precipitation experiments. Both axial and radial viewing measurement positions were aligned using Mn 257.610 nm emission line, with radial viewing height set at 15.0 mm. All rare earth elements were measured using axial viewing, while radial viewing of the plasma was used in the analysis of some of the matrix elements.

TABLE 11 Instrument description and typical operating conditions for PerkinElmer Optima 8300 used throughout the work.

Sample introduction	Cyclonic spray chamber with GemCone Low-Flow nebulizer, or Scott type double-pass spray chamber with cross flow nebulizer
RF-Generator	40 MHz FlatPlate™ (figure 6)
Torch	Quartz torch with an alumina injector, 2 mm inner diameter
Plasma viewing	Axial viewing: plasma central channel, radial viewing height: 15.0 mm
Grating	Echelle, ruling density of 79 lines per mm
Detectors	Two Segmented array, Charge-coupled device detectors, wavelength range: 165–782 nm
RF power (W)	1,500
Plasma gas flow rate (l min ⁻¹)	8
Carrier gas flow rate (l min ⁻¹)	0.6
Auxiliary gas flow rate (l min ⁻¹)	0.2
Sample introduction rate (ml min ⁻¹)	1.5
Integration time (s)	Automatic, 1–10
Replicates	3

Calibration of the ICP-OES instruments for rare earth element analysis was performed using four-point calibration. Solutions used for the calibration contained rare earth elements in the following concentrations: 0, 0.08, 0.40, and 2.00 mg l⁻¹ (diluted from multi-element standard solution 1 containing 10 mg l⁻¹ of REEs). Calibration solutions also contained 20 % (v/v) *aqua regia* as a matrix. The correlation coefficient of the regression was at least 0.9999. In order to test

the stability of the measurement, the calibration was checked periodically (each 15th sample) with the analysis of a standard solution. Internal standard (Be II 313.107 nm) was used mainly when analyzing liquid-liquid extraction samples. Selection of internal standard was done based on the lack of Be in fly ash samples and the use of ionic line, as all REE lines were ionic. Concentrations of matrix elements were determined using two-point calibration. This semi-quantitative analysis contained 40 elements and calibration was done using a blank solution and multi-element standard solutions 2 and 3, which contained 10 mg l⁻¹ of elements presented in table 10.

A Perkin Elmer DRCII ICP-MS was used to confirm rare earth element concentrations. The analyses were conducted at the University of Hull in the United Kingdom. SEM pictures and elemental analysis were performed using a Bruker Quantax400 EDS and Zeiss EVO-50XVP. Fly ash was attached onto carbon tape for imaging and analysis; hence, results for carbon in fly ash can be skewed. Particle size of fly ash was determined using a Fritsch analysette 22 economy. Fly ash was mixed with water to form a slurry for the laser-based analysis, where an integrated ultrasonic emitter is used to break down agglomerates.

3.4 Optimization of ICP-OES measurement

ICP-OES measurement for determination of rare earth element concentrations was developed by selecting appropriate wavelengths, calculating limits of detection, evaluating linearity of the working range, and assessing accuracy of the analysis using reference material NIST SRM 1633b. Several real fly ash samples were also analyzed, and results are presented as an example for one fly ash sample. *Aqua regia* and sulfuric acid matrices were used to determine robust plasma conditions, after which rare earth element recovery was examined in robust and non-robust plasma conditions using synthetic samples.

Several wavelengths were selected for each analyte, and on the basis of analysis of real samples, the background correction points were adjusted and inappropriate wavelengths removed. Final selection of wavelengths was done after application of standard addition technique, for ruling out the presence of systematic errors, and comparison analysis using ICP-MS. In standard addition, two different concentrations of rare earth elements were added into digested fly ash samples, and one sample was also prepared with no standard additions to be the blank solution. The concentrations of standard additions varied between 0.006-1.800 mg l⁻¹ for different rare earth elements, and were selected according to the concentrations present in real samples. Calibration was done individually for each sample, after which the linearity of emission intensity was evaluated. Linearity of emission signal was also estimated for external calibration, which was normally used in calibration of ICP-OES.

Reference material NIST SRM1633b was used to evaluate the accuracy of the measurement, and several real fly ash samples were analyzed to assess the

applicability of the new REE analysis method. The same sample preparation procedures and analyses were applied to reference material and real samples. Ultrasound- and microwave-assisted digestions were used in sample dissolution (section 3.5.1), after which the samples were analyzed with ICP-OES and ICP-MS. Trueness of the ICP-OES analysis was evaluated by comparing the results to informational concentrations in the certificate (table 8) and results by ICP-MS. Precision was assessed by calculating standard deviations for three replicate samples.

Plasma robustness was optimized using two sample matrices, *aqua regia* and sulfuric acid, that represent most of the samples analyzed in this thesis. *Aqua regia* tests were done using *aqua regia* leachate of fly ash, which had been diluted in order to get magnesium's concentration to a suitable level. Matrix elements were added to the diluted sample to match the concentrations in real samples. Sulfuric acid tests were done using five synthetic samples, which had different sulfuric acid concentrations: 0.01, 0.10, 0.30, 0.50, and 0.70 mol l⁻¹. Synthetic sulfuric acid samples contained main matrix elements found in sulfuric acid ash leachates (table 12) and also beryllium as an internal standard.

Robustness of the plasma was determined by measuring the intensities of magnesium's ion and atom lines and comparing their ratio: Mg II (280.270 nm)/Mg I (285.213 nm). Robust plasma conditions can be reached with a Mg II/Mg I line intensity ratio of 8 or higher. Plasma power and nebulizer gas flow rate have a significant effect on the robustness, and their effect was studied by keeping plasma power at 1,300/1,400/1,500 W and by varying nebulizer gas flow rate between 0.4–0.9 l min⁻¹. Sample introduction was carried out using either a Scott type double-pass spray chamber with a cross flow nebulizer or a cyclonic spray chamber with a GemCone Low-Flow™ nebulizer (figure 6). Measurements were performed using both axial and radial plasma viewing, and with a plasma gas flow rate of 8.0 l min⁻¹ and an auxiliary gas flow rate of 0.2 l min⁻¹.

TABLE 12 Element concentrations (mg l⁻¹) in synthetic sulfuric acid samples.

Element	Concentrations (mg l ⁻¹)
Ca	300
Fe	300
Al	100
Si	50
K	20
Na	10
Mn	10
Mg	5
Be	1
REEs	0.5

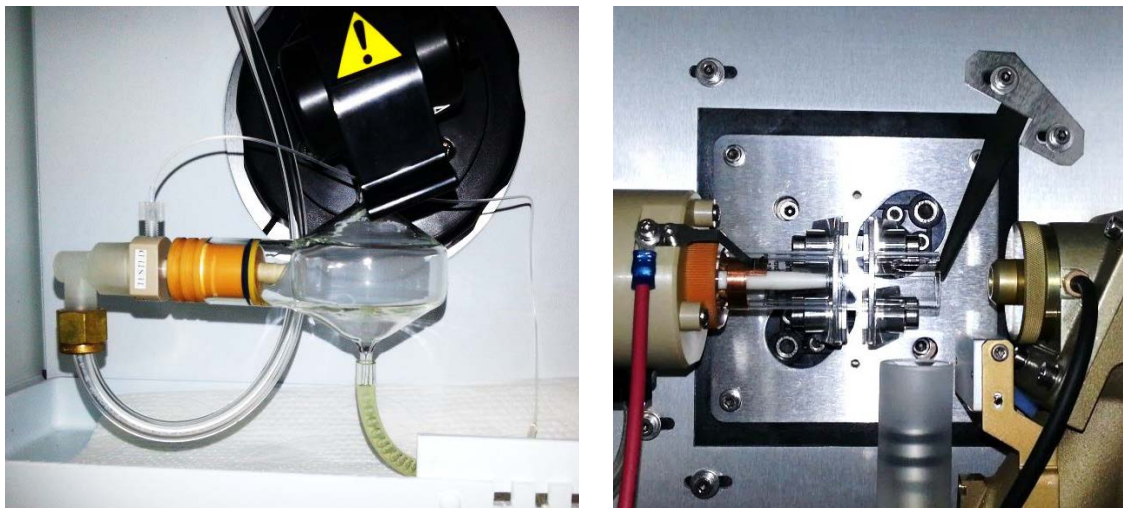


FIGURE 6 GemCone Low-Flow™ nebulizer with cyclonic spray chamber left and PerkinElmer Optima 8300 Flat Plate™ right.

Rare earth element recovery from synthetic samples was studied in robust and non-robust plasma conditions, which were determined according to the procedure described above. The aim was to compare these two operating conditions, and also to evaluate the trueness of the REE analysis using synthetic samples. Recovery tests were conducted for the same two sample matrices that were used in determining Mg II/I ratio, ergo *aqua regia*, and sulfuric acid. For the *aqua regia* recovery test, a synthetic sample with 20 % (v/v) *aqua regia* was used, and for the sulfuric acid recovery test a synthetic sample with a sulfuric acid concentration of 0.5 mol l⁻¹. Both samples also had elemental concentrations, as presented in table 12. Calibration standards contained the same acid matrices as the samples, 20 % *aqua regia* and 0.5 mol l⁻¹ sulfuric acid, respectively; otherwise, calibration was done as described in Section 3.3. Robust plasma conditions used here were as follows: a plasma power of 1,500 W and a nebulizer gas flow rate of 0.6 l min⁻¹; and non-robust conditions: 1,300 W and 0.8 l min⁻¹, respectively. Measurements were conducted using axial plasma viewing and with/without beryllium as an internal standard.

3.5 Experimental procedures

Experimental procedures presented here give a simplified introduction into the experimental work involved in this thesis. Numerous optimization tests were conducted during the development of fly ash processing techniques, and consequently, only the basic procedures with condition ranges are described in the experimental section. All the tests have been carried out with several fly ash samples to be certain that the procedures apply to a variety of ash samples independent of the batch.

Fly ash digestion has been performed using ultrasound- and microwave-assisted digestions, where the majority of the analytes in the sample are released into the solution. Total concentration of rare earth elements in fly ash has been determined using these digestions. These techniques were accepted as well-functioning and tested methods and were hence used without further development.^{101, 102}

Fly ash leaching procedure was developed and optimized in order to release the rare earth elements into solution without excess impurities. Leaching of rare earth elements from fly ash was done using dilute sulfuric acid as the leaching reagent. This was preceded by leaching the fly ash with an oxalate containing leaching reagent in order to dissolve other valuable components from the fly ash. The results presented here focus on the sulfuric acid leaching of the fly ash, while the oxalate leaching is beyond the scope of this thesis.

Rare earth element recovery from the sulfuric acid leachate was assessed using oxalate precipitation and liquid-liquid extraction. For both of these procedures, several sulfuric acid leachates of different fly ashes were used as samples. The sulfuric acid leachates for these tests were prepared using the optimized leaching procedure (section 4.4.5).

3.5.1 Digestion

Ultrasound-assisted digestion (modified from Ilander and Väisänen¹⁰¹)

A sample of about 500 mg was accurately weighed into a 50 ml plastic centrifuge tube, into which 2.0 ml of HNO₃, 6.0 ml of HCl and 0.5 ml of HF was added. The tube was closed and placed into a 650 W, 35 kHz, Model Transsonic 820/H ultrasonic water bath (ELMA, Singen, Germany) at a temperature of approximately 60 °C.

Procedure 1: The optimized sonication procedure lasted 9 minutes and was conducted in 3 minute intervals.

Procedure 2: The sample was sonicated for 3 minutes, then left to stand for 3 minutes, and then shaken by hand to prevent sedimentation. This was repeated six times altogether.

After the extraction procedure, the sample solution was filtered (Whatman No. 41) into a 50 ml volumetric flask and the filtrate diluted to volume with water. Rare earth element and matrix element concentrations were determined using ICP-OES.

Microwave-assisted digestion (modified from EPA-Method 3052¹⁰²)

A sample of about 350 mg was accurately weighed into a 100 ml TFM (tetrafluoromethaxil) vessel, into which 2.0 ml of HNO₃, 6.0 ml of HCl, and 0.5 ml of HF was added. After one hour, the sample was placed into an ETHOS PLUS microwave digestion system (Milestone, Sorisole, Italy) and heated with a digestion program containing the following steps:

- 1) Power 600 W (ramp time 5 min) for 5 min (5 bar) and

2) Power 1,000 W (ramp time 5 min) for 15 min (15 bar).

After digestion, the sample solution was filtered (Whatman No. 41) into a 50 ml volumetric flask and the filtrate diluted to volume with water. Rare earth element and matrix element concentrations were determined using ICP-OES.

3.5.2 Leaching

*Two-stage leaching*¹⁰³

A fly ash sample of about 1,000 mg was accurately weighed into a 50 ml plastic centrifuge tube. 20 ml of oxalic acid water solution was added into the tube with the ash sample, and the sample vessel was closed and placed in an ultrasonic water bath at a temperature of 25–75 °C. The sample was treated in the bath for at least an hour using ultrasound occasionally to expedite the procedure. The sample was then centrifuged at 3,500 rpm for 10 minutes with Thermo Scientific Heraeus Labofuge 400 Centrifuge. The oxalic acid leachate was removed from on top of the ash sample with a pipette and diluted to 50 ml volume with water in a volumetric flask. If ash particles were transferred with the leachate into the solution, it was filtered using Whatman No. 42 filter paper.

In the second leaching stage, 20 ml of leaching reagent containing 0.20–1.00 mol l⁻¹ sulfuric acid and 0–0.18 mol l⁻¹ nitric acid was added into the ash sample residue. The sample vessel was closed and placed in a heated ultrasonic water bath. The sample was treated in the water bath for at least 18 minutes with occasional application of ultrasound to facilitate the leaching process. After leaching, the sample solution was filtered using Whatman No. 42 filter paper into a 50 ml volumetric flask and diluted to volume with water. When larger volumes of leachate were required (for example in liquid-liquid extraction experiments), 10 g of ash sample was weighed into a 500 ml erlenmeyer bottle (figure 7), and the leaching reagent volumes were increased accordingly.

Rare earth element and matrix element concentrations were determined from the leachates using ICP-OES. The results are presented as leaching percentages: concentrations in leachate are compared to concentrations reached with ultrasound-assisted *aqua regia* digestion.

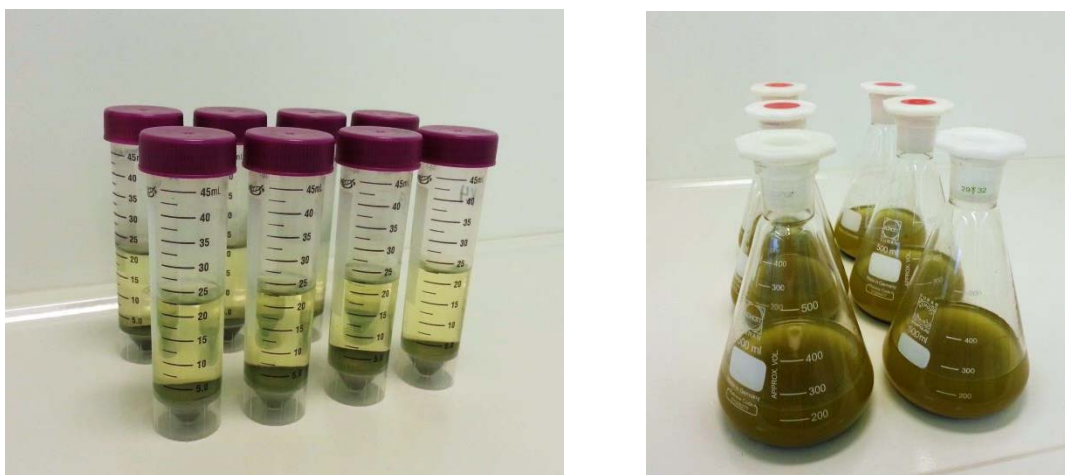


FIGURE 7 Two-stage ash leaching in centrifuge tubes and erlenmeyers.

Re-circulation of leachate

Two re-circulation studies were conducted, where sulfuric acid leaching was done after either an oxalic acid leaching or water wash. The first re-circulation experiment comprised of 10 rounds of two-stage leaching described earlier in this section. The same leachate (in the first stage: oxalic acid, in the second stage: sulfuric acid) circulated through 10 fresh fly ash samples. The leaching parameters used in the study are presented in table 13.

The second experiment consisted of four rounds of two stage leaching: first stage was leaching with water, and the second stage was sulfuric acid leaching. The leaching step with water was added to reduce basicity and impurities in the ash. Parameters used in the experiment are collected in table 13. Rare earth element and matrix element concentrations in leachates were determined with ICP-OES after rounds 1, 4, 7, and 10 in the first experiment and after rounds 1, 2, 3, and 4 in the second experiment. Leachates were diluted to 50 ml volume in a volumetric flask before analysis.

TABLE 13. Parameters used in re-circulation experiments.

Parameter	1 st experiment	2 nd experiment
Solid concentration	75 g l ⁻¹	75 g l ⁻¹
Volume of leachate	30 ml	20 ml
Concentration of sulfuric acid	0.5 mol l ⁻¹	1.0 mol l ⁻¹
Temperature of water bath	25 °C	25 °C
Leaching time	20 min	20 min

3.5.3 Precipitation

Precipitation experiments were performed using sulfuric acid leachate of fly ash as a sample.¹⁰³ Typically, 20 ml of leachate was pipetted into a 50 ml centrifuge

tube, into which an appropriate volume of oxalic acid solution was added. Using ammonia solution, the pH of the sample was adjusted to 1.0–3.0. The precipitation was visible as a drop of ammonia solution was added. The sample was transferred into a water bath at a temperature of 20–80 °C and stirred for 0–60 minutes. The sample was centrifuged at the speed of 3,500 rpm for 10 minutes, after which the solution was separated from the precipitate using a pipette. The precipitate was fully dissolved in 2 ml of *aqua regia* after a few minutes of ultrasonic treatment. Dissolved precipitate was diluted to a volume of 10 ml in a volumetric flask.

In a few tests, the oxalate precipitate was first dried in air and then calcined into an oxide in an oven at 800 °C temperature during 2 h. After calcination, the precipitate was dissolved using *aqua regia* as described above. Rare earth element and matrix element concentrations were determined from the original leachate, leachate separated from the precipitate and dissolved precipitate using ICP-OES. Results are presented as precipitation percentages, where the concentration in the precipitate is compared to the concentration in the original leachate.

3.5.4 Liquid-liquid extraction

The organic phase consisted of 2.5–40 % (v/v) D2EHPA in kerosene, with an altogether volume of 10 ml. Feed solution of 20 ml of sulfuric acid leachate, in which pH had been adjusted to 0.75–2.0 with an ammonia solution, was added into the separatory funnel with the organic phase. The mixture was shaken for 5–40 minutes and the phases were left to settle, after which the raffinate was drained from the funnel. Other A:O-ratios were also studied.

5 ml of 4–6 mol l⁻¹ mineral acid (nitric, hydrochloric, or sulfuric acid) was added into the separatory funnel, and the mixture was shaken for 5–40 minutes. The phases were left to separate, and the stripping reagent was drained from the funnel. Other A:O-ratios were also studied.

Rare earth element and matrix element concentrations were determined with ICP-OES from the original leachate, the raffinate, and the stripping reagent. Samples were diluted 1:5 with a matrix of 20 % (v/v) *aqua regia*. The results are given as extraction percentages for liquid-liquid extraction, where the concentration in the raffinate is subtracted from the concentration in the feed solution, and the result is compared to concentration in the feed solution (formula 11). Results for stripping are also presented as percentages, where concentration in the stripping solution is compared to the concentration in the feed solution ergo sulfuric acid leachate of fly ash.

$$\text{Extraction \%} = \frac{c(\text{feed solution}) - c(\text{raffinate})}{c(\text{feed solution})} \cdot 100 \% \quad (11)$$

4 RESULTS AND DISCUSSION

4.1 Development of REE analysis

In the beginning of the study several wavelengths were selected for rare earth elements' ICP-OES analysis (table 14). All REE wavelengths used are ionic lines due to rare earth elements' low ionization energies of 5.5–6.2 eV. During this work, one wavelength was selected for each element after taking into account sensitivity, lack of spectral interferences, and accuracy. Selected wavelengths are underlined in table 14.

The working range in REE analysis was 0–2.00 mg l⁻¹, which resulted in excellent linearity between emission signal and concentration: correlation coefficients of the external calibration^{98 pp. 111–114} are presented in table 14. Calibration was done using three calibration standards and a blank solution. Standard addition technique was used to evaluate the linearity of the emission signal in the real fly ash sample matrix. This allows systematic errors to be ruled out in the newly developed method. Analysis of the standard addition samples, blank and two standards with REE additions in the range of 0–1.80 mg l⁻¹, gave correlation coefficients of at least 0.999, except for erbium at 349.910 nm with a correlation coefficient of 0.9988. The emission intensity was found to behave linearly with the concentrations added into the samples.

Detection limits were calculated for REEs after each analysis according to formula 10, and typical values for LODs are presented in table 14. LODs are in the µg l⁻¹ range for all rare earth elements. All lines used were very sensitive especially with axial viewing, and detection limits restricted analysis only with a few elements, e.g. terbium and tulium, which were present in the fly ash in very low concentrations.

Precision of the ICP-OES measurement was evaluated according to analysis of real fly ash samples, where the RSD values of the instrument were assessed (table 14). Typical RSD values of the instrument were found to be between 0.60–2.73 % for all rare earth elements.

TABLE 14 Rare earth element wavelengths used in ICP-OES analyses (selected wavelengths are underlined), correlation coefficients of the external calibration, limits of detection (mg l^{-1}), and RSD (%) ranges.

Element	Wavelength (nm)	Correlation coeff.	LOD (mg l^{-1})	RSD (%)
La	<u>408.672</u>	0.999999	0.015	0.85–2.45
Ce	<u>413.380</u> , 413.764, 418.660	1.000000	0.008	1.34–2.53
Pr	414.311, <u>422.293</u>	1.000000	0.008	1.99–2.29
Nd	<u>406.109</u> , 430.358	1.000000	0.009	0.78–1.37
Sm	<u>359.260</u> , 388.529, 442.434	1.000000	0.011	1.18–2.22
Eu	<u>381.967</u> , 412.970	0.999985	0.021	0.60–1.69
Gd	335.047, <u>342.247</u>	1.000000	0.015	1.10–1.52
Tb	<u>350.917</u>	1.000000	0.011	1.13–2.40
Dy	<u>353.170</u>	0.999999	0.017	1.33–1.75
Ho	<u>339.898</u> , 345.600	1.000000	0.012	2.00–2.73
Er	<u>349.910</u>	1.000000	0.012	1.14–1.67
Tm	313.126, <u>346.220</u>	0.999999	0.013	0.95–2.15
Yb	<u>328.937</u> , 369.419	0.999989	0.008	1.03–1.75
Lu	<u>261.542</u> , 291.139	0.999993	0.003	1.89–2.41
Y	360.073, <u>371.029</u>	0.999992	0.022	0.85–2.45
Sc	<u>361.383</u> , 424.683	0.999996	0.024	1.20–2.53

The precision and trueness of rare earth element analysis were studied using standard reference material SRM 1633b. Digestion of reference material was conducted using ultrasound-assisted digestion and microwave-assisted digestion (as presented in 3.5.1), and rare earth elements were analyzed using ICP-OES and ICP-MS techniques. Informational concentrations were given in the certificate for selected rare earth elements.

The two analysis techniques resulted in similar concentrations for rare earth elements, but with LREEs (excluding cerium), ICP-MS is closer to informational values and with HREEs ICP-OES (table 15). This might be due to the increase in atomic number from lanthanum to lutetium, which affects m/z in the ICP-MS technique. Concentrations for scandium with ICP-MS are quite high compared to the informational value, and ICP-OES's results are closer to the values given in the certificate. It is possible that there is a systematic error present in scandium's ICP-MS analysis. Values given in the certificate are, however, only informational and cannot be considered as true values. It can be speculated that determination of rare earth elements from the reference material has been challenging, as the values are not certified but only informational. Concentrations of praseodymium, holmium, erbium and yttrium are not given in the certificate; hence, no comparison can be made, but results using ICP-OES and ICP-MS are similar for these elements.

When the two digestion methods are compared, microwave-assisted digestion seems to be slightly more efficient in dissolving REEs from the fly ash (table 15). This can be seen for both analysis methods used. Standard deviations are also slightly smaller when microwave-assisted digestion is used. The differ-

ences between digestion methods are, however, quite small. In comparison, the ultrasound-assisted digestion is significantly faster, and is done under atmospheric pressure, hence being safer than microwave-assisted digestion.

TABLE 15 REE mean concentrations and standard deviations (mg kg^{-1}) in NIST SRM 1633b ($n=3$) dissolved using two different methods, ultrasound and microwave, analyzed using ICP-OES and ICP-MS, and informational concentrations (mg kg^{-1}) for selected REEs.

Element	ICP-OES		ICP-MS		Informational
	Ultrasound	Microwave	Ultrasound	Microwave	
La	64±3	70±2	72±5	82±2	94
Ce	177±9	189±4	153±11	173±4	190
Pr	14.8±0.7	16.8±0.3	18.4±1.3	20.8±0.5	
Nd	68±4	78±2	73±5	82±3	85
Sm	14.5±0.5	17.4±0.8	15.5±1.2	17.4±0.8	20
Eu	4.0±0.1	4.8±0.1	3.7±0.3	4.0±0.2	4.1
Gd	17±1	22±1	16.5±1.0	18.4±0.6	13
Tb	2.7±0.2	3.5±0.3	2.6±0.2	2.9±0.3	2.6
Dy	13.1±0.5	13.7±0.4	10.0±0.7	10.2±0.4	17
Ho	<LOD	<LOD	2.7±0.3	3.0±0.2	
Er	7.5±0.3	7.7±0.3	7.3±0.7	8.1±0.4	
Tm	2.1±0.1	2.6±0.1	0.81±0.07	0.90±0.06	2.1
Yb	6.9±0.3	7.9±0.3	4.8±0.4	5.4±0.3	7.6
Lu	1.8±0.1	2.9±0.1	0.81±0.07	0.90±0.03	1.2
Y	67±2	70±1	71±4	75±2	
Sc	31±2	33±4	73±3	67±4	41

A similar assessment that was carried out to SRM 1633b was also administered on real fly ash samples collected from a Finnish power plant. Digestion methods were ultrasound- and microwave-assisted, and rare earth element concentrations were analyzed using ICP-OES and ICP-MS techniques. Concentrations determined using ICP-OES and ICP-MS are comparable except for praseodymium and scandium (table 16). In the case of praseodymium, it is not clear which of the results is closer to the actual concentration because there was no informational value given in the certificate in the case of analysis of NIST SRM 1633b. For scandium it can be said that analysis with ICP-OES results in concentrations closer to the actual values due to ICP-MS's overestimation observed in analysis of SRM 1633b. Microwave and ultrasound seem to be similarly effective in digesting wood/peat incineration fly ash, but microwave is slightly more effective for some LREEs such as lanthanum and cerium. Standard deviations are somewhat smaller when ultrasound is used.

TABLE 16 REE mean concentrations and standard deviations (mg kg^{-1}) in fly ash A ($n = 3$) dissolved using two different methods, ultrasound and microwave, and analyzed using ICP-OES and ICP-MS.

Element	ICP-OES		ICP-MS	
	Ultrasound	Microwave	Ultrasound	Microwave
La	39±2	42±3	49±3	53±3
Ce	98±2	104±5	92±4	100±5
Pr	2.4±0.2	2.1±0.4	11.4±0.5	12.3±0.8
Nd	39±3	42±3	43±3	47±3
Sm	8.5±0.3	8.2±0.6	8.0±0.5	8.5±0.8
Eu	2.2±0.1	2.4±0.2	2.0±0.1	2.2±0.3
Gd	10.1±0.4	10.7±0.6	8.2±0.5	8.7±1.2
Tb	2.1±0.1	2.0±0.2	1.2±0.1	1.2±0.3
Dy	<LOD	<LOD	4.6±0.3	4.6±1.1
Ho	<LOD	<LOD	1.2±0.1	1.2±0.3
Er	3.5±0.2	3.4±0.6	3.6±0.2	3.4±1.1
Tm	1.3±0.1	1.3±0.2	0.42±0.03	0.39±0.14
Yb	3.7±0.2	3.5±0.9	2.7±0.2	2.5±1.2
Lu	1.6±0.1	1.7±0.2	0.47±0.03	0.43±0.20
Y	28±2	29±2	31±2	24±15
Sc	10.0±0.4	10.7±0.4	44±2	47±10

Rare earth element concentrations in 10 fly ash samples were studied using ultrasound-assisted *aqua regia* digestion. The results are presented in table 17 with concentrations of REEs in coal fly ash^{53, 67} and in crust^{18 p. 58} for comparison. Most rare earth elements, especially the LREEs, are concentrated in peat/biomass fly ash compared to concentrations in crust. Only concentrations of Dy, Er, Yb, Y, and Sc in the measured ash samples are in the range of the crust or lower. In one analyzed fly ash sample, the total concentration of rare earth elements was up to 560 mg kg^{-1} , which might be high enough for profitable utilization. Rare earth element concentrations in coal fly ash are slightly higher or in the same range than in the samples analyzed here, except for Tb, Tm, and Lu, which have higher concentrations in peat/biomass fly ash.

TABLE 17 REE concentration range (mg kg⁻¹) in 10 peat/biomass fly ash samples, coal fly ash from United Kingdom, Poland, and China^{53, 67}, and in crust (modified from Extractive Metallurgy of Rare Earths^{18 p. 58}).

Element	Rare earth element concentration range (mg kg ⁻¹)		
	Peat/biomass fly ash	Coal fly ash ^{53, 67}	Crust ^{18 p. 58}
La	26-104	41.9-110	5-39
Ce	57-243	86.6-225	20-70
Pr	2.2-21	9.4-27	3.5-9.2
Nd	24-63	37.2-106	12-41.5
Sm	5.4-18	7.1-20	4.5-8
Eu	1.4-5.8	1.7-4.1	0.14-2.0
Gd	4.1-13	7.4-20.1	4.5-8.0
Tb	1.1-4.6	1.2-2.8	0.7-2.5
Dy	<LOD-7.8	6.9-15.8	4.5-7.5
Ho	<LOD-5.0	1.4-3.1	0.7-1.7
Er	2.3-6.7	3.7-9	2.5-6.5
Tm	1.3-5.3	0.5-1.3	0.2-1
Yb	1.9-6.4	3.4-8.4	0.33-8
Lu	0.9-4.8	0.5-1.2	0.8-1.7
Y	18-52	37.3-86	28-70
Sc	7.3-18	-	5-22

- Value was not given

4.2 Optimization of measurement conditions

4.2.1 Robustness of plasma with *aqua regia* samples

Robust plasma conditions were optimized for *aqua regia* samples using two *aqua regia* leachate samples: SRM 1633b fly ash and peat/wood incineration fly ash. There were no notable differences between the two leachate samples, and results for the peat/wood incineration fly ash leachate are presented in figure 8. Similar trends are observed for both cyclonic and the Scott spray chamber: radial viewing of the plasma gives higher Mg II/I ratios, and the increase in plasma power results in more robust plasma. This was to be expected based on literature and knowledge of the instrument construction. The optimum nebulizer gas flow is 0.5-0.6 l min⁻¹ when axial viewing is used and 0.6-0.7 l min⁻¹ using radial viewing.

The intensities of the Mg II line using axial viewing are presented in figure 9, where it is clearly seen that cyclonic spray chamber produces higher intensities than the Scott spray chamber. The intensity maximum for cyclonic spray chamber is approximately 27.3 million cps at a plasma power of 1500 W and a nebulizer gas flow rate of 0.5 l min⁻¹. For the Scott spray chamber, the maximum

is approximately 19.1 million cps at a plasma power of 1400 W and a nebulizer gas flow rate of 0.6–0.7 l min⁻¹. In trace element analysis, the cyclonic spray chamber is therefore a better choice as a sample introduction system. When the Scott spray chamber is used the decrease in nebulizer gas flow rate from 0.6 to 0.5 l min⁻¹ causes a dramatic drop in intensity. For the cyclonic spray chamber, the behavior is quite different: the drop in intensity occurs steadily when the nebulizer gas flow rate is increased toward 0.9 l min⁻¹.

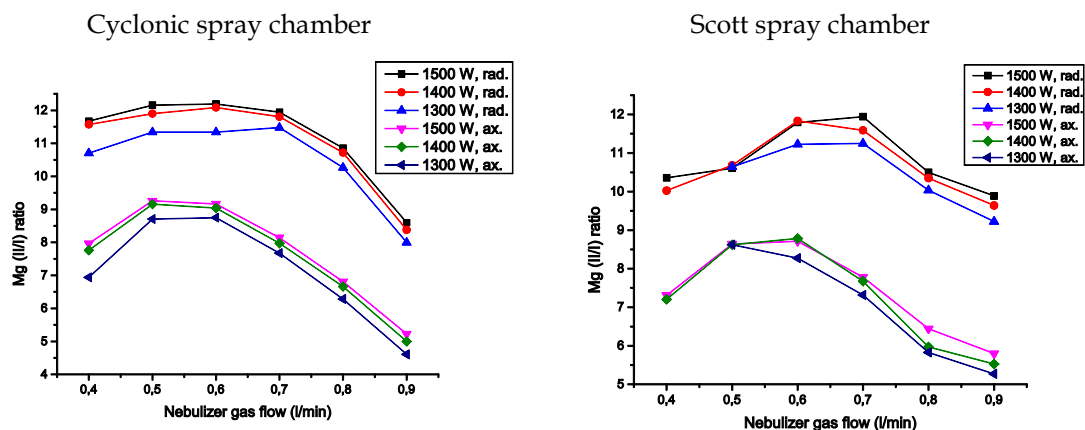


FIGURE 8 Magnesium II/I line intensity ratio as a function of nebulizer gas flow rate (l min⁻¹) with three different plasma power (W) settings and with radial and axial plasma viewing. Sample: *aqua regia* leachate of fly ash B containing approximately 5 mg l⁻¹ of Mg.

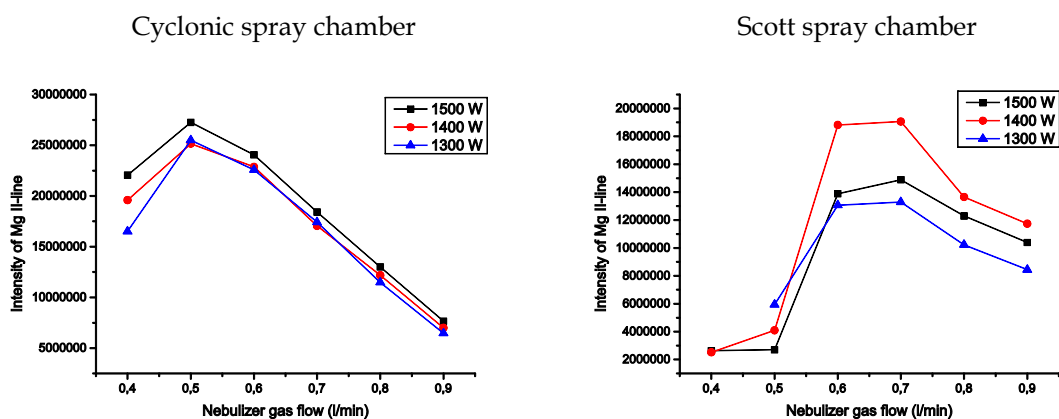


FIGURE 9 Magnesium II line intensity as a function of nebulizer gas flow rate (l min⁻¹) with three different plasma power (W) settings and axial plasma viewing. Sample: *aqua regia* leachate of sample B containing approximately 5 mg l⁻¹ of Mg.

4.2.2 Robustness of plasma with sulfuric acid samples

Robust plasma conditions were optimized for sulfuric acid solutions using five concentrations of sulfuric acid: 0.01–0.70 mol l⁻¹. Synthetic solutions also contained main elements found in ash leachates. The results were similar for all sulfuric acid concentrations studied, and graphs for sulfuric acid concentration 0.50 mol l⁻¹ are shown in figure 10. The graphs are quite similar for both sample introduction systems used, and the same trends are observed as with *aqua regia* samples: radial viewing and higher plasma power result in a higher Mg II/I ratio and, therefore, more robust plasma. Nebulizer gas flow rate results in the highest Mg II/I ratio at 0.5–0.6 l min⁻¹ with axial viewing and at 0.6 l min⁻¹ with radial viewing.

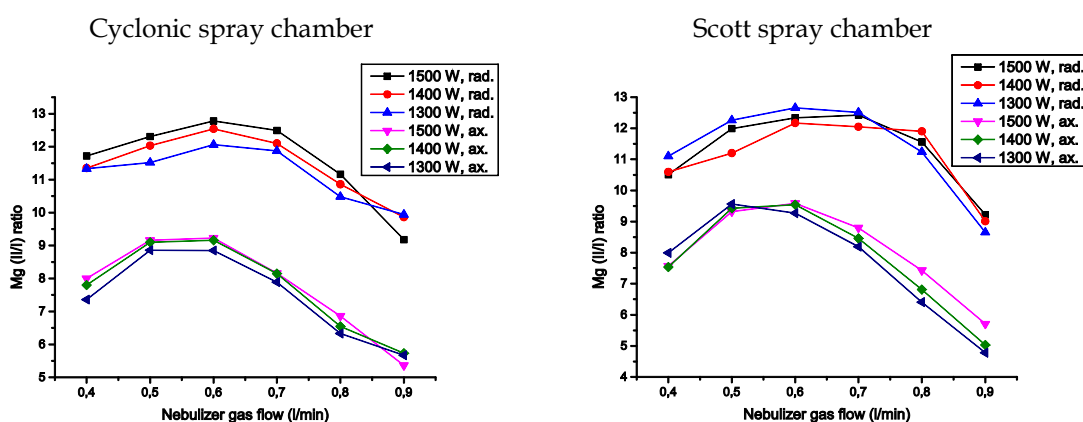


FIGURE 10 Magnesium II/I line intensity ratio as function of nebulizer gas flow rate with three different plasma power settings and with radial and axial plasma viewing. Sample: synthetic 0.5 mol l⁻¹ sulfuric acid sample containing 5 mg l⁻¹ of Mg.

The intensities of the Mg II line with axial viewing are illustrated in figure 11. The maximum intensity using the cyclonic spray chamber is approximately 17.9 million cps with a nebulizer gas flow rate of 0.5 l min⁻¹, and using the Scott-type spray chamber, 6.6 million cps with a 0.7 l min⁻¹ nebulizer gas flow rate. Signal suppression by sulfuric acid is evident compared to results with *aqua regia*. The acid effect observed with *aqua regia* is complex, as it is a mixture of two acids.

For both *aqua regia* and sulfuric acid matrices, lower nebulizer gas flow rate is preferred when the cyclonic spray chamber is used. The difference in line intensity between the two sample introduction systems is noticeable; hence, the use of the Scott spray chamber is justified when the samples have hydrofluoric acid or high dissolved solids content, but otherwise the cyclonic spray chamber is preferable especially in trace element analysis.

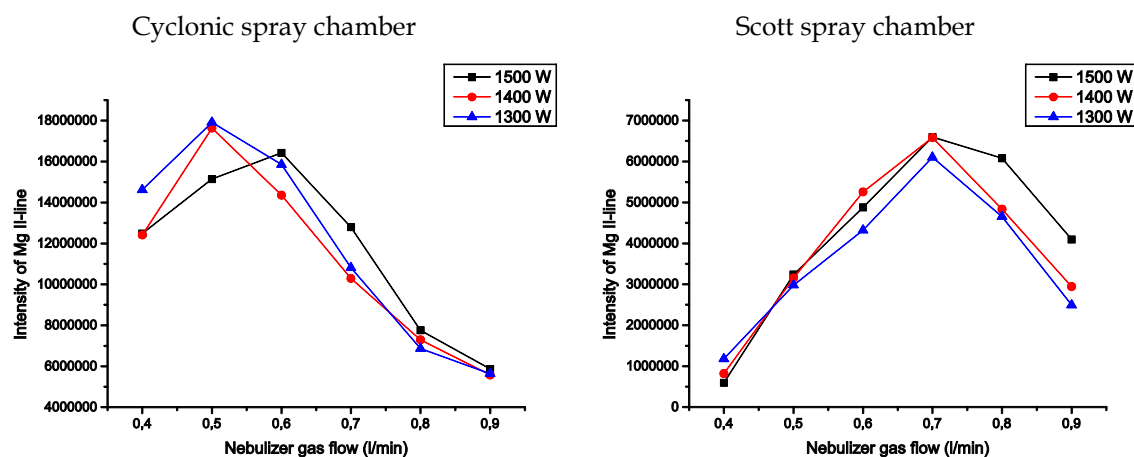


FIGURE 11 Magnesium II line intensity as function of nebulizer gas flow rate (l min^{-1}) with three different plasma power settings using axial plasma viewing. Sample: synthetic 0.5 mol l^{-1} sulfuric acid sample, Mg concentration 5 mg l^{-1} .

4.2.3 Acid effect in sulfuric acid samples

The acid effect occurring in the measurement of samples containing sulfuric acid was examined using synthetic samples with different concentrations of sulfuric acid: 0.01, 0.10, 0.30, 0.50, and 0.70 mol l^{-1} . The intensities of magnesium I and II emission lines were found to decrease as the concentration of sulfuric acid was increased (Mg II line intensities in figure 12). The decrease in intensity was in the range of 8-16 % with different measurement conditions. When robust plasma conditions were used, the intensities decreased to a lesser extent compared to non-robust conditions. In robust plasma conditions the acid effect is mainly due to processes of aerosol generation and transport, while in non-robust plasma conditions changes in the plasma itself also contribute to the acid effect.¹⁰⁴ Hence, acid effect is more pronounced in non-robust conditions, as observed in these experiments also.

Cyclonic spray chamber is less sensitive to acid effects than Scott double-pass spray chamber⁸⁷, as observed here, the Scott spray chamber resulted in a more evident decrease in intensities especially in non-robust conditions. Acid effect by sulfuric acid was also found to be slightly more prominent using axial viewing than radial viewing. The use of internal standard beryllium corrected the decrease in intensities to a limited extent. The decrease in intensities was also observed in rare earth element measurement using axial viewing and cyclonic spray chamber, and resulted in 8-11 % decrease in intensities for sulfuric acid concentration 0.7 mol l^{-1} . Due to this effect, samples with sulfuric acid have been diluted in order to decrease the severity of the acid effect in ICP-OES measurement.

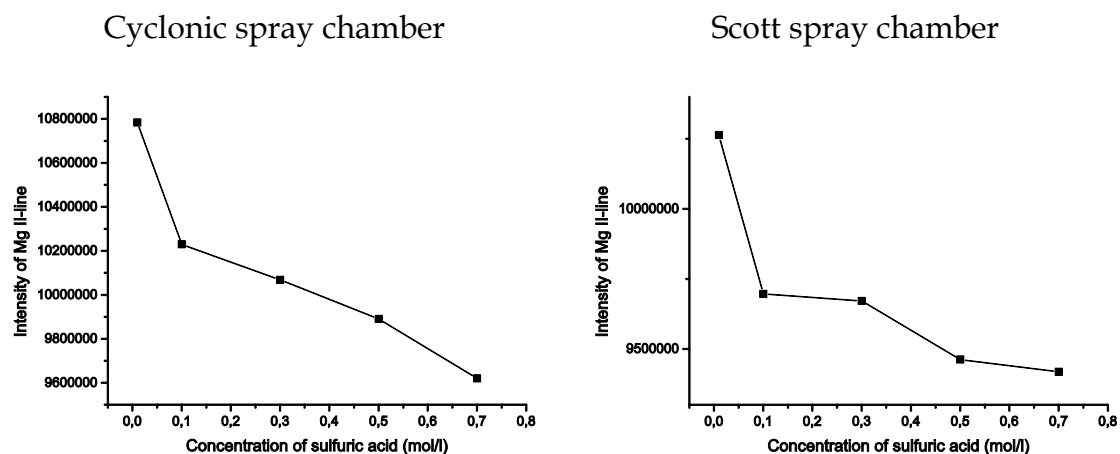


FIGURE 12 Magnesium II line intensity as a function of sulfuric acid concentration using axial viewing in robust plasma conditions.

4.2.4 REE recovery in robust and non-robust plasma conditions

The effect of plasma conditions on rare earth element measurement was studied with synthetic *aqua regia* and sulfuric acid samples containing 0.50 mg l^{-1} rare earth elements. Results for the test are presented in table 18 for *aqua regia* sample and in table 19 for the sulfuric acid sample. In the analysis of *aqua regia* sample robust plasma conditions resulted in overall appropriate recoveries whether an internal standard is used or not. The use on beryllium was beneficial in the case of praseodymium, neodymium, europium and thulium. In non-robust plasma conditions rare earth element recoveries were fairly low at approximately 90 %, and the use of an internal standard increases the recoveries to slightly over 100 %. The recoveries of cerium, samarium and gadolinium are better without the use of the internal standard.

As can be seen from table 19, in robust conditions, the yield of REEs in the 0.50 mol l^{-1} sulfuric acid sample is approximately 20 % higher than the added concentration, and in non-robust conditions approximately 15 % lower. Use of Be as an internal standard, however, improves the yield close to 100 % when using robust conditions, except for gadolinium with 121 % recovery. In non-robust conditions, the yield is approximately 10 % over the added concentration even with the internal standard. It is clear from these results that internal standardization is more difficult in non-robust conditions. When a synthetic sample containing 0.01 mol l^{-1} of sulfuric acid was analyzed, the yield was very close to 100 % in both robust and non-robust conditions, and even without the use of an internal standard. Hence, the acid effect is evident in 0.50 mol l^{-1} sulfuric acid sample compared to the 0.01 mol l^{-1} sample.

Trueness of the REE analysis was also evaluated after these recovery tests, since due to matrix matching, synthetic samples represent real samples well. REE determination from *aqua regia* samples using robust plasma conditions and internal standard for praseodymium, neodymium, europium and thulium, results in good recoveries with deviations from the true value at maximum of 6 %.

TABLE 18 Recovery percentages of REEs in 20 % *aqua regia* measured in robust (power 1,500 W and nebulizer gas flow 0.6 l min⁻¹) and non-robust (power 1,300 W and nebulizer gas flow 0.8 l min⁻¹) plasma conditions using cyclonic spray chamber and GemCone Low-Flow nebulizer.

Element	Robust plasma conditions, istd:		Non-robust plasma conditions, istd:	
	None	Be	None	Be
La	96.2	107.8	89.1	107.5
Ce	99.4	111.2	94.3	113.8
Pr	89.2	99.6	83.3	100.3
Nd	93.4	104.8	86.4	104.2
Sm	100.2	112.3	93.9	113.3
Eu	91.6	102.3	87.7	105.5
Gd	105.9	118.7	98.4	118.9
Tb	95.1	106.5	88.5	106.6
Dy	94.5	105.8	88.5	106.6
Ho	94.4	105.7	88.2	106.4
Er	94.0	105.1	88.1	106.1
Tm	91.0	101.8	85.0	102.4
Yb	99.4	111.3	89.3	107.6
Lu	94.1	105.4	88.2	106.3
Y	99.3	111.3	91.0	109.7
Sc	99.0	110.9	90.7	109.3

TABLE 19 Recovery percentages of REEs in 0.50 mol l⁻¹ sulfuric acid measured in robust (power 1,500 W and nebulizer gas flow 0.6 l min⁻¹) and non-robust (power 1,300 W and nebulizer gas flow 0.8 l min⁻¹) plasma conditions using cyclonic spray chamber and GemCone Low-Flow nebulizer.

Element	Robust plasma conditions, istd:		Non-robust plasma condition, istd:	
	None	Be	None	Be
La	121.4	101.2	84.3	107.6
Ce	127.4	106.2	88.9	113.8
Pr	113.0	94.1	80.6	102.8
Nd	119.1	98.7	83.7	107.0
Sm	128.6	107.2	90.4	115.7
Eu	120.7	100.6	81.8	104.2
Gd	144.5	120.8	100.4	129.0
Tb	125.6	104.6	88.0	112.6
Dy	124.2	103.6	87.7	111.9
Ho	124.6	102.7	86.9	111.3
Er	122.8	102.5	86.1	110.0
Tm	120.8	100.6	84.4	107.8
Yb	126.0	105.2	86.9	111.1
Lu	124.8	104.1	88.6	113.3
Y	127.3	106.2	87.0	111.1
Sc	127.8	106.9	87.2	111.2

In robust plasma conditions and with the use of internal standard REE recoveries in sulfuric acid synthetic sample had a maximum deviation of 7 % compared to the added concentration, except for gadolinium, which has a recovery of 121 %. For determination of gadolinium from sulfuric acid samples, it is important to dilute the samples prior to analysis.

4.3 Properties of fly ash

Several properties of fly ash samples were determined during this work, and the most relevant studies are presented here. Main elemental composition of fly ash samples was studied using SEM; an example of a typical sample composition is presented in table 20. The amount of oxygen confirms the presence of oxides that form in the combustion processes, and the main components present are CaO, SiO₂, Al₂O₃, and Fe₂O₃. Compared to typical results for coal fly ash (table 6), peat/biomass fly ash contains more calcium originating from the fuel.

The appearance of peat/biomass fly ash was captured using SEM. Figure 13 shows two SEM images of fly ash with a magnification of 400 times on the left and 800 times on the right. Ash particles were glued onto carbon tape for imaging which appears as the black background in the images. Porous particles and spheres of varying sizes are evident in the images. One sphere collapsed during electron bombardment, and it appears to be hollow, as shown in the picture on the right.

TABLE 20 Weight percentages of main elements in fly ash determined using SEM (Fly ash sample A)

Element	Concentration (w/w, %)
O	36.3
Ca	14.2
Si	4.71
C	3.96*
Al	2.66
Fe	1.83
K	1.43
S	1.24
Mg	0.86
Na	0.49
Mn	0.44
P	0.42

* Result for carbon is skewed due to carbon tape used in analysis.

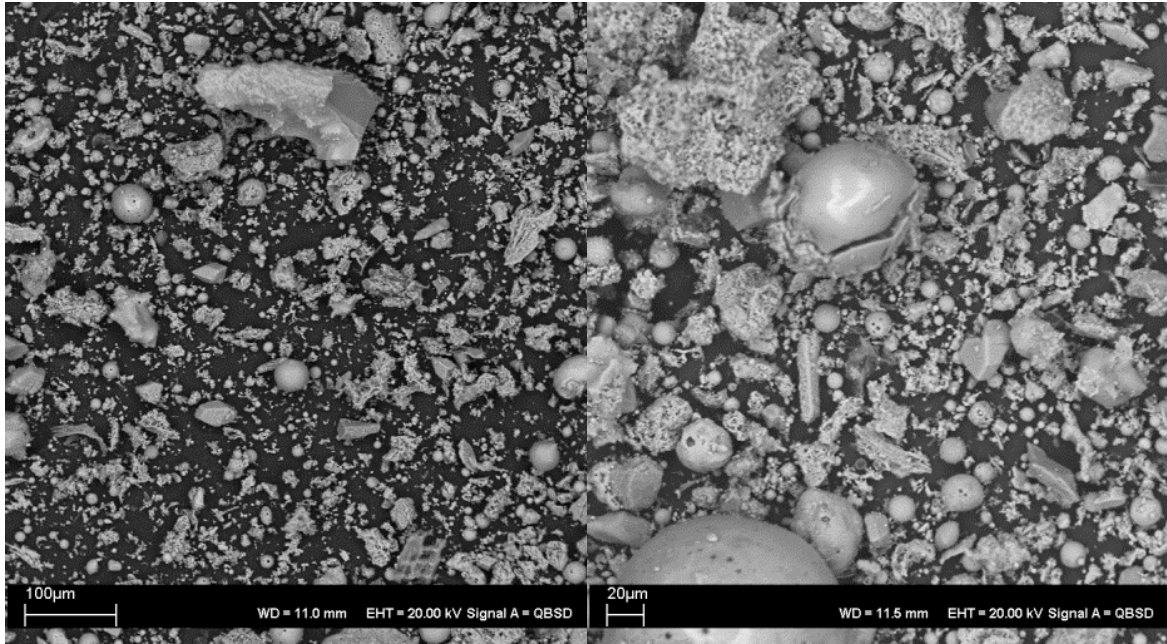


FIGURE 13 SEM pictures of fly ash A with 400 and 800 time magnifications.

Particle size distribution of fly ash was determined for two different ash samples. In figure 14, particle distribution of sample A is presented. 90 % of the particles are smaller than 100 μm in sample A. The larger particles are unburned carbon, which are visible in the fly ash samples. The particle size distribution for sample B displayed slightly bigger particles than in sample A, which is probably due to differences in combustion processes.

Magnetic qualities of fly ash were studied to ascertain whether it would be possible to separate concentrated metallic fractions from the ash. The experiment was conducted by moving a strong magnet straight above thinly spread fly ash. The fraction that stuck to the magnet as well as the original sample were dissolved in *aqua regia* and analyzed using ICP-OES. Rare earth elements were concentrated roughly 50 % more in the magnetic fraction than in the original sample. This applies also to other metals in the sample; they were concentrated in the range of 30–50 % compared to the original ash sample. This implies that rare earth elements are bound to magnetic fractions in the fly ash, such as iron oxides. However, magnetic separation is probably not a viable option due to the low increase in concentration observed in the test, although more sophisticated magnetic separation could be beneficial in rare earth element concentration.

Basicity of ash was determined using a slurry method, where the ash is mixed with water and the pH measured after one day of settling. The measured pH values were 10.6–12.6 for different peat/biomass fly ash samples. Basicity of the ash raises the pH value of acidic leaching solutions, and some of the leaching efficiency is lost.

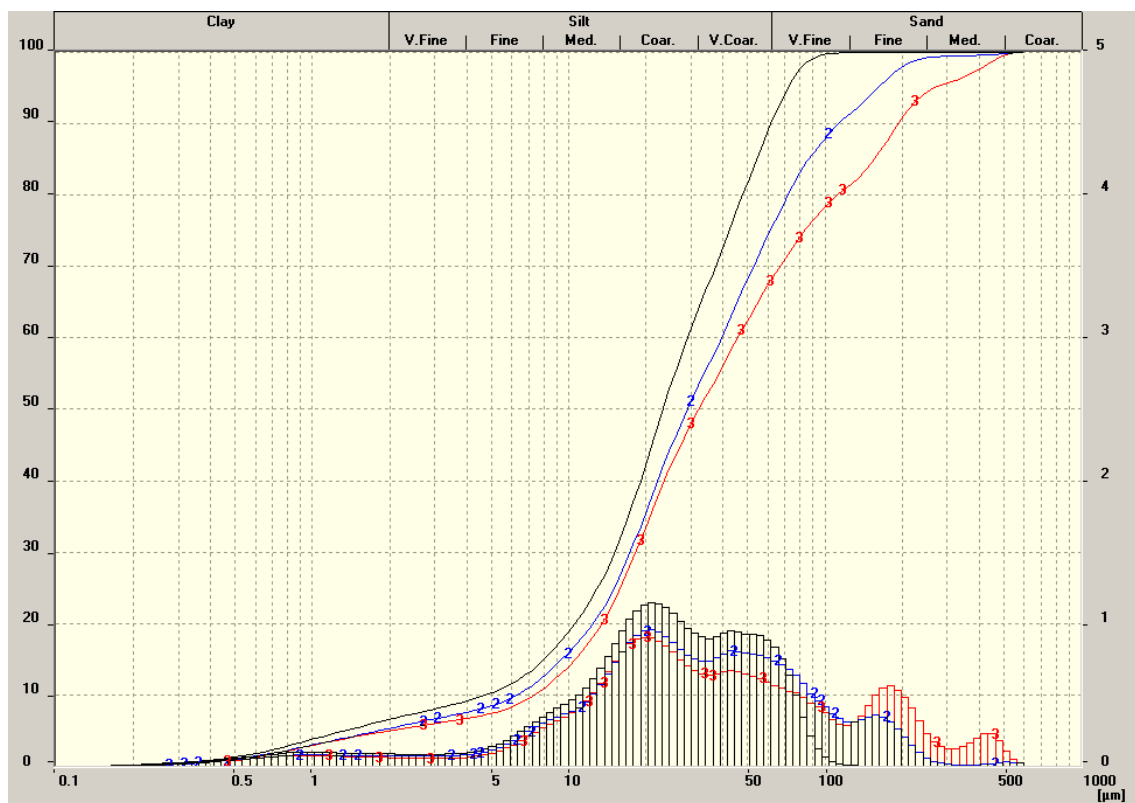


FIGURE 14 Particle size distribution of sample A (three replicate measurements), i.e. cumulative percentage (left y-axis) and as function of particle diameter (μm) on a logarithmic scale.

4.4 Leaching of REEs from fly ash

4.4.1 Initial leaching experiments

Sulfuric acid is widely used in leaching of rare earth elements from different solid matrices; hence it was selected to be used in the initial leaching tests. To improve the leaching efficiency, a mixture of sulfuric and nitric acid was used in the first tests. A two-stage leaching procedure was developed, where the first leaching solution contains oxalate and leaches other precious metals from the ash, while the rare earth elements are not leached. In the second stage sulfuric acid is used to leach the rare earth elements from the fly ash. Optimization of sulfuric acid leaching is presented further in the following sections.

Three stage leaching was also tested, where nitric acid leaching was added as a first step with the intention of removing some impurities from the ash before the actual leaching procedure. However, unacceptable concentrations of rare earth elements were lost in the nitric acid leachate, and this was not pursued further.

Solid concentration was studied between 50–150 g l⁻¹. Results showed that dissolution improves when the volume of leachate is increased with respect to

the weight of the fly ash sample. However, it is not economical to use large volumes of leachates even though dissolution is somewhat improved, especially when rare earth element concentrations in the leachate get lower. A compromise was made to use 75 g l^{-1} solid concentration in the following studies.

4.4.2 Concentration of sulfuric and nitric acid

Concentration of the leaching reagent was optimized between $0.2\text{--}1.0 \text{ mol l}^{-1}$ of sulfuric acid. The leaching of rare earth elements is poor when 0.2 mol l^{-1} sulfuric acid is used, but increases as the concentration is raised to 0.4 mol l^{-1} (figure 15). The highest leaching percentages for rare earth elements are achieved when sulfuric acid concentration is 0.4 mol l^{-1} , and when sulfuric acid concentration is increased further, the leaching percentages decline steadily. This might be due to REEs being precipitated as double-sulfates. Sulfuric acid concentration was further studied in smaller increments between $0.3\text{--}0.5 \text{ mol l}^{-1}$. In this experiment it was found that there is no advantage in using more concentrated acid than 0.35 mol l^{-1} (figure 16). Consequently, 0.4 mol l^{-1} sulfuric acid was chosen as the leaching reagent. Leaching percentages for scandium are higher than 100 % in the latter experiment, which might be due to heterogeneity in the fly ash sample.

Addition of nitric acid into the leaching reagent with sulfuric acid was studied by keeping sulfuric acid concentration at a constant, and by varying the nitric acid concentration between $0\text{--}0.18 \text{ mol l}^{-1}$. No clear differences were observed in leaching efficiencies as the concentration of nitric acid was raised, as all samples had similar leaching percentages for rare earth elements. Addition of nitric acid into the leaching reagent was not continued in the following tests.

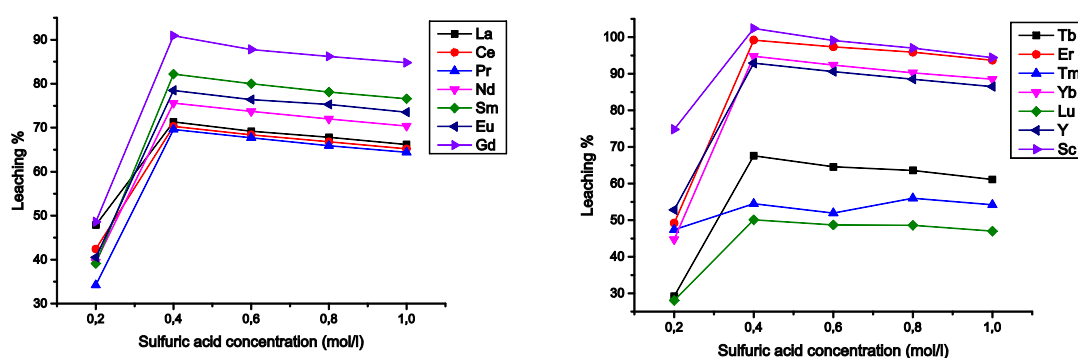


FIGURE 15 Leaching percentage of rare earth elements as function of sulfuric acid concentration ($0.2\text{--}1.0 \text{ mol l}^{-1}$), sample B.

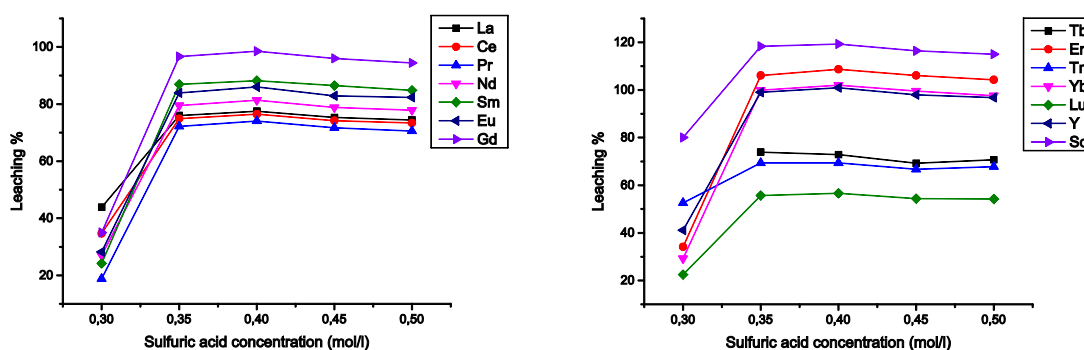


FIGURE 16 Leaching percentage of rare earth elements as function of sulfuric acid concentration (0.3–0.5 mol l⁻¹), sample B.

4.4.3 Leaching time and temperature

Leaching time was optimized using a water bath, and the test was carried out with and without ultrasound. Ultrasound can facilitate the leaching process by creating hot spots in the solution and by eroding the fly ash particles.¹⁰⁵ Leaching time was investigated between 18–138 minutes with the application of ultrasound every three minutes for three minutes. Increasing the leaching time did not seem to improve rare earth element leaching in this experiment, and the optimum leaching time is approximately 20 minutes.

When samples were held in a water bath without ultrasound, the leaching time was studied between 18–54 minutes. The samples were shaken every six minutes to allow better contact between the leaching reagent and fly ash. In this experiment, rare earth element leaching percentages increased very slightly when leaching time was increased but not significantly enough to make it reasonable to increase leaching time very much.

The advantage of ultrasound was studied lastly by doing 18, 36, and 54 minute leaching tests with and without ultrasound (table 21). There are no clear differences in results with or without ultrasound, and it can be concluded that rare earth elements are easily leached in 20 minutes and use of ultrasound is not necessary.

Temperature of the water bath was also studied using the following temperatures: 25, 50, and 75 °C. The rise in water bath temperature increases rare earth element recovery for approximately 10–20 percentage points. Elevated water bath temperature is required to achieve good dissolution of REEs.

TABLE 21 Rare earth element's leaching percentages with three leaching times, and with or without ultrasound, sample B.

Element	With ultrasound			No ultrasound		
	18 min	36 min	54 min	18 min	36 min	54 min
La	72.1	69.9	69.8	71.2	71.2	73.2
Ce	71.0	68.8	68.6	70.1	70.3	72.5
Pr	67.1	64.4	64.0	67.3	67.0	69.6
Nd	75.0	72.9	72.6	73.3	74.1	76.2
Sm	81.6	79.3	79.0	80.9	82.1	83.2
Eu	77.9	76.0	76.3	75.7	76.8	79.1
Gd	90.2	87.3	87.7	88.3	89.4	91.3
Tb	65.8	67.2	67.1	62.1	61.5	65.4
Er	100.0	96.9	96.6	98.5	99.4	102.2
Tm	47.4	50.2	55.3	54.9	58.6	58.1
Yb	93.2	90.2	90.2	90.2	91.5	94.1
Lu	48.1	47.3	48.3	46.9	47.7	49.8
Y	93.2	90.2	90.0	91.8	92.3	95.0
Sc	109.7	107.1	106.9	110.3	111.1	114.2

4.4.4 Leachate re-circulation

Re-circulation of leachate was studied in order to achieve higher rare earth element concentrations in the sulfuric acid leachate. The first experiment was done by re-circulating 0.5 mol l⁻¹ sulfuric acid via ten new fly ash samples. Results of the test are presented in table 22. Increase in rare earth element concentrations was approximately twofold from round one to round four. In rounds seven and ten, REE concentrations stayed at the same level as in round four; hence, there seems to be no advantage in re-circulating the leachate much more than four rounds. It is noteworthy that holmium is present in the leachate during the first round, but not in the latter rounds, which suggests that it might precipitate during the circulation. The same might be true for dysprosium also, as its concentration increases from round one to four, but decreases towards the latter rounds.

The second re-circulation test was conducted using 1.0 mol l⁻¹ sulfuric acid in leaching and by re-circulating the leachate through four new ash samples. Results of the second test are shown in table 23. The same trend is observed also in the second experiment: rare earth element concentrations increase approximately twofold during four rounds.

A similar re-circulation test was run using 3.0 mol l⁻¹ sulfuric acid, where it was re-circulated via four new ash samples. This experiment resulted in the leachate turning into a gel as the re-circulation proceeded; thus, using a more concentrated sulfuric acid is not a viable option in the process.

TABLE 22. Rare earth element concentrations (mg l^{-1}) in rounds 1, 4, 7, and 10 of first re-circulation experiment, sulfuric acid concentration was 0.5 mol l^{-1} , sample B.

Element	Concentration (mg l^{-1})			
	1. round	4. round	7. round	10. round
La	4.25	8.17	7.92	8.30
Ce	9.29	18.84	17.46	18.23
Pr	0.79	1.91	1.78	1.72
Nd	3.44	7.53	7.22	7.44
Sm	0.82	1.82	1.60	1.62
Eu	0.12	0.34	0.37	0.37
Gd	0.67	1.88	2.13	2.16
Tb	0.06	0.16	0.20	0.20
Dy	0.49	0.99	0.75	0.58
Ho	0.09	<LOD	<LOD	<LOD
Er	0.29	0.71	0.79	0.80
Tm	0.05	0.82	1.43	1.56
Yb	0.26	0.65	0.79	0.80
Lu	0.04	0.16	0.21	0.21
Y	2.85	6.83	7.90	8.16
Sc	0.81	1.98	2.16	1.92

TABLE 23. Rare earth element concentrations (mg l^{-1}) in rounds 1–4 of second re-circulation experiment, sulfuric acid concentration was 1.0 mol l^{-1} , sample B.

Element	Concentration (mg l^{-1})			
	1. round	2. round	3. round	4. round
La	2.97	4.36	5.60	6.22
Ce	6.68	9.58	12.54	13.66
Pr	0.60	0.93	1.28	1.42
Nd	2.68	3.94	5.21	5.73
Sm	0.59	0.87	1.15	1.27
Eu	0.10	0.17	0.25	0.29
Gd	0.63	1.06	1.50	1.76
Tb	0.05	0.09	0.14	0.17
Dy	0.23	0.36	0.48	0.52
Ho	0.02	0.03	0.04	0.05
Er	0.24	0.42	0.60	0.71
Tm	0.03	0.05	0.08	0.09
Yb	0.22	0.39	0.56	0.68
Lu	0.05	0.09	0.13	0.16
Y	2.37	4.14	5.90	7.03
Sc	0.59	1.04	1.52	1.82

In an ideal situation, the recovery of rare earth elements from fly ash would stay constant during the re-circulation, and concentrations would increase linearly as re-circulation proceeded. In these experiments, however, the concentrations increase twofold from round one to round four, and so half of the possibly recoverable rare earth elements remain in the fly ash.

4.4.5 Optimized leaching procedure

According to the previous optimization tests, the highest leaching efficiency is achieved using 0.4 mol l⁻¹ sulfuric acid as the leaching reagent. Addition of nitric acid into the leaching reagent was not found beneficial. Ultrasound was studied in speeding up the leaching procedure, but it was discovered that a short leaching time is enough to leach rare earth elements from the fly ash, and that the use of ultrasound is not necessary. The temperature of the water bath was found to be significant for rare earth element leaching, as the increase in temperature resulted in better REE leaching percentages. Re-circulation of leachate was found to be beneficial to a maximum of four rounds, and even then, a part of the recoverable rare earth elements remained in the fly ash.

Results for the optimized procedure are presented in table 24. The recovery of rare earth elements is approximately 70 %, while some rare earth elements are leached almost quantitatively. Leaching efficiency of lutetium and europium is lower than with the other rare earth elements.

TABLE 24 Leaching percentages of REEs using the optimized leaching procedure, percentages are calculated by comparing to *aqua regia* digestion, average of 5 replicates, sample B.

Element	Leaching %
La	68.3
Ce	59.2
Pr	63.2
Nd	61.3
Sm	71.1
Eu	49.2
Gd	82.9
Tb	71.4
Dy	90.8
Ho	>100
Er	73.7
Tm	<LOD
Yb	73.2
Lu	34.1
Y	78.2
Sc	94.8

4.5 REE precipitation as oxalates

4.5.1 Initial precipitation experiments

Rare earth elements can be precipitated from solution using oxalic acid. Sulfuric acid leachate is very acidic (pH between 0-1); therefore, the pH has to be adjusted above pH 1 using an alkaline solution to achieve precipitation. From common bases ammonia was selected to be used. Sodium hydroxide solution was rejected to prevent sodium build up. Oxalic acid volume, pH, mixing time, and temperature were optimized to achieve maximum precipitation without excess impurities in the precipitate.

4.5.2 Effects of pH

The first experiments were conducted in pH 1.5. The original pH of sulfuric acid leachate was close to 0.8, and the precipitation of rare earth elements started just under pH 1 when ammonia solution was added drop-wise. Precipitation of REEs was close to complete. In experiments where pH was adjusted to 2.0-3.0, more impurities precipitated without an increase in rare earth element's precipitation. Based on the preliminary experiments, a pH range of 1.0-1.6 was investigated further using two different sulfuric acid leachates (figures 17 and 18). The optimum pH for oxalate precipitation appears to be 1.1-1.2 for the two leachate solutions tested. Precipitation percentages for holmium and praseodymium are higher than 100 % due to low concentrations close to limits of detection.

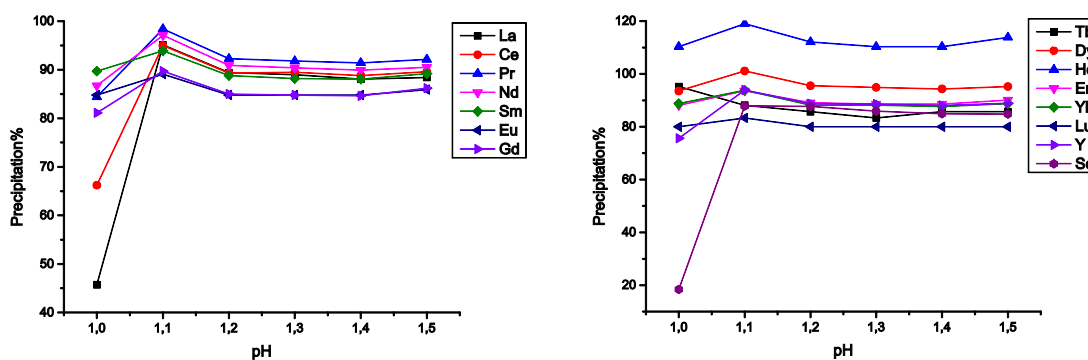


FIGURE 17 Precipitation percentage of REE's as a function of precipitation pH, sample: fly ash B's leaching solution.

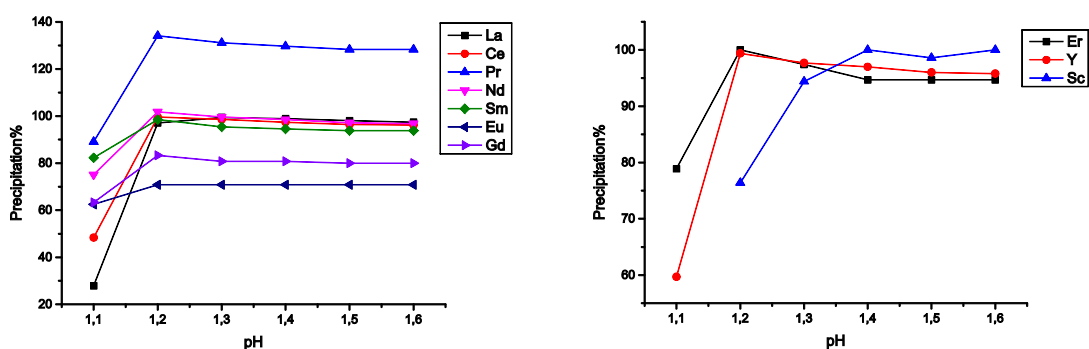


FIGURE 18 Precipitation percentage of REE's as a function of precipitation pH, sample: fly ash C's leaching solution.

Precipitation of impurity elements is presented in figure 19. Precipitation of rare earth elements is based on co-precipitation of calcium oxalate; therefore, the main impurity in the precipitate is calcium. The concentration of impurity elements in the precipitate can be minimized by using the lowest pH, while rare earth elements still precipitate.

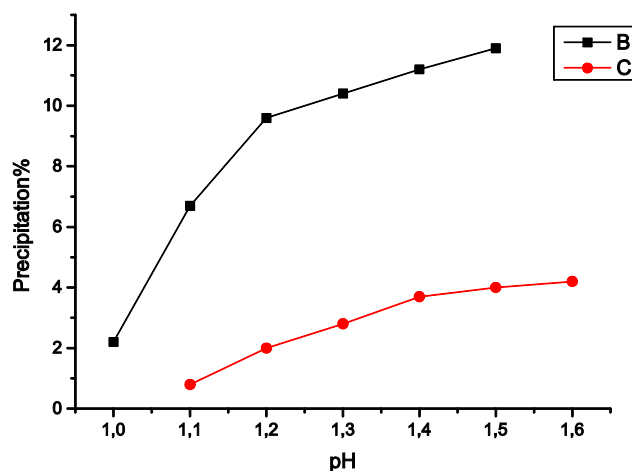


FIGURE 19 Precipitation percentage of the sum of all impurity elements as function of pH, samples B and C.

4.5.3 Molar amount of oxalic acid

An oxalic acid solution was used as a precipitating agent in these studies. Initial experiments were performed using excess oxalic acid, and in later experiments, oxalic acid concentration was optimized using four sulfuric acid leach solutions. The molar ratio of oxalic acid was varied between 5–300 times the molar amount of rare earth elements in the sample solution (table 25).

As can be seen from table 25, there seems to be no advantage in using more oxalic acid than 5 times the molar amount of rare earth elements in the

sample solution: precipitation percentages of REE's are relatively same in all samples. In addition, the concentration of impurity elements in precipitate increases when the molar amount of oxalic acid is increased. Therefore, the ideal molar amount of oxalic acid is 1.5–5 times the molar amount of REEs in the sample solution.

TABLE 25 REE precipitation percentages using different molar amounts of oxalic acid (compared to REE's molar amount in sample solution), sample D's leaching solution.

Element	Molar amount of oxalic acid:					
	5	10	20	50	100	300
La	94.5	95.0	95.4	92.9	94.3	94.1
Ce	94.6	94.4	94.6	92.2	93.4	93.1
Nd	94.6	95.1	95.3	92.6	93.7	93.4
Sm	92.9	93.9	93.9	90.9	91.9	91.9
Eu	86.1	88.9	88.9	86.1	86.1	86.1
Gd	85.4	86.5	86.0	83.7	85.4	84.3
Tb	83.3	88.9	88.9	83.3	83.3	83.3
Dy	<LOD	<LOD	<LOD	<LOD	<LOD	<LOD
Ho	<LOD	<LOD	<LOD	<LOD	<LOD	<LOD
Er	92.1	93.4	92.1	90.8	90.8	92.1
Tm	35.0	35.0	35.0	35.0	35.0	35.0
Yb	92.6	92.6	92.6	91.2	91.2	91.2
Lu	75.0	75.0	75.0	66.7	75.0	75.0
Y	94.7	95.3	95.3	93.0	94.3	94.0
Sc	94.3	94.3	94.3	92.0	93.2	92.0

4.5.4 Mixing time and temperature

During initial testing, the sample solution was mixed with a magnetic stirrer for 20 minutes in a 60 °C water bath after oxalic acid addition and pH adjustment. When mixing temperature was modified between 20 °C and 80 °C, no clear differences in rare earth element's or impurity element's precipitation were observed. Consequently, ambient temperature is suitable for oxalate precipitation.

Mixing time was optimized by doing 0, 20, 40, and 60 minute tests, and it was found that rare earth element precipitation increases up to 20 min, after which it stays fairly constant (figure 20). Lastly, the gap between 0 to 20 minutes was studied using 5-minute intervals, and it was verified that precipitation increases up to 20 minutes of mixing time.

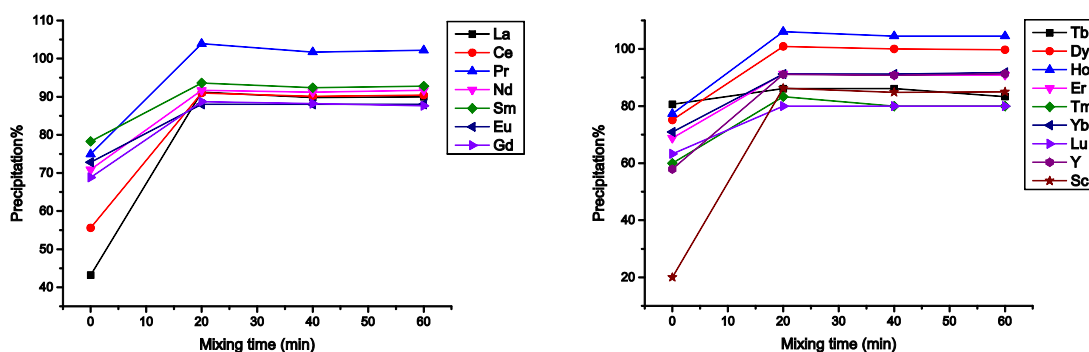


FIGURE 20 Precipitation percentage of REEs as function of mixing time, sample: fly ash B's leachate.

4.5.5 Optimized precipitation procedure

As mentioned before, the main constituent of precipitate is calcium oxalate at 60 weight percentages (table 26). Rare earth element oxalate is a minor component in the precipitate at under 1 w/w, %. Calcination of the precipitate turns oxalates into oxides but does not improve the quality of the precipitate. Precipitation can be used to separate rare earth elements from the solution, but the low concentration of REEs and high concentration of impurity elements (mainly calcium) in leachate lead to a poor quality precipitate. These results give rise to study other methods for recovering rare earth elements from the leachate.

TABLE 26 Composition (w/w, %) of precipitate and calcined precipitate.

Element	Precipitate	Calcined precipitate
REE	0.7	1.4
Ca	18.7	47.9
S	2.7	3.2
Fe	0.1	0.2
Al	0.1	0.1
Sr	0.1	0.2

4.6 REE concentration using liquid-liquid extraction

4.6.1 Initial liquid-liquid extraction experiments

Liquid-liquid extraction of rare earth elements was studied using the most widely used rare earth element extractant D2EHPA. EHEHPA was also considered as a possible extractant, but it was rejected due to its poor availability outside China. In the first experiments D2EHPA was used without dilution, and in later testing it was diluted with kerosene. Phases were mixed via shaking by hand for 5 minutes, except for mixing time optimization where the phases were

mixed using magnetic stirrers for 5–40 minutes. Nearly quantitative recovery was achieved for rare earth elements already in the first experiments.

The sample solution's pH was found to be a very important factor in the extraction. LREEs are extracted properly into the organic phase in higher pH values, while HREEs are extracted easily even when the pH is lower. Precipitation of rare earth elements was found to be a limiting factor when pH was raised above 1.5.

Stripping of the organic phase was studied first with hydrochloric and nitric acids. The recovery of rare earth elements improved when concentration of acid was increased. Very concentrated acids, however, have negative effects on D2EHPA's physical properties; hence, 4 mol l⁻¹ acids were used in stripping in later testing.

4.6.2 Optimization of liquid-liquid extraction

Choice of solvent

Kerosene was studied as a solvent for D2EHPA due to its wide use in industry and affordable pricing. The volume percentage of D2EHPA in kerosene was evaluated from 2.5 to 25.0 % using 2.5 and 5.0 percent increments. The results of the experiment are presented in table 27, and it can be seen that HREEs are efficiently extracted into the organic phase using 5 % D2EHPA. For LREEs, a more concentrated D2EHPA is needed to achieve efficient extraction, and even with 25 % D2EHPA, recovery of LREEs remains low.

TABLE 27 REE extraction percentages into organic phase with different dilutions of D2EHPA with kerosene, sample B's leachate.

Element	Volume percentage of D2EHPA in the organic phase:					
	2.5 %	5 %	10 %	15 %	20 %	25 %
La	<LOD	1.9	3.5	<LOD	<LOD	12.6
Ce	<LOD	2.4	4.3	<LOD	1.0	16.2
Pr	<LOD	2.6	4.0	<LOD	2.8	17.5
Nd	<LOD	0.9	6.7	1.4	2.4	19.7
Sm	<LOD	2.0	11.8	21.8	37.4	50.0
Eu	<LOD	13.8	30.0	52.0	100.0	100.0
Gd	<LOD	17.3	33.8	46.7	56.5	65.4
Tb	-	-	-	-	-	-
Dy	41.7	100.0	100.0	100.0	100.0	100.0
Ho	-	-	-	-	-	-
Er	100.0	100.0	100.0	100.0	100.0	100.0
Tm	-	-	-	-	-	-
Yb	100.0	100.0	100.0	100.0	100.0	100.0
Lu	-	-	-	-	-	-
Y	81.9	97.9	100.0	100.0	100.0	100.0
Sc	100.0	100.0	100.0	100.0	100.0	100.0

- Concentration of the element was <LOD in the sulfuric acid leachate.

pH of the sample solution

The pH of the sample solution was studied initially by adjusting the pH to 0.75, 1.0, 1.5, and 2.0. Extraction of rare earth elements improves as the pH is raised, but the precipitation of rare earth elements becomes a prohibiting factor above pH 1.5. To optimize the appropriate pH for liquid-liquid extraction, pH adjustment of sulfuric acid leachate was assessed. The sample solution's pH was raised using an ammonia solution (5 mol l⁻¹) from original pH of 0 in 0.5 increments to pH 3.0. There was no precipitate observed in pH 0.5, and from a pH of 1.0 onwards, a precipitate was formed.

In figure 21, rare earth element percentages in leachate solution are presented as a function of pH. At a pH of 1.5 there seems to be a critical point where precipitation becomes significant. Some HREEs precipitate already at a pH of 1.0, their recovery in solution being approximately 90 %. The optimum pH for liquid-liquid extraction seems to be slightly over 1.0, where precipitation is not yet prominent, but at the same time, pH is high enough for REEs to be efficiently extracted into the organic phase. In another experiment, the pH of the sample solution was raised to a value of 4.5, where the precipitate starts to dissolve and rare earth elements are released back into the solution. Scandium exhibits different behavior compared to the other rare earth elements, as it does not precipitate similarly when the pH is raised. This is due to its different chemical properties.

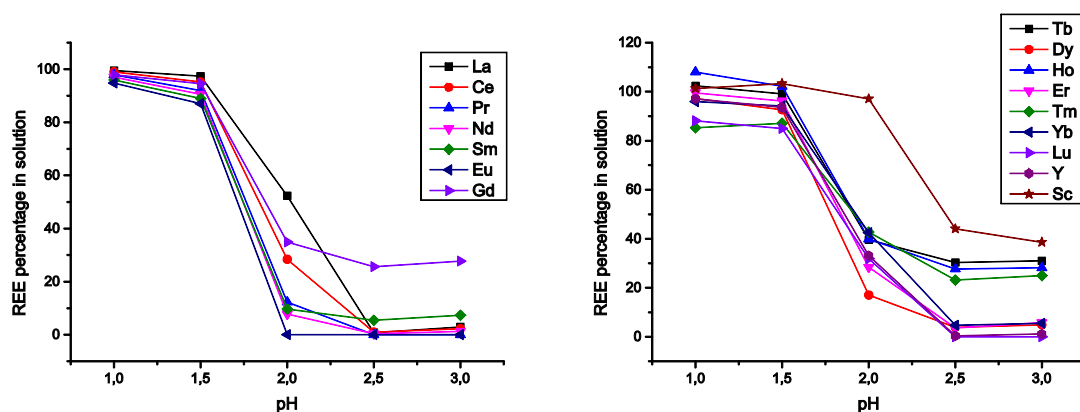


FIGURE 21 Rare earth element percentage in sulfuric acid leachate solution as function of sample solution pH, sample C's leachate.

A:O-ratio

Aqueous to organic ratio was studied using 10:1 to 1:5 A:O-ratios. From table 28 it is evident that HREEs are easily extracted into the organic phase, even at A:O-ratio of 10:1, while LREEs need a higher volume of D2EHPA to be extracted properly. For any given A:O-ratio the recovery of REEs increases steadily along the lanthanoid series with increasing atomic number. Thulium, ytterbium, lutetium, yttrium, and scandium are recovered completely with all A:O-ratios test-

ed here. This gives rise to the possibility of separating LREE and HREE fractions using D2EHPA.

TABLE 28 REE extraction percentages into the organic phase using different A:O-ratios, sample B's leachate.

Element	A:O-ratio:					
	10:1	5:1	2:1	1:1	1:2	1:5
La	3.6	11.8	35.9	54.5	71.3	85.0
Ce	11.6	25.4	51.9	69.2	82.4	91.5
Pr	14.8	27.7	57.9	74.7	87.7	94.4
Nd	16.3	33.2	61.1	75.9	86.8	93.7
Sm	56.0	69.8	82.9	89.4	91.1	94.8
Eu	83.8	93.1	99.4	100.0	100.0	100.0
Gd	59.1	68.0	77.8	85.5	90.3	92.5
Tb	52.3	60.9	67.1	76.6	76.4	74.7
Dy	94.7	95.5	97.6	97.6	98.7	100.0
Ho	72.7	77.1	71.8	73.0	67.5	68.9
Er	90.0	86.7	87.4	85.0	86.3	86.7
Tm	100.0	100.0	100.0	100.0	100.0	100.0
Yb	93.7	94.5	96.0	96.8	96.6	97.1
Lu	100.0	100.0	100.0	100.0	100.0	100.0
Y	100.0	100.0	100.0	100.0	100.0	100.0
Sc	99.1	99.7	100.0	100.0	100.0	100.0

Mixing time

Required mixing time in liquid-liquid extraction was studied using 5-, 10-, 20- and 40-minute mixing times. Results are presented in table 29, and they show no clear differences between 5–40 minute mixing times. Extraction percentages of matrix elements are similar with different mixing times, besides iron, which extracts into the organic phase better when mixing time is increased. On the basis of these results, 5 minutes of mixing is enough to achieve good extraction of rare earth elements and minimize iron extraction.

In the same test, separation time of the organic and aqueous phase was observed. The phases separated quickly; hence, a few minutes of separation time is enough in liquid-liquid extraction. Similar results were observed for stripping of the organic phase, where 5 minutes of mixing time and a few minutes of phase separation were adequate.

TABLE 29 REE extraction percentages into organic phase with 5–40 minute mixing times, sample B's leachate.

Element	Mixing time (min):			
	5	10	20	40
La	51.0	54.2	50.5	49.2
Ce	69.4	71.2	68.9	67.8
Pr	74.7	75.7	74.2	73.2
Nd	76.4	77.7	76.2	75.4
Sm	92.3	92.6	91.7	92.1
Eu	96.9	97.2	97.0	97.0
Gd	89.3	89.8	89.5	90.0
Tb	98.3	99.6	99.0	99.6
Dy	100.0	100.0	100.0	100.0
Ho	99.5	99.5	100.0	100.0
Er	100.0	100.0	100.0	100.0
Tm	100.0	100.0	100.0	100.0
Yb	97.4	97.4	97.4	97.6
Lu	97.1	97.4	97.3	97.6
Y	100.0	100.0	100.0	98.2
Sc	100.0	100.0	100.0	100.0

4.6.3 Optimization of stripping

Choice of stripping reagent

Rare earth elements were first extracted from fly ash sulfuric acid leachate to 40 % D2EHPA/kerosene mixture using A:O-ratio of 2:1. The extraction percentage of rare earth elements was on average 92 %. 4 mol l⁻¹ nitric acid, hydrochloric acid and sulfuric acid were tested as stripping reagents using an A:O-ratio of 1:1. Results are presented in table 30. For LREEs, nitric acid and hydrochloric acid were found to be slightly more efficient than sulfuric acid, and for HREEs, hydrochloric acid and sulfuric acid were more efficient than nitric acid. In general, mineral acids studied here extract LREEs more easily than HREEs, and especially scandium appears to stick to D2EHPA very tightly. Hydrochloric acid appears to be the most suitable option as a stripping reagent; however, other tested mineral acids also work well.

When sulfuric acid was used in stripping, the formation of a precipitate was observed after phases were left to separate. This is probably due to REEs precipitating as double-sulfates. If sulfuric acid were used in stripping, the formation of this precipitate would have to be studied further, as it could complicate the extraction process.

TABLE 30 Rare earth element recovery percentage from organic phase using three mineral acids as stripping reagents, sample B's leachate.

Element	HNO ₃	HCl	H ₂ SO ₄
La	98.3	97.4	93.0
Ce	98.0	98.3	93.1
Pr	97.3	97.5	89.8
Nd	90.6	91.5	86.3
Sm	92.8	97.1	90.1
Eu	-	-	-
Gd	85.4	91.9	82.8
Tb	86.3	96.3	>100
Dy	61.4	82.0	83.5
Ho	63.4	90.7	>100
Er	31.7	56.0	89.4
Tm	-	-	-
Yb	5.5	10.7	28.9
Lu	-	-	-
Y	25.3	52.4	79.7
Sc	3.2	3.2	0.4

- Concentration of the element was <LOD in the sulfuric acid leachate

Effect of solvent percentage on stripping

The influence of solvent percentage on stripping was evaluated. An A:O-ratio of 2:1 was used in liquid-liquid extraction and 1:1 in stripping using 6 mol l⁻¹ nitric acid as the stripping reagent. Results are presented in table 31. In previous tests, a low recovery for HREEs from organic phase has been observed; here, a high yield of approximately 90 % for HREEs is achieved using 5 % D2EHPA. When the percentage of D2EHPA is increased in the organic phase, HREE recovery from organic phase decreases, as for LREEs, recovery increases slightly when percentage of D2EHPA rises. This indicates to HREEs being more tightly bound to D2EHPA; hence, using smaller concentrations of D2EHPA in the organic phase allows heavy REEs to be released more easily into the stripping reagent.

A:O ratio in stripping

The effect of A:O-ratio on stripping was studied, and results are presented in table 32. Recovery of rare earth elements is reduced from A:O of 1:1 to 1:8, but yields remain reasonable still at 1:4. The decrease in recoveries is most severe with HREEs. Even though overall recovery decreases, concentration of rare earth elements from the original 40 mg l⁻¹ in sulfuric acid leachate improves notably to nearly 200 mg l⁻¹ in the hydrochloric acid stripping reagent using an A:O-ratio of 1:8.

TABLE 31 Rare earth element recovery percentage from organic phase using 6 mol l⁻¹ nitric acid. Composition of organic phase is altered from 5% to 25 % of D2EHPA in kerosene, sample B's leachate.

Element	Percentage of D2EHPA in organic phase:				
	5	10	15	20	25
La	94.8	69.7	78.4	77.4	80.6
Ce	88.1	79.3	86.2	84.4	86.6
Pr	78.1	60.9	75.7	80.7	85.8
Nd	86.9	82.7	90.5	79.7	84.2
Sm	89.0	85.8	94.0	95.2	97.2
Eu	86.9	87.9	90.1	90.5	91.3
Gd	81.9	92.4	94.5	94.4	93.9
Tb	91.9	94.5	94.5	91.7	90.2
Dy	95.8	96.9	96.1	92.5	89.1
Ho	94.2	92.9	89.3	84.4	79.4
Er	93.2	88.0	81.1	72.2	64.5
Tm	89.3	74.2	59.6	46.0	36.5
Yb	81.3	50.6	33.0	23.2	17.1
Lu	71.6	35.4	20.7	12.6	8.6
Y	92.7	87.4	79.5	72.4	66.1
Sc	<LOD	<LOD	<LOD	<LOD	<LOD

TABLE 32 Recovery percentage of REEs from organic phase to 4 mol l⁻¹ hydrochloric acid, sample B's leachate.

Element	A:O-ratio:		
	1:1	1:4	1:8
La	97.4	95.4	91.9
Ce	98.3	95.5	91.8
Pr	97.5	93.4	89.6
Nd	91.5	88.0	85.0
Sm	97.1	91.0	85.8
Eu	>100	92.4	88.7
Gd	91.9	86.6	78.6
Tb	96.3	72.5	59.3
Dy	82.0	55.3	35.9
Ho	90.7	39.0	16.6
Er	56.0	20.6	10.4
Tm	<LOD	<LOD	<LOD
Yb	10.7	3.2	1.9
Lu	<LOD	<LOD	<LOD
Y	52.4	19.9	9.0
Sc	3.2	2.5	2.3

4.6.4 Scandium stripping

Scandium was the only rare earth element that was not extracted properly into any of the mineral acids used in stripping. Sodium hydroxide was suggested in the literature^{34, 40, 106} to be able to extract scandium from D2EHPA. Concentrations of 0.5, 1.0, 2.0, and 5.0 mol l⁻¹ NaOH were tested, and the phase separation was adequate only using the two higher concentrations of sodium hydroxide. When the percentage of D2EHPA in the organic phase was 40 %, scandium was not stripped from the organic phase. However, when 2 % D2EHPA in kerosene was used, scandium extraction was almost quantitative. This is in agreement with scandium's high affinity for D2EHPA. The other rare earth elements were not extracted into the 2 % D2EHPA organic phase, except for HREEs in low concentrations. This suggests a two-step D2EHPA extraction if scandium is to be recovered from the solution: first, dilute D2EHPA is used to extract scandium from the sulfuric acid leachate and then sodium hydroxide to strip scandium from the organic phase. In the second extraction, the rest of the rare earth elements are extracted into 40 % D2EHPA in kerosene and then stripped using a mineral acid.

4.6.5 Scrubbing of organic phase

Scrubbing of organic phase after liquid-liquid extraction and before stripping was carried out using 0.2 mol l⁻¹ nitric acid. The objective was to remove some of the impurities from the organic phase without major losses of rare earth elements. Main impurities extracted into the organic phase are aluminum, calcium, and iron (table 33). Calcium is extracted from the organic phase using 0.2 mol l⁻¹ nitric acid, while rare earth element extraction is very low. Thus, diluted nitric acid is a viable option in removing calcium from the organic phase. Other diluted mineral acids might work in impurity removal as well.

TABLE 33 Concentrations (mg l⁻¹) of aluminium, calcium, and iron in the organic phase and in dilute (0.2 mol l⁻¹) nitric acid using different A:O-ratios, sample B's leachate.

Element	Organic phase	A:O-ratio		
		1:1	1:4	1:8
Al	17.1	0.67	0.49	0.75
Ca	285.7	229.3	341.4	217.8
Fe	152.0	0.03	0.09	0.08

4.6.6 Optimized liquid-liquid extraction procedure

Liquid-liquid extraction should be done using a higher concentration of D2EHPA in kerosene when light REEs are collected, and if heavy REEs are collected, a more dilute D2EHPA is optimal. The sample solution's pH should be raised using a base but kept low enough not to precipitate the rare earth ele-

ments. In order to concentrate the REEs, A:O-ratio should be at least 2:1 in the loading of the organic phase and at least 1:2 in the stripping stage. A mixing time of 5 minutes is adequate in both liquid-liquid extraction and stripping, and the separation of phases is fast, taking only a few minutes. Before stripping, organic phase can be scrubbed using a dilute mineral acid to remove calcium and other impurities. Nitric, hydrochloric, and sulfuric acids work well in stripping, and hydrochloric acid was found to be the most efficient. The result is an acid solution containing approximately 200 mg l⁻¹ of REEs, with the majority of them being light REEs.

5 CONCLUSIONS

A method for the determination of rare earth element concentrations in fly ash has been developed utilizing ultrasound-assisted *aqua regia* digestion and ICP-OES analysis. Ultrasound was used to facilitate the digestion procedure by creating hot spots in the leaching solution and by eroding the fly ash particles. Operating conditions for ICP-OES were optimized using a magnesium ion and atomic line intensity ratio in order to achieve as robust plasma conditions as possible. The analysis of rare earth element concentrations was verified by comparison with the ICP-MS instrument and analysis of NIST 1633b standard reference material and synthetic samples. Robust plasma conditions, where the introduction of samples with different acid matrices and matrix element concentrations does not affect the excitation processes in the plasma, were achieved using lower nebulizer gas flow rate (0.6 l min^{-1}) and high plasma power (1,500 W). Use of axial viewing and the cyclonic spray chamber with a GemCone Low-Flow nebulizer in sample introduction resulted in the highest sensitivity. Using axial viewing, all rare earth elements have detection limits in the $\mu\text{g l}^{-1}$ range and can be analyzed with high accuracy from fly ash samples. When samples contain hydrofluoric acid, the sample introduction is performed using the Scott double-pass spray chamber with a cross flow nebulizer. Dilution of samples, especially sulfuric acid samples, decreased the amount of matrix effects present in the analysis. When difficult sample matrices are analyzed, for example, aqueous phases from liquid-liquid extractions, the use of internal standard is recommended; especially, when the samples cannot be diluted.

Rare earth element concentrations were determined from industrial fly ash generated in a combustion process using peat and biomass as fuels using the optimized method. Samples contain considerable concentrations of rare earth elements, up to 560 mg kg^{-1} in total. These concentrations are high enough to initiate further research into recovery of rare earth elements from fly ash. In light of high rare earth element concentration in fly ash, a leaching procedure for rare earth elements was developed, where dilute sulfuric acid was used to treat fly ash. The leaching procedure was optimized to achieve good dissolution of rare earth elements, yet low concentrations of impurity elements in the re-

sulting leachate. It was found that an optimum concentration of sulfuric acid can be found, and that using a higher concentration of sulfuric acid does not necessarily lead to optimum results. The optimized leaching procedure resulted in approximately 70 % of rare earth elements being leached from fly ash.

Rare earth element recovery from sulfuric acid leachate was studied using the precipitation and liquid-liquid extraction. Recovery of rare earth elements using oxalate precipitation was quantitative but non-specific as the precipitate contained calcium oxalate as the major component, and hence was not a rational option. Liquid-liquid extraction using D2EHPA in kerosene as an extractant was found suitable in concentrating rare earth elements before oxalate precipitation. Dilute D2EHPA was found to recover heavy rare earth elements from sulfuric acid leachate; however, light rare earth element recovery requires a more concentrated D2EHPA to be used in liquid-liquid extraction. Sulfuric acid leachate's pH has to be raised in order to achieve a good yield of rare earth elements in liquid-liquid extraction, but not too high to precipitate REEs from the sample solution. Stripping of rare earth elements from the organic phase can be achieved using nitric, hydrochloric, and sulfuric acids, while the optimum recovery was achieved using hydrochloric acid. Scandium was not stripped from the organic phase using mineral acids as the rest of the rare earth elements, but it can be recovered by loading it into dilute D2EHPA and stripping with sodium hydroxide. The stripping solutions containing higher concentration of rare earth elements than the original sulfuric acid leachates could be treated with oxalic acid to precipitate the rare earth elements as oxalates.

A comprehensive study of determination and recovery of rare earth elements from fly ash samples has been described. The process can be modified to fit different types of ashes; hence, it could have major applications. The economy of the process developed depends highly on the rare earth price development, which determines the commercial possibilities of this method.

REFERENCES

1. J. Gambogi, U.S. Geological Survey, Mineral Commodity Summaries, Rare Earths, February 2014, 128-129, http://minerals.usgs.gov/minerals/pubs/commodity/rare_earths/mcs-2014-raree.pdf (13.6.2014).
2. Report on critical raw material for the EU, Report of the Ad hoc Working Group on defining critical raw materials, European Commission, May 2014, 1-41.
3. Report on critical raw materials for the EU, Report of the Ad-hoc Working group on defining critical raw materials, European Commission, 30.7.2010, 1-85.
4. Critical Materials Strategy, U.S. Department of Energy, December 2011, 1-190.
5. K. Binnemans, P.T. Jones, B. Blanpain, T. Van Gerven, Y. Yang, A. Walton and M. Buchert, Recycling of rare earths: a critical review, *J. Cleaner Prod.*, **2013**, *51*, 1-22.
6. R.S. Blissett and N.A. Rowson, A review of the multi-component utilisation of coal fly ash, *Fuel*, **2012**, *97*, 1-23.
7. V.V. Seredin and S. Dai, Coal deposits as potential alternative sources for lanthanides and yttrium, *Int. J. Coal Geol.*, **2012**, *94*, 67-93.
8. F.-S. Zhang, S. Yamasaki and K. Kimura, Rare earth element content in various waste ashes and the potential risk to Japanese soils, *Environ. Int.*, **2001**, *27*(5), 393-398.
9. P. Thy, C. Leshner, B. Jenkins, M. Gras and R. Shiraki, Trace metal mobilization during combustion of biomass fuels, PIER Final Project Report, California Energy Commission, June 2008, 1-112.
10. L. Zhao, F.-S. Zhang and J. Zhang, Chemical properties of rare earth elements in typical medical waste incinerator ashes in China, *J. Hazard. Mater.*, **2008**, *158*(2-3), 465-470.
11. L.S. Morf, R. Gloor, O. Haag, M. Haupt, S. Skutan, F. Di Lorenzo and D. Böni, Precious metals and rare earth elements in municipal solid waste – Sources and fate in a Swiss incineration plant, *Waste Manage.*, **2013**, *33*(3), 634-644.

12. M. Izquierdo and X. Querol, Leaching behaviour of elements from coal combustion fly ash: An overview, *Int. J. Coal Geol.*, **2012**, *94*, 54-66.
13. P.B. Joshi, D.V. Preda, D.A. Skyler, A. Tsinberg, B.D. Green and W.J. Marinelli, Recovery of rare earth elements and compounds from coal ash, *U.S. Patent*, US 20130287653, Oct 31, 2013.
14. G.-y. Adachi, N. Imanaka and S. Tamura, Research trends in rare earths: A preliminary analysis, *J. Rare Earths*, **2010**, *28*, 843-846.
15. A. Jordens, Y.P. Cheng and K.E. Waters, A review of the beneficiation of rare earth element bearing minerals, *Miner. Eng.*, **2013**, *41*, 97-114.
16. J.-C.G. Bünzli, *Lanthanides in Kirk-Othmer Encyclopedia of Chemical Technology*, John Wiley and Sons, Inc., 2013, 1-43.
17. I. McGill, *Rare Earth Elements in Ullmann's Encyclopedia of Industrial Chemistry*, Wiley-VCH Verlag GmbH & Co. KGaA, Weinheim, 2012, 183-228.
18. C.K. Gupta and N. Krishnamurthy, *Extractive Metallurgy of Rare Earths*, CRC Press, Boca Raton, Florida, 2004, 1-504.
19. J.B. Hedrick, U.S. Geological Survey, Mineral Commodity Summaries, Rare Earths, January 2010, 128-129, http://minerals.usgs.gov/minerals/pubs/commodity/rare_earths/mcs-2010-raree.pdf (29.8.2014).
20. K.R. Long, B.S. Van Gosen, N.K. Foley and D. Cordier, The principal rare earth elements deposits of the United States - A summary of domestic deposits and a global perspective, U.S. Department of the Interior, U.S. Geological Survey, Reston, Virginia, 2010, 1-96.
21. "Bastnasite-155010" by Rob Lavinsky/iRocks.com, from <http://commons.wikimedia.org/wiki/File:Bastnasite-155010.jpg#mediaviewer/File:Bastnasite-155010.jpg>, (17.9.2014).
22. "Monazite-(Ce)-202137" by Rob Lavinsky/iRocks.com, from [http://commons.wikimedia.org/wiki/File:Monazite-\(Ce\)-202137.jpg#mediaviewer/File:Monazite-\(Ce\)-202137.jpg](http://commons.wikimedia.org/wiki/File:Monazite-(Ce)-202137.jpg#mediaviewer/File:Monazite-(Ce)-202137.jpg), (17.9.2014).
23. "Xenotime with Rutile-08-2-78aa" by Rob Lavinsky/iRocks.com from http://commons.wikimedia.org/wiki/File:Xenotime_with_Rutile-08-2-78aa.jpg#mediaviewer/File:Xenotime_with_Rutile-08-2-78aa.jpg, (17.9.2014).

24. Z. Chen, Global rare earth resources and scenarios of future rare earth industry, *J. Rare Earths*, **2011**, 29(1), 1-6.
25. F. Xie, T.A. Zhang, D. Dreisinger and F. Doyle, A critical review on solvent extraction of rare earths from aqueous solutions, *Miner. Eng.*, **2014**, 56, 10-28.
26. S. Massari and M. Ruberti, Rare earth elements as critical raw materials: Focus on international markets and future strategies, *Resour. Policy*, **2013**, 38(1), 36-43.
27. S. Kihlman and L.S. Lauri, Kriittiset metallit ja mineraalit sekä niiden alueellinen jakautuminen ja esiintymispotentiaali Suomen ja Fennoskandian alueilla, Geologian tutkimuskeskus, Rovaniemi, 2013, 1-21.
28. Mineralprices.com - The Global Source for Metal Pricing, Mineral Fund Advisory PTY, <http://mineralprices.com/default.aspx#Rare> (5.9.2014).
29. R. Chi and Z. Xu, A solution chemistry approach to the study of rare earth element precipitation by oxalic acid, *Metall. Mater. Trans. B*, **1999**, 30B, 189-195.
30. D.A. Bertuol, A.M. Bernardes and J.A.S. Tenório, Spent NiMH batteries – The role of selective precipitation in the recovery of valuable metals, *J. Power Sources*, **2009**, 193(2), 914-923.
31. L. Pietrelli, B. Bellomo, D. Fontana and M. R. Montereali, Rare earths recovery from NiMH spent batteries, *Hydrometallurgy*, **2002**, 66(1-3), 135-139.
32. R.D. Abreu and C.A. Morais, Purification of rare earth elements from monazite sulphuric acid leach liquor and the production of high-purity ceric oxide, *Miner. Eng.*, **2010**, 23(6), 536-540.
33. H.-C. Kao, P.-S. Yen and R.-S. Juang, Solvent extraction of La(III) and Nd(III) from nitrate solutions with 2-ethylhexylphosphonic acid mono-2-ethylhexyl ester, *Chem. Eng. J. (Amsterdam, Neth.)*, **2006**, 119(2-3), 167-174.
34. W. Wang, Y. Pranolo and C.Y. Cheng, Recovery of scandium from synthetic red mud leach solutions by solvent extraction with D2EHPA, *Sep. Purif. Technol.*, **2013**, 108, 96-102.
35. J. Kraikaew, W. Srinuttrakul and C. Chayavadhanakur, Solvent extraction study of rare earths from nitrate medium by the mixtures of TBP and D2EHPA in kerosene, *J. Met., Mater. Miner.*, **2005**, 15(2), 89-95.

36. N. Song, X. Zhao, Q. Jia, W. Zhou and W. Liao, Extraction of rare earths using mixtures of sec-octylphenoxy acetic acid and organophosphorus acids, *Korean J. Chem. Eng.*, **2010**, 27(4), 1258-1261.
37. S. Radhika, B.N. Kumar, M.L. Kantam and B.R. Reddy, Liquid-liquid extraction and separation possibilities of heavy and light rare-earths from phosphoric acid solutions with acidic organophosphorus reagents, *Sep. Purif. Technol.*, **2010**, 75(3), 295-302.
38. S. Radhika, B. Nagaphani Kumar, M. Lakshmi Kantam and B. Ramachandra Reddy, Solvent extraction and separation of rare-earths from phosphoric acid solutions with TOPS 99, *Hydrometallurgy*, **2011**, 110(1-4), 50-55.
39. A.E. Giles, C. Aldrich and J.S.J. van Deventer, Modelling of rare earth solvent extraction with artificial neural nets, *Hydrometallurgy*, **1996**, 43(1-3), 241-255.
40. M. Ochsenkühn-Petropulu, T. Lyberopulu and G. Parissakis, Selective separation and determination of scandium from yttrium and lanthanides in red mud by a combined ion exchange/solvent extraction method, *Anal. Chim. Acta*, **1995**, 315(1-2), 231-237.
41. H. Chang, M. Li, Z. Liu, Y. Hu and F. Zhang, Study on separation of rare earth elements in complex system, **2010**, 28(Supplement 1), *J. Rare Earths*, 116-119.
42. D. Wu, Q. Zhang and B. Bao, Solvent extraction of Pr and Nd (III) from chloride-acetate medium by 8-hydroquinoline with and without 2-ethylhexyl phosphoric acid mono-2-ethylhexyl ester as an added synergist in heptane diluent, *Hydrometallurgy*, **2007**, 88(1-4), 210-215.
43. M.-S. Lee, J.-Y. Lee, J.-S. Kim and G.-S. Lee, Solvent extraction of neodymium ions from hydrochloric acid solution using PC88A and saponified PC88A, *Sep. Purif. Technol.*, **2005**, 46(1-2), 72-78.
44. P. Miranda Jr. and L.B. Zinner, Separation of samarium and gadolinium solutions by solvent extraction, *J. Alloys Compd.*, **1997**, 249(1-2), 116-118.
45. D. Fontana and L. Pietrelli, Separation of middle rare earths by solvent extraction using 2-ethylhexylphosphonic acid mono-2-ethylhexyl ester as an extractant, *J. Rare Earths*, **2009**, 27(5), 830-833.
46. V.V. Belova, A.A. Voshkin, N.S. Egorova and A.I. Kholkin, Solvent extraction of rare earth metals from nitrate solutions with di(2,4,4-trimethylpentyl) phosphinate of methyltrioctylammonium, *J. Mol. Liq.*, **2012**, 172, 144-146.

47. M. Anitha, M.K. Kotekar, D.K. Singh, R. Vijayalakshmi and H. Singh, Solvent extraction studies on rare earths from chloride medium with organo-phosphorous extractant dinonyl phenyl phosphoric acid, *Hydrometallurgy*, **2014**, *146*, 128-132.
48. Q. Jia, S. Tong, Z. Li, W. Zhou, H. Li and S. Meng, Solvent extraction of rare earth elements with mixtures of sec-octylphenoxy acetic acid and bis(2,4,4-trimethylpentyl) dithiophosphinic acid, *Sep. Purif. Technol.*, **2009**, *64*(3), 345-350.
49. K. Kondo, L.X. Tao and M. Matsumoto, Extraction equilibrium and kinetics of neodymium with diisodecylphosphoric acid, *Hydrometallurgy*, **1997**, *44*(3), 321-330.
50. J.S. Preston, P.M. Cole, W.M. Craig and A.M. Feather, The recovery of rare earth oxides from a phosphoric acid by-product. Part 1: Leaching of rare earth values and recovery of a mixed rare earth oxide by solvent extraction, *Hydrometallurgy*, **1996**, *41*(1), 1-19.
51. S.V. Vassilev, D. Baxter, L.K. Andersen and C.G. Vassileva, An overview of the composition and application of biomass ash. Part 1. Phase-mineral and chemical composition and classification, *Fuel*, **2013**, *105*, 40-76.
52. S.V. Vassilev, D. Baxter, L.K. Andersen and C.G. Vassileva, An overview of the composition and application of biomass ash. Part 2. Potential utilisation, technological and ecological advantages and challenges, *Fuel*, **2013**, *105*, 19-39.
53. R.S. Blissett, N. Smalley and N.A. Rowson, An investigation into six coal fly ashes from the United Kingdom and Poland to evaluate rare earth element content, *Fuel*, **2014**, *119*, 236-239.
54. J.C. Hower, J.G. Groppo, P. Joshi, S. Dai, D.P. Moecher and M.N. Johnston, Location of cerium in coal-combustion fly ashes: Implications for recovery of lanthanides, *Coal Combustion and Gasification Products*, **2013**, *5*, 73-78.
55. C.J. Warren and M.J. Dudas, Leachability and partitioning of elements in ferromagnetic fly ash particles, *Sci. Total Environ.*, **1989**, *83*(1-2), 99-111.
56. J.C. Hower, S. Dai, V.V. Seredin, L. Zhao, I.J. Kostova, L.F.O. Silva, S.M. Mardon and G. Gurdal, A note on the occurrence of yttrium and rare earth elements in coal combustion products, *Coal Combustion and Gasification Products*, **2013**, *5*, 39-47.

57. M.P. Ketris and Y.E. Yudovich, Estimations of clarkes for carbonaceous biolithes: World averages for trace element contents in black shales and coals, *Int. J. Coal Geol.*, **2009**, 78(2), 135-148.
58. S.M. Mardon and J.C. Hower, Impact of coal properties on coal combustion by-product quality: examples from a Kentucky power plant, *Int. J. Coal Geol.*, **2004**, 59(3-4), 153-169.
59. D. Smolka-Danielowska, Rare earth elements in fly ashes created during the coal burning process in certain coal-fired power plants operating in Poland – Upper Silesian industrial region, *J. Environ. Radioact.*, **2010**, 101(11), 965-968.
60. Y. Zhang, Z. Jiang, M. He and B. Hu, Determination of trace rare earth elements in coal fly ash and atmospheric particulates by electrothermal vaporization inductively coupled plasma mass spectrometry with slurry sampling, *Environ. Pollut. (Amsterdam, Neth.)*, **2007**, 148(2), 459-467.
61. C. Block and R. Dams, Study of fly ash emission during combustion of coal, *Environ. Sci. Technol.*, **1976**, 10(10), 1011-1017.
62. C. Block and R. Dams, Inorganic composition of Belgian coals and coal ashes, *Environ. Sci. Technol.*, **1975**, 9(2), 146-150.
63. J.A. Campbell, J.C. Laul, K.K. Nielson and R.D. Smith, Separation and chemical characterization of finely-sized fly-ash particles, *Anal. Chem.*, **1978**, 50(8), 1032-1040.
64. D.G. Coles, R.C. Ragaini, J.M. Ondov, G.L. Fisher, D. Silberman and B.A. Prentice, Chemical studies of stack fly ash from a coal-fired power plant, *Environ. Sci. Technol.*, **1979**, 13(4), 455-459.
65. L.D. Hansen and G.L. Fisher, Elemental distribution in coal fly ash particles, *Environ. Sci. Technol.*, **1980**, 14(9), 1111-1117.
66. J. Ribeiro, B. Valentim, C. Ward and D. Flores, Comprehensive characterization of anthracite fly ash from a thermo-electric power plant and its potential environmental impact, *Int. J. Coal Geol.*, **2011**, 86(2-3), 204-212.
67. L.F.O. Silva, A. Jasper, M.L. Andrade, C.H. Sampaio, S. Dai, X. Li, T. Li, W. Chen, X. Wang, H. Liu, L. Zhao, S.G. Hopps, R.F. Jewell and J.C. Hower, Applied investigation on the interaction of hazardous elements binding on ultrafine and nanoparticles in Chinese anthracite-derived fly ash, *Sci. Total Environ.*, **2012**, 419, 250-264.

68. D.B. Mayfield and A.S. Lewis, Environmental review of coal ash as a resource for rare earth and strategic elements, *World of Coal Ash (WOCA) Conference*, Lexington, Kentucky, USA, 2013.
69. H. Hasegawa, I.M. Rahman, Y. Egawa, H. Sawai, Z.A. Begum, T. Maki and S. Mizutani, Recovery of the Rare Metals from Various Waste Ashes with the Aid of Temperature and Ultrasound Irradiation Using Chelants, *Water, Air, Soil Pollut.*, **2014**, 225(9), 1-13.
70. S. Kashiwakura, Y. Kumagai, H. Kubo and K. Wagatsuma, Dissolution of rare earth elements from coal fly ash particles in a dilute H₂SO₄ solvent, *Open J. Phys. Chem.*, **2013**, 3(2), 69-75.
71. V.V. Seredin, A new method for primary evaluation of the outlook for rare earth element ores, *Geol. Ore Deposits (Transl. of Geol. Rudn. Mestorozhd.)*, **2010**, 52(5), 428-433.
72. J. Nölte, *ICP Emission Spectrometry: A Practical Guide*, Wiley-VCH Verlag GmbH & Co., Weinheim, 2003, 1-267.
73. Optima 8x00 Series ICP-OES Flat Plate Plasma System, Technical note, PerkinElmer Inc., Waltham, USA, 2012, http://www.perkinelmer.com/CMSResources/Images/44-136952TCH_Optima8x00FlatPlatePlasmaSys.pdf, (10.10.2014).
74. P.W.J.M. Boumans, *Inductively Coupled Plasma Emission Spectroscopy Part. 1: Methodology, Instrumentation, and Performance, in Chemical Analysis, Vol. 90*, John Wiley & Sons, Inc., New York, USA, 1987, 1-583.
75. Meinhard high efficiency glass concentric nebulizers, <https://www.meinhard.com/index.cfm/category/109/high-efficiency-nebulizers-glass.cfm>, Meinhard, (22.11.2014).
76. Agilent OneNeb nebulizer, <http://www.chem.agilent.com/en-US/promotions/pages/oneneb.aspx>, Agilent, (22.11.2014).
77. J.-L. Todoli, J.-M. Mermet, *Liquid Sample Introduction in ICP Spectrometry: A Practical Guide*, Elsevier, Amsterdam, The Netherlands, 2008, 1-289.
78. Glass Expansion Tracey TFE - HF-resistant spray chambers for ICP-OES, http://www.geicp.com/cgi-bin/site/wrapper.pl?c1=Products_spray_bytype_tracetfe, (22.11.2014).

79. E. Tognoni, M. Hidalgo, A. Canals, G. Cristoforetti, S. Legnaioli, A. Salvetti and V. Palleschi, Combination of the ionic-to-atomic line intensity ratios from two test elements for the diagnostic of plasma temperature and electron number density in inductively coupled plasma atomic emission spectroscopy, *Spectrochim. Acta, Part B*, **2007**, 62B(5), 435-443.
80. J.-M. Mermet, Use of magnesium as a test element for inductively coupled plasma atomic emission spectrometry diagnostics, *Anal. Chim. Acta*, **1991**, 250(1), 85-94.
81. J. Dennaud, A. Howes, E. Poussel and J.-M. Mermet, Study of ionic-to-atomic line intensity ratios for two axial viewing-based inductively coupled plasma atomic emission spectrometers, *Spectrochim. Acta, Part B*, **2001**, 56B(1), 101-112.
82. N. Velitchkova, S. Velichkov and N. Daskalova, Inductively coupled plasma atomic emission spectrometry – Optimization of the operating conditions in the determination of trace of elements in line-rich emission matrices, *Spectrochim. Acta, Part B*, **2007**, 62B(4), 386-402.
83. Fitted Background Correction (FBC) - fast, accurate and fully automated background correction, Technical Overview, 5100 ICP-OES, Agilent Technologies, 2014,
http://www.chem.agilent.com/Library/technicaloverviews/Public/5991-4836EN_TechOview_5100_FBC.pdf (13.10.2014).
84. J.-L. Todolí and J.-M. Mermet, Acid interferences in atomic spectrometry: analyte signal effects and subsequent reduction, *Spectrochim. Acta, Part B*, **1999**, 54B(6), 895-929.
85. M. Grotti, R. Leardi and R. Frache, Combined effects of inorganic acids in inductively coupled plasma optical emission spectrometry, *Spectrochim. Acta, Part B*, **2002**, 57B(12), 1915-1924.
86. J.-L. Todoli, S. Maestre, J. Mora, A. Canals and V. Hernandis, Comparison of several spray chambers operating at very low liquid flow rates in inductively coupled plasma atomic emission spectrometry, *Fresenius' J. Anal. Chem.*, **2000**, 368(8), 773-779.
87. S. Maestre, J. Mora, J.-L. Todoli and A. Canals, Evaluation of several commercially available spray chambers for use in inductively coupled plasma atomic emission spectrometry, *J. Anal. At. Spectrom.*, **1999**, 14(1), 61-67.

88. M.S. Pavlovic, M.M. Kuzmanovic, V.M. Pavelkic and M. Marinkovic, The role of demixing effect in analyte emission enhancement by easily ionized elements in d.c. plasma, *Spectrochim. Acta, Part B*, **2000**, 55B(8), 1373-1384.
89. X. Romero, E. Poussel and J.-M. Mermet, The effect of sodium on analyte ionic line intensities in inductively coupled plasma atomic emission spectrometry: influence of the operating conditions, *Spectrochim. Acta, Part B*, **1997**, 52B(4), 495-502.
90. I.B. Brenner, J.M. Mermet, I. Segal and G.L. Long, Effect of nitric and hydrochloric acids on rare earth element (REE) intensities in inductively coupled plasma emission spectrometry, *Spectrochim. Acta, Part B*, **1995**, 50B(4-7), 323-331.
91. I.B. Brenner, I. Segal, M. Mermet and J.M. Mermet, Study of the depressive effects of nitric acid on the line intensities of rare earth elements in inductively coupled plasma atomic emission spectrometry, *Spectrochim. Acta, Part B*, **1995**, 50B(4-7), 333-340.
92. Real-time spectral correction of complex samples using FACT spectral deconvolution software, Technical Overview, 5100 ICP-OES, Agilent Technologies, 2014,
http://www.chem.agilent.com/Library/technicaloverviews/Public/5991-4837EN_TechOview_5100_FACT.pdf (13.10.2014).
93. Multicomponent Spectral Fitting, Technical note, PerkinElmer Inc., Waltham, USA, 2009,
http://www.perkinelmer.com/CMSResources/Images/44-130615TCH_OptimaMSF.pdf, (10.10.2014).
94. H. Kola and P. Perämäki, The study of the selection of emission lines and plasma operating conditions for efficient internal standardization in inductively coupled plasma optical emission spectrometry, *Spectrochim. Acta, Part B*, **2004**, 59B(2), 231-242.
95. X. Romero, E. Poussel and J.M. Mermet, Influence of the operating conditions on the efficiency of internal standardization in inductively coupled plasma atomic emission spectrometry, *Spectrochim. Acta, Part B*, **1997**, 52B(4), 487-493.
96. C. Dubuisson, E. Poussel and J.M. Mermet, Comparison of ionic line-based internal standardization with axially and radially viewed inductively coupled plasma atomic emission spectrometry to compensate for sodium effects on accuracy, *J. Anal. At. Spectrom.*, **1998**, 13(11), 1265-1269.

97. D.C. Baxter and I. Rodushkin, *Calibration Approaches for Trace Element Determination*, in *Comprehensive Analytical Chemistry*, edited by D. Barceló, Volume XLI, Elsevier, Amsterdam, The Netherlands, 2003, 47-92.
98. J.C. Miller and J.N. Miller, *Statistics and Chemometrics for Analytical Chemistry*, 4th Edition, Pearson Education Limited, Harlow, U.K., 2000, 1-271.
99. International vocabulary of metrology - Basic and general concepts and associated terms (VIM), 3rd edition, JGCM 200:2012, 1-91.
100. P. Quevauviller, *Sample Preparation for Trace Element Analysis*, in *Comprehensive Analytical Chemistry*, edited by D. Barceló, Volume XLI, Elsevier, Amsterdam, The Netherlands, 2003, 93-115.
101. A. Ilander and A. Väisänen, An ultrasound-assisted digestion method for the determination of toxic element concentrations in ash samples by inductively coupled plasma optical emission spectrometry, *Anal. Chim. Acta.*, **2007**, 602(2), 195-201.
102. EPA-Method 3052, Microwave assisted acid digestion of siliceous and organically based matrices, 1996.
103. A. Väisänen, J. Valkonen, S. Perämäki, V. Soikkeli and R. Ryymin, Menetelmä tuhkan, erityisesti lentotuhkan, käsittelemiseksi, Patent number 123432, 2013, 1-20.
104. A. Canals, V. Hernandis, J.L. Todolí and R.F. Browner, Fundamental studies on pneumatic generation and aerosol transport in atomic spectrometry: effect of mineral acids on emission intensity in inductively coupled plasma atomic emission spectrometry, *Spectrochim. Acta, Part B*, **1995**, 50B(4-7), 305-321.
105. T.J. Mason, *Sonochemistry: The Uses of Ultrasound in Chemistry*, The Royal Society of Chemistry, Cambridge, 1990, 1-157.
106. W. Wang and C.Y. Cheng, Separation and purification of scandium by solvent extraction and related technologies: a review, *J. Chem. Technol. Biotechnol.*, **2011**, 86(10), 1237-1246.

DEPARTMENT OF CHEMISTRY, UNIVERSITY OF JYVÄSKYLÄ
RESEARCH REPORT SERIES

1. Vuolle, Mikko: Electron paramagnetic resonance and molecular orbital study of radical ions generated from (2.2)metacyclophane, pyrene and its hydrogenated compounds by alkali metal reduction and by thallium(III)trifluoroacetate oxidation. (99 pp.) 1976
2. Pasanen, Kaija: Electron paramagnetic resonance study of cation radical generated from various chlorinated biphenyls. (66 pp.) 1977
3. Carbon-13 Workshop, September 6-8, 1977. (91 pp.) 1977
4. Laihia, Katri: On the structure determination of norbornane polyols by NMR spectroscopy. (111 pp.) 1979
5. Nyrönen, Timo: On the EPR, ENDOR and visible absorption spectra of some nitrogen containing heterocyclic compounds in liquid ammonia. (76 pp.) 1978
6. Talvitie, Antti: Structure determination of some sesquiterpenoids by shift reagent NMR. (54 pp.) 1979
7. Häkli, Harri: Structure analysis and molecular dynamics of cyclic compounds by shift reagent NMR. (48 pp.) 1979
8. Pitkänen, Ilkka: Thermodynamics of complexation of 1,2,4-triazole with divalent manganese, cobalt, nickel, copper, zinc, cadmium and lead ions in aqueous sodium perchlorate solutions. (89 pp.) 1980
9. Asunta, Tuula: Preparation and characterization of new organometallic compounds synthesized by using metal vapours. (91 pp.) 1980
10. Sattar, Mohammad Abdus: Analyses of MCPA and its metabolites in soil. (57 pp.) 1980
11. Bibliography 1980. (31 pp.) 1981
12. Knuutila, Pekka: X-Ray structural studies on some divalent 3d metal compounds of picolinic and isonicotinic acid N-oxides. (77 pp.) 1981
13. Bibliography 1981. (33 pp.) 1982
14. 6th National NMR Symposium, September 9-10, 1982, Abstracts. (49 pp.) 1982
15. Bibliography 1982. (38 pp.) 1983
16. Knuutila, Hilikka: X-Ray structural studies on some Cu(II), Co(II) and Ni(II) complexes with nicotinic and isonicotinic acid N-oxides. (54 pp.) 1983
17. Symposium on inorganic and analytical chemistry May 18, 1984, Program and Abstracts. (100 pp.) 1984
18. Knuutinen, Juha: On the synthesis, structure verification and gas chromatographic determination of chlorinated catechols and guaiacols occurring in spent bleach liquors of kraft pulp mill. (30 pp.) 1984
19. Bibliography 1983. (47 pp.) 1984
20. Pitkänen, Maija: Addition of BrCl, B₂ and Cl₂ to methyl esters of propenoic and 2-butenic acid derivatives and ¹³C NMR studies on methyl esters of saturated aliphatic mono- and dichlorocarboxylic acids. (56 pp.) 1985
21. Bibliography 1984. (39 pp.) 1985
22. Salo, Esa: EPR, ENDOR and TRIPLE spectroscopy of some nitrogen heteroaromatics in liquid ammonia. (111 pp.) 1985
23. Humppi, Tarmo: Synthesis, identification and analysis of dimeric impurities of chlorophenols. (39 pp.) 1985
24. Aho, Martti: The ion exchange and adsorption properties of sphagnum peat under acid conditions. (90 pp.) 1985
25. Bibliography 1985 (61 pp.) 1986
26. Bibliography 1986. (23 pp.) 1987
27. Bibliography 1987. (26 pp.) 1988
28. Paasivirta, Jaakko (Ed.): Structures of organic environmental chemicals. (67 pp.) 1988
29. Paasivirta, Jaakko (Ed.): Chemistry and ecology of organo-element compounds. (93 pp.) 1989
30. Sinkkonen, Seija: Determination of crude oil alkylated dibenzothiophenes in environment. (35 pp.) 1989
31. Kolehmainen, Erkki (Ed.): XII National NMR Symposium Program and Abstracts. (75 pp.) 1989
32. Kuokkanen, Tauno: Chlorocymenes and Chlorocymenenes: Persistent chlorocompounds in spent bleach liquors of kraft pulp mills. (40 pp.) 1989
33. Mäkelä, Reijo: ESR, ENDOR and TRIPLE resonance study on substituted 9,10-anthraquinone radicals in solution. (35 pp.) 1990
34. Veijanen, Anja: An integrated sensory and analytical method for identification of off-flavour compounds. (70 pp.) 1990
35. Kasa, Seppo: EPR, ENDOR and TRIPLE resonance and molecular orbital studies on a substitution reaction of anthracene induced by thallium(III) in two fluorinated carboxylic acids. (114 pp.) 1990
36. Herve, Sirpa: Mussel incubation method for monitoring organochlorine compounds in freshwater recipients of pulp and paper industry. (145 pp.) 1991
37. Pohjola, Pekka: The electron paramagnetic resonance method for characterization of Finnish peat types and iron (III) complexes in the process of peat decomposition. (77 pp.) 1991

DEPARTMENT OF CHEMISTRY, UNIVERSITY OF JYVÄSKYLÄ
RESEARCH REPORT SERIES

38. Paasivirta, Jaakko (Ed.): Organochlorines from pulp mills and other sources. Research methodology studies 1988-91. (120 pp.) 1992
39. Veijanen, Anja (Ed.): VI National Symposium on Mass Spectrometry, May 13-15, 1992, Abstracts. (55 pp.) 1992
40. Rissanen, Kari (Ed.): The 7. National Symposium on Inorganic and Analytical Chemistry, May 22, 1992, Abstracts and Program. (153 pp.) 1992
41. Paasivirta, Jaakko (Ed.): CEOEC'92, Second Finnish-Russian Seminar: Chemistry and Ecology of Organo-Element Compounds. (93 pp.) 1992
42. Koistinen, Jaana: Persistent polychloroaromatic compounds in the environment: structure-specific analyses. (50 pp.) 1993
43. Virkki, Liisa: Structural characterization of chlorolignins by spectroscopic and liquid chromatographic methods and a comparison with humic substances. (62 pp.) 1993
44. Helenius, Vesa: Electronic and vibrational excitations in some biologically relevant molecules. (30 pp.) 1993
45. Leppä-aho, Jaakko: Thermal behaviour, infrared spectra and x-ray structures of some new rare earth chromates(VI). (64 pp.) 1994
46. Kotila, Sirpa: Synthesis, structure and thermal behavior of solid copper(II) complexes of 2-amino-2-hydroxymethyl-1,3-propanediol. (111 pp.) 1994
47. Mikkonen, Anneli: Retention of molybdenum(VI), vanadium(V) and tungsten(VI) by kaolin and three Finnish mineral soils. (90 pp.) 1995
48. Suontamo, Reijo: Molecular orbital studies of small molecules containing sulfur and selenium. (42 pp.) 1995
49. Hämäläinen, Jouni: Effect of fuel composition on the conversion of fuel-N to nitrogen oxides in the combustion of small single particles. (50 pp.) 1995
50. Nevalainen, Tapio: Polychlorinated diphenyl ethers: synthesis, NMR spectroscopy, structural properties, and estimated toxicity. (76 pp.) 1995
51. Aittola, Jussi-Pekka: Organochloro compounds in the stack emission. (35 pp.) 1995
52. Harju, Timo: Ultrafast polar molecular photophysics of (dibenzylmethine)borondifluoride and 4-aminophthalimide in solution. (61 pp.) 1995
53. Maatela, Paula: Determination of organically bound chlorine in industrial and environmental samples. (83 pp.) 1995
54. Paasivirta, Jaakko (Ed.): CEOEC'95, Third Finnish-Russian Seminar: Chemistry and Ecology of Organo-Element Compounds. (109 pp.) 1995
55. Huuskonen, Juhani: Synthesis and structural studies of some supramolecular compounds. (54 pp.) 1995
56. Palm, Helena: Fate of chlorophenols and their derivatives in sawmill soil and pulp mill recipient environments. (52 pp.) 1995
57. Rantio, Tiina: Chlorohydrocarbons in pulp mill effluents and their fate in the environment. (89 pp.) 1997
58. Ratilainen, Jari: Covalent and non-covalent interactions in molecular recognition. (37 pp.) 1997
59. Kolehmainen, Erkki (Ed.): XIX National NMR Symposium, June 4-6, 1997, Abstracts. (89 pp.) 1997
60. Matilainen, Rose: Development of methods for fertilizer analysis by inductively coupled plasma atomic emission spectrometry. (41 pp.) 1997
61. Koistinen, Jari (Ed.): Spring Meeting on the Division of Synthetic Chemistry, May 15-16, 1997, Program and Abstracts. (36 pp.) 1997
62. Lappalainen, Kari: Monomeric and cyclic bile acid derivatives: syntheses, NMR spectroscopy and molecular recognition properties. (50 pp.) 1997
63. Laitinen, Eira: Molecular dynamics of cyanine dyes and phthalimides in solution: picosecond laser studies. (62 pp.) 1997
64. Eloranta, Jussi: Experimental and theoretical studies on some quinone and quinol radicals. (40 pp.) 1997
65. Oksanen, Jari: Spectroscopic characterization of some monomeric and aggregated chlorophylls. (43 pp.) 1998
66. Häkkänen, Heikki: Development of a method based on laser-induced plasma spectrometry for rapid spatial analysis of material distributions in paper coatings. (60 pp.) 1998
67. Virtapohja, Janne: Fate of chelating agents used in the pulp and paper industries. (58 pp.) 1998
68. Airola, Karri: X-ray structural studies of supramolecular and organic compounds. (39 pp.) 1998
69. Hyötyläinen, Juha: Transport of lignin-type compounds in the receiving waters of pulp mills. (40 pp.) 1999
70. Ristolainen, Matti: Analysis of the organic material dissolved during totally chlorine-free bleaching. (40 pp.) 1999
71. Eklin, Tero: Development of analytical procedures with industrial samples for atomic emission and atomic absorption spectrometry. (43 pp.) 1999

DEPARTMENT OF CHEMISTRY, UNIVERSITY OF JYVÄSKYLÄ
RESEARCH REPORT SERIES

72. Väliisaari, Jouni: Hygiene properties of resol-type phenolic resin laminates. (129 pp.) 1999
73. Hu, Jiwei: Persistent polyhalogenated diphenyl ethers: model compounds syntheses, characterization and molecular orbital studies. (59 pp.) 1999
74. Malkavaara, Petteri: Chemometric adaptations in wood processing chemistry. (56 pp.) 2000
75. Kujala Elena, Laihia Katri, Nieminen Kari (Eds.): NBC 2000, Symposium on Nuclear, Biological and Chemical Threats in the 21st Century. (299 pp.) 2000
76. Rantalainen, Anna-Lea: Semipermeable membrane devices in monitoring persistent organic pollutants in the environment. (58 pp.) 2000
77. Lahtinen, Manu: *In situ* X-ray powder diffraction studies of Pt/C, CuCl/C and Cu₂O/C catalysts at elevated temperatures in various reaction conditions. (92 pp.) 2000
78. Tamminen, Jari: Syntheses, empirical and theoretical characterization, and metal cation complexation of bile acid-based monomers and open/closed dimers. (54 pp.) 2000
79. Vatanen, Virpi: Experimental studies by EPR and theoretical studies by DFT calculations of α -amino-9,10-anthraquinone radical anions and cations in solution. (37 pp.) 2000
80. Kotilainen, Risto: Chemical changes in wood during heating at 150-260 °C. (57 pp.) 2000
81. Nissinen, Maija: X-ray structural studies on weak, non-covalent interactions in supramolecular compounds. (69 pp.) 2001
82. Wegelius, Elina: X-ray structural studies on self-assembled hydrogen-bonded networks and metallosupramolecular complexes. (84 pp.) 2001
83. Paasivirta, Jaakko (Ed.): CEOEC'2001, Fifth Finnish-Russian Seminar: Chemistry and Ecology of Organo-Element Compounds. (163 pp.) 2001
84. Kiljunen, Toni: Theoretical studies on spectroscopy and atomic dynamics in rare gas solids. (56 pp.) 2001
85. Du, Jin: Derivatives of dextran: synthesis and applications in oncology. (48 pp.) 2001
86. Koivisto, Jari: Structural analysis of selected polychlorinated persistent organic pollutants (POPs) and related compounds. (88 pp.) 2001
87. Feng, Zhinan: Alkaline pulping of non-wood feedstocks and characterization of black liquors. (54 pp.) 2001
88. Halonen, Markku: Lahon havupuun käyttö sulfaattiprosessin raaka-aineena sekä havupuun lahontorjunta. (90 pp.) 2002
89. Falábu, Dezső: Synthesis, conformational analysis and complexation studies of resorcarene derivatives. (212 pp.) 2001
90. Lehtovuori, Pekka: EMR spectroscopic studies on radicals of ubiquinones Q-n, vitamin K₃ and vitamin E in liquid solution. (40 pp.) 2002
91. Perkkalainen, Paula: Polymorphism of sugar alcohols and effect of grinding on thermal behavior on binary sugar alcohol mixtures. (53 pp.) 2002
92. Ihalainen, Janne: Spectroscopic studies on light-harvesting complexes of green plants and purple bacteria. (42 pp.) 2002
93. Kunttu, Henrik, Kiljunen, Toni (Eds.): 4th International Conference on Low Temperature Chemistry. (159 pp.) 2002
94. Väisänen, Ari: Development of methods for toxic element analysis in samples with environmental concern by ICP-AES and ETAAS. (54 pp.) 2002
95. Luostarinen, Minna: Synthesis and characterisation of novel resorcarene derivatives. (200 pp.) 2002
96. Louhelainen, Jarmo: Changes in the chemical composition and physical properties of wood and nonwood black liquors during heating. (68 pp.) 2003
97. Lahtinen, Tanja: Concave hydrocarbon cyclophane B-prisms. (65 pp.) 2003
98. Laihia, Katri (Ed.): NBC 2003, Symposium on Nuclear, Biological and Chemical Threats – A Crisis Management Challenge. (245 pp.) 2003
99. Oasmaa, Anja: Fuel oil quality properties of wood-based pyrolysis liquids. (32 pp.) 2003
100. Virtanen, Elina: Syntheses, structural characterisation, and cation/anion recognition properties of nano-sized bile acid-based host molecules and their precursors. (123 pp.) 2003
101. Nättinen, Kalle: Synthesis and X-ray structural studies of organic and metallo-organic supramolecular systems. (79 pp.) 2003
102. Lampiselkä, Jarkko: Demonstraatio lukion kemian opetuksessa. (285 pp.) 2003
103. Kallioinen, Jani: Photoinduced dynamics of Ru(dcbpy)₂(NCS)₂ – in solution and on nanocrystalline titanium dioxide thin films. (47 pp.) 2004
104. Valkonen, Arto (Ed.): VII Synthetic Chemistry Meeting and XXVI Finnish NMR Symposium. (103 pp.) 2004
105. Vaskonen, Kari: Spectroscopic studies on atoms and small molecules isolated in low temperature rare gas matrices. (65 pp.) 2004
106. Lehtovuori, Viivi: Ultrafast light induced dissociation of Ru(dcbpy)(CO)₂I₂ in solution. (49 pp.) 2004
107. Saarenketo, Pauli: Structural studies of metal complexing schiff bases, Schiff base derived

DEPARTMENT OF CHEMISTRY, UNIVERSITY OF JYVÄSKYLÄ
RESEARCH REPORT SERIES

- N*-glycosides and cyclophane π -prisms. (95 pp.) 2004
108. Paasivirta, Jaakko (Ed.): CEOEC'2004, Sixth Finnish-Russian Seminar: Chemistry and Ecology of Organo-Element Compounds. (147 pp.) 2004
109. Suontamo, Tuula: Development of a test method for evaluating the cleaning efficiency of hard-surface cleaning agents. (96 pp.) 2004
110. Güneş, Minna: Studies of thiocyanates of silver for nonlinear optics. (48 pp.) 2004
111. Ropponen, Jarmo: Aliphatic polyester dendrimers and dendrons. (81 pp.) 2004
112. Vu, Mân Thi Hong: Alkaline pulping and the subsequent elemental chlorine-free bleaching of bamboo (*Bambusa procera*). (69 pp.) 2004
113. Mansikkamäki, Heidi: Self-assembly of resorcinarenes. (77 pp.) 2006
114. Tuononen, Heikki M.: EPR spectroscopic and quantum chemical studies of some inorganic main group radicals. (79 pp.) 2005
115. Kaski, Saara: Development of methods and applications of laser-induced plasma spectroscopy in vacuum ultraviolet. (44 pp.) 2005
116. Mäkinen, Riika-Mari: Synthesis, crystal structure and thermal decomposition of certain metal thiocyanates and organic thiocyanates. (119 pp.) 2006
117. Ahokas, Jussi: Spectroscopic studies of atoms and small molecules isolated in rare gas solids: photodissociation and thermal reactions. (53 pp.) 2006
118. Busi, Sara: Synthesis, characterization and thermal properties of new quaternary ammonium compounds: new materials for electrolytes, ionic liquids and complexation studies. (102 pp.) 2006
119. Mäntykoski, Keijo: PCBs in processes, products and environment of paper mills using wastepaper as their raw material. (73 pp.) 2006
120. Laamanen, Pirkko-Leena: Simultaneous determination of industrially and environmentally relevant aminopolycarboxylic and hydroxycarboxylic acids by capillary zone electrophoresis. (54 pp.) 2007
121. Salmela, Maria: Description of oxygen-alkali delignification of kraft pulp using analysis of dissolved material. (71 pp.) 2007
122. Lehtovaara, Lauri: Theoretical studies of atomic scale impurities in superfluid ^4He . (87 pp.) 2007
123. Rautiainen, J. Mikko: Quantum chemical calculations of structures, bonding, and spectroscopic properties of some sulphur and selenium iodine cations. (71 pp.) 2007
124. Nummelin, Sami: Synthesis, characterization, structural and retrostructural analysis of self-assembling pore forming dendrimers. (286 pp.) 2008
125. Sopo, Harri: Uranyl(VI) ion complexes of some organic aminobisphenolate ligands: syntheses, structures and extraction studies. (57 pp.) 2008
126. Valkonen, Arto: Structural characteristics and properties of substituted cholanoates and *N*-substituted cholanamides. (80 pp.) 2008
127. Lähde, Anna: Production and surface modification of pharmaceutical nano- and microparticles with the aerosol flow reactor. (43 pp.) 2008
128. Beyeh, Ngong Kodiah: Resorcinarenes and their derivatives: synthesis, characterization and complexation in gas phase and in solution. (75 pp.) 2008
129. Väliisaari, Jouni, Lundell, Jan (Eds.): Kemiaan opetuksen päivät 2008: uusia oppimisympäristöjä ja ongelmalähtöistä opetusta. (118 pp.) 2008
130. Myllyperkiö, Pasi: Ultrafast electron transfer from potential organic and metal containing solar cell sensitizers. (69 pp.) 2009
131. Käkölä, Jaana: Fast chromatographic methods for determining aliphatic carboxylic acids in black liquors. (82 pp.) 2009
132. Koivukorpi, Juha: Bile acid-arene conjugates: from photoswitchability to cancer cell detection. (67 pp.) 2009
133. Tuuttila, Tero: Functional dendritic polyester compounds: synthesis and characterization of small bifunctional dendrimers and dyes. (74 pp.) 2009
134. Salorinne, Kirsi: Tetramethoxy resorcinarene based cation and anion receptors: synthesis, characterization and binding properties. (79 pp.) 2009
135. Rautiainen, Riikka: The use of first-thinning Scots pine (*Pinus sylvestris*) as fiber raw material for the kraft pulp and paper industry. (73 pp.) 2010
136. Ilander, Laura: Uranyl salophens: synthesis and use as ditopic receptors. (199 pp.) 2010
137. Kiviniemi, Tiina: Vibrational dynamics of iodine molecule and its complexes in solid krypton - Towards coherent control of bimolecular reactions? (73 pp.) 2010
138. Ikonen, Satu: Synthesis, characterization and structural properties of various covalent and non-covalent bile acid derivatives of N/O-heterocycles and their precursors. (105 pp.) 2010
139. Siitonen, Anni: Spectroscopic studies of semiconducting single-walled carbon nanotubes. (56 pp.) 2010
140. Raatikainen, Kari: Synthesis and structural studies of piperazine cyclophanes –

- Supramolecular systems through Halogen and Hydrogen bonding and metal ion coordination. (69 pp.) 2010
141. Leivo, Kimmo: Gelation and gel properties of two- and three-component Pyrene based low molecular weight organogelators. (116 pp.) 2011
142. Martiskainen, Jari: Electronic energy transfer in light-harvesting complexes isolated from *Spinacia oleracea* and from three photosynthetic green bacteria *Chloroflexus aurantiacus*, *Chlorobium tepidum*, and *Prosthecochloris aestuarii*. (55 pp.) 2011
143. Wichmann, Oula: Syntheses, characterization and structural properties of [O,N,O,X] aminobisphenolate metal complexes. (101 pp.) 2011
144. Ilander, Aki: Development of ultrasound-assisted digestion methods for the determination of toxic element concentrations in ash samples by ICP-OES. (58 pp.) 2011
145. The Combined XII Spring Meeting of the Division of Synthetic Chemistry and XXXIII Finnish NMR Symposium. Book of Abstracts. (90 pp.) 2011
146. Valto, Piia: Development of fast analysis methods for extractives in papermaking process waters. (73 pp.) 2011
147. Andersin, Jenni: Catalytic activity of palladium-based nanostructures in the conversion of simple olefinic hydro- and chlorohydrocarbons from first principles. (78 pp.) 2011
148. Aumanen, Jukka: Photophysical properties of dansylated poly(propylene amine) dendrimers. (55 pp.) 2011
149. Kärnä, Minna: Ether-functionalized quaternary ammonium ionic liquids – synthesis, characterization and physicochemical properties. (76 pp.) 2011
150. Jurček, Ondřej: Steroid conjugates for applications in pharmacology and biology. (57 pp.) 2011
151. Nauha, Elisa: Crystalline forms of selected Agrochemical actives: design and synthesis of cocrystals. (77 pp.) 2012
152. Ahkola, Heidi: Passive sampling in monitoring of nonylphenol ethoxylates and nonylphenol in aquatic environments. (92 pp.) 2012
153. Helttunen, Kaisa: Exploring the self-assembly of resorcinarenes: from molecular level interactions to mesoscopic structures. (78 pp.) 2012
154. Linnanto, Juha: Light excitation transfer in photosynthesis revealed by quantum chemical calculations and exciton theory. (179 pp.) 2012
155. Roiko-Jokela, Veikko: Digital imaging and infrared measurements of soil adhesion and cleanability of semihard and hard surfaces. (122 pp.) 2012
156. Noponen, Virpi: Amides of bile acids and biologically important small molecules: properties and applications. (85 pp.) 2012
157. Hulkko, Eero: Spectroscopic signatures as a probe of structure and dynamics in condensed-phase systems – studies of iodine and gold ranging from isolated molecules to nanoclusters. (69 pp.) 2012
158. Lappi, Hanna: Production of Hydrocarbon-rich biofuels from extractives-derived materials. (95 pp.) 2012
159. Nykänen, Lauri: Computational studies of Carbon chemistry on transition metal surfaces. (76 pp.) 2012
160. Ahonen, Kari: Solid state studies of pharmaceutically important molecules and their derivatives. (65 pp.) 2012
161. Pakkanen, Hannu: Characterization of organic material dissolved during alkaline pulping of wood and non-wood feedstocks (76 pp.) 2012
162. Moilanen, Jani: Theoretical and experimental studies of some main group compounds: from closed shell interactions to singlet diradicals and stable radicals. (80 pp.) 2012
163. Himanen, Jatta: Stereoselective synthesis of Oligosaccharides by *De Novo* Saccharide welding. (133 pp.) 2012
164. Bunzen, Hana: Steroidal derivatives of nitrogen containing compounds as potential gelators. (76 pp.) 2013
165. Seppälä, Petri: Structural diversity of copper(II) amino alcohol complexes. Syntheses, structural and magnetic properties of bidentate amino alcohol copper(II) complexes. (67 pp.) 2013
166. Lindgren, Johan: Computational investigations on rotational and vibrational spectroscopies of some diatomics in solid environment. (77 pp.) 2013
167. Giri, Chandan: Sub-component self-assembly of linear and non-linear diamines and diacylhydrazines, formylpyridine and transition metal cations. (145 pp.) 2013
168. Riisiö, Antti: Synthesis, Characterization and Properties of Cu(II)-, Mo(VI)- and U(VI) Complexes With Diaminotetraphenolate Ligands. (51 pp.) 2013
169. Kiljunen, Toni (Ed.): Chemistry and Physics at Low Temperatures. Book of Abstracts. (103 pp.) 2013
170. Hänninen, Mikko: Experimental and Computational Studies of Transition Metal Complexes with Polydentate Amino- and Aminophenolate Ligands: Synthesis, Structure, Reactivity and Magnetic Properties. (66 pp.) 2013

DEPARTMENT OF CHEMISTRY, UNIVERSITY OF JYVÄSKYLÄ
RESEARCH REPORT SERIES

171. Antila, Liisa: Spectroscopic studies of electron transfer reactions at the photoactive electrode of dye-sensitized solar cells. (53 pp.) 2013
172. Kemppainen, Eeva: Mukaiyama-Michael reactions with α -substituted acroleins – a useful tool for the synthesis of the pectenotoxins and other natural product targets. (190 pp.) 2013
173. Virtanen, Suvi: Structural Studies Of Dielectric Polymer Nanocomposites. (49 pp.) 2013
174. Yliniemelä-Sipari, Sanna: Understanding The Structural Requirements for Optimal Hydrogen Bond Catalyzed Enolization – A Biomimetic Approach.(160 pp.) 2013
175. Leskinen, Mikko V: Remote β -functionalization of β^{γ} -keto esters (105 pp.) 2014
176. 12th European Conference on Research in Chemistry Education (ECRICE2014). Book of Abstracts. (166 pp.) 2014.
177. Peuronen, Anssi: N-Monoalkylated DABCO-Based N-Donors as Versatile Building Blocks in Crystal Engineering and Supramolecular Chemistry. (54 pp.) 2014